N_2O emissions from eutrophic lakes: sources and significance

A thesis presented in partial fulfilment of the requirements for the degree of

Master of Engineering

in

Chemical and Bioprocess Engineering

at Massey University, Manawatu, New Zealand

Laura TEUMA

2022

Abstract

For decades, high emissions of the greenhouse gas and ozone-depleting pollutant nitrous oxide (N_2O) have been repeatedly reported from eutrophic environments. Acknowledging this fact, the Intergovernmental Panel on Climate Change (IPCC) recently increased the emission factor (EF) used to compute indirect N_2O emissions from wastewater discharge into eutrophic and nutrient-impacted aquatic environments from 0.005 to 0.019 kg N_2O-N emitted per kg of N received. However, because the IPCC still considers that bacterial nitrification and denitrification are the only significant N_2O biological mechanisms, it computes N_2O emissions by assuming a linear relationship between the amount of N_2O emitted from an aquatic environment and the amount of nitrogen (N) reaching this environment. This bacteria-centric assumption may be challenged by the ability of microalgae to synthesize significant amount of N_2O. Indeed, as microalgae blooms can be triggered by N and/or phosphorus (P) pollution, the ability of these organisms to produce N_2O may mean that N_2O emissions from eutrophic environments cannot only be correlated to N inputs. Thus, we hypothesize that microalgae significantly contribute to N_2O emissions in eutrophic aquatic environments and that P inputs should also be considered to accurately estimate N_2O emissions from eutrophic aquatic environments.

This thesis initially sought to determine if algae-rich eutrophic ecosystems indeed generate significant N_2O emissions and if microalgae indeed contribute to these emissions. To reduce the scope of the research, emphasis was given to the study of eutrophic lakes as a 'worse-case environment'. Our methodology was based around field monitoring and laboratory assays testing artificial and natural microalgae-based microcosms.

Preliminary data gathered from the eutrophic Lake Horowhenua (Levin, New Zealand) show that the lake is a source of N_2O (0.4 – 8.7 g $N\text{-}N_2O \cdot ha^{-1} \cdot yr^{-1}$, n = 29 sampling events). However, no relationship between algal biomass concentration and N_2O production could be evidenced. In parallel, laboratory batch assays were performed to investigate physiological conditions influencing microalgal N_2O synthesis and the potential enzymes involved. Preliminary data showed that wild type *Chlamydomonas reinhardtii* produced N_2O up to 31.5 ± 10.7 µmole $N_2O \cdot g\ DW^{-1}$ over 24 hours in autotrophic conditions and when supplied 10 mM NO_2^-. Inhibiting the electron flow coming from PSII in the same conditions inhibited N_2O production, suggesting that the electron transport chain is involved in N_2O synthesis. These results informed us on the N_2O synthesis pathways that should be investigated during future field work and allowed us to identify candidate strains to create a mutant unable to synthesize N_2O for future microcosms study.

Because accurate data is paramount to robust policy, this research is the first step to establish the significance of a new N_2O source that is not necessarily linked to N pollution and could trigger a paradigm shift in how N_2O emissions are estimated in greenhouse gas inventories. This may in turn affect how N_2O sources are prioritized for mitigation strategies and, if deemed necessary, will also provide the methodologies and knowledge needed for efficient monitoring of eutrophic aquatic bodies, including marine environments.

Acknowledgements

Firstly, I would like to thank my main supervisor Dr Maxence Plouviez for his constant support and guidance during this research. His unfailing help encouraged me to always improve my work. I also wish to extend my thanks to my first co-supervisor Prof. Benoit Guieysse for his continuous advice and who has been a continuing source of reassurance and optimism throughout. I am also grateful to my second co-supervisor Dr Emanuel Sanz-Luque for his guidance and who has offered valuable advice on molecular biology.

I would like to express my gratitude to Prof. Jonathan Procter and members of the Lake Horowhenua Trust for their assistance and access to Lake Horowhenua and to Steve Langevad and the Palmerston North City Council for access to the Turitea reservoir that allowed me to undertake my research.

Thanks also to Prof. Emilio Fernandez and Prof. Aurora Galvan and the University of Cordoba for hosting me during the first months of my studies. I would like to thank my colleague Carmen Bellido-Pedraza for her help during my time in Spain.

I must thank the Massey University scholarship office for their financial support which enabled me to undertake my research.

Many thanks to Massey University staff, especially Ann-Marie Jackson, John Edwards and Kylie Evans for their help in the laboratory. I wish to extend my thanks to the administrative staff, especially Karen Pickering and Dilantha Punchihewa for their assistance during this challenging time as a student.

I wish to thank my colleagues Alex Cliff, Florencia Ocampo and Federico Fabisik for their help and extend my gratitude to all the School of Food and Advanced Technology for creating a positive work place environment.

Finally, I welcome this opportunity to thank my friends Angela Bravo Nunez, Rayen Leon Quezada, Hien Truong, Merit Mathew and Kevin Gimenez for their support. I would like to give special thanks to my family for their trust and constant support.

Table of contents

List of illustrations

List of tables

1. Introduction

The Nature Education knowledge project defines eutrophication as "excessive plant and algal growth due to the increased availability of one or more limiting growth factors needed for photosynthesis (Schindler 2006), such as sunlight, carbon dioxide, and nutrient fertilizers" (Chislock et al., 2013). The New Zealand Ministry for the Environment is more specific and states that "eutrophication is the result of nutrients built up in a body of water, frequently due to run-off from land, which causes dense growth of aquatic plants or algae"(*Assessment of the Eutrophication Susceptibility of New Zealand's Estuaries*, 2019). Indeed, the artificial input of nitrogen (N) and phosphorus (P) in water bodies has considerably increased the occurrence of eutrophication to an extent that it is now considered a global environmental issue and the overgrowth of algae and aquatic plants causes deterioration of water taste and odour, loss of transparency, and even toxicity in some cases (Xu et al., 2010; Aubriot et al., 2020; Huang et al., 2020). For example, the water quality of Rotorua Lakes in New Zealand has declined since the 1950s due to the intensive use of fertilizers and urbanisation (Morgenstern et al., 2015), even leading to the closure of Lake Rotoiti for 2 months during summer 2003 because of the toxicity of a large microalgal bloom (Hamilton, 2003). The New Zealand Ministry for the Environment has estimated that around half of New Zealand monitored lakes are eutrophic or worse (Ministry for the Environment & Stats NZ, 2020). Globally, the figure is similar with 30 – 40% of all lakes being eutrophic (Yang et al., 2008).

Another potential and poorly known consequence of eutrophication is the emission of nitrous oxide (N_2O), a potent greenhouse gas (GHG) and ozone-depleting atmospheric pollutant (Ravishankara et al., 2009). Several authors have indeed estimated that global N_2O emissions from eutrophic lakes could represent 52 to 211 Tg CO_2·$year^{-1}$ (DelSontro et al., 2018; Plouviez et al., 2019a; Plouviez & Guieysse, 2020), which represent 3 to 12% of all direct anthropogenic N_2O emissions from agriculture, the largest contributor to anthropogenic N_2O emissions globally (Tian et al., 2020). However, and while significant N_2O emissions have been repeatedly reported in microalgae-rich aquatic ecosystems (e.g. eutrophic lakes), we still do not know the magnitude of these emissions and how much of these emissions are directly caused by microalgae (Ciais et al., 2013; Plouviez et al., 2019a). This is particularly relevant when we consider that the ability of microalgae to produce N_2O has now been unambiguously demonstrated in the laboratory (Burlacot et al., 2020; Guieysse et al., 2013; Plouviez et al., 2019a; Weathers, 1984; Weathers & Niedzielski, 1986).

Acknowledging that high N_2O emissions have indeed been often recorded from "nutrient-impacted waters such as eutrophic lakes", the Intergovernmental Panel on Climate Change (IPCC) recently increased the value of the Tier 3 emission factor used to compute N_2O emissions from "waters

receiving treated or untreated effluent" (see section 2.1 for explanation) from 0.05 to 0.019 kg N_2O-N emitted per kg of N received (Bartram et al., 2019). However, it is clear from its narrative that the IPCC still assumes these N_2O emissions are only occurring via bacterial nitrification and denitrification. This 'bacteria-centric' view implies that current N_2O field monitoring and budgeting methodologies may not be accurate in eutrophic environments. This also means that mitigation strategies based solely on N control may not be efficient because microalgae growth can be triggered by P, meaning a dual control of nutrients might be required to reduce N_2O emissions from eutrophic aquatic environments (Conley et al., 2009; Paerl et al., 2016). To identify knowledge gaps and propose a tangible research methodology, the following review is divided in 6 sections:

- Section 2.1 describes how N_2O emissions are currently computed from aquatic environments and how these estimations compare to field data. This section identifies the knowledge gaps in the current assumptions and methodology used to estimate N_2O emissions.

- Section 2.2 describes the currently known microbial N_2O synthesis pathways, with emphasis on microalgae. This section provides the knowledge needed to understand the assumptions behind current N_2O budgeting methodologies, and the uncertainty these assumptions are causing.

- Section 2.3 briefly describes the diversity of freshwater lakes and the tools used to evaluate their water quality. This section provides the basic knowledge to measure lakes' trophic level.

- Section 2.4 describes the eutrophication process of lakes with emphasis on the nutrients involved and the proposed mitigation strategies. This section outlines the assumptions used in current mitigation strategies and help understand their potential inadequacy in microalgae-rich ecosystems.

- Section 2.5 describes fundamentals in algae cell biology with emphasis on algal N and P metabolisms. This section evidences the importance of understanding how N and P impact algal growth and, by extension, algal N_2O synthesis.

- Section 2.6 outlines the 'research gaps' identified from the literature review, formulates our research hypothesis and concludes the review.

The literature review (Section 2) is followed by the description of the proposed research strategy and methodology (Sections 3 to 5). Finally, preliminary results are presented and discussed (Section 6).

2. Literature review

2.1. Anthropogenic N_2O emissions from inland and coastal waters

N_2O is an ozone-depleting pollutant (Ravishankara et al., 2009) and greenhouse gas (GHG) with a global warming potential 273 times higher than CO_2 on a 100-year time scale (Masson-Delmotte et al., 2021). Anthropogenic N_2O emissions have increased by 23% over the past 40 years, reaching 7,300 kt N-N_2O·year^{-1} between 2007 and 2016. Observed atmospheric N_2O concentrations are even starting to surpass all predictions by the IPCC (Tian et al., 2020).

Box 1: Intergovernmental Panel on Climate Change (IPCC).

The IPCC was founded in 1988 by the United Nations Environment Programme and the World Meteorological Organization to assess the science related to climate change. Its main objectives are to provide governments and policy makers with the tools to estimate GHG emissions, regular assessment reports regarding climate change, the consequences and risks resulting from climate change, and to come up with recommendations about adaptation and mitigation strategies.

The global sources of N_2O are presented in Figure 1 (Tian et al., 2020) and further detailed in Appendix A. As can be seen, global N_2O emissions from aquatic environments were estimated to 4,300 kt N-N_2O·year^{-1} from 2007 to 2016, with anthropogenic emissions from aquatic environments representing 14% of these emissions.

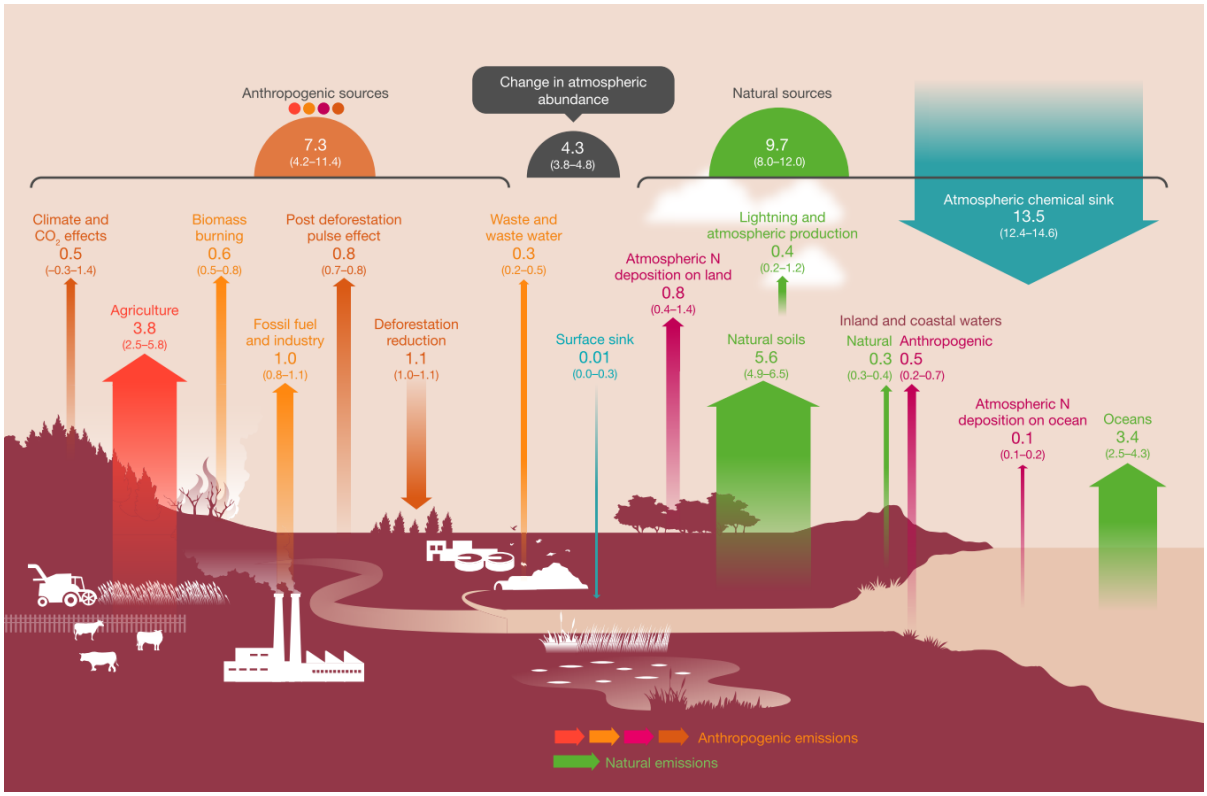

Figure 1: Global N_2O budget. N_2O fluxes are in Tg N·yr^{-1} for 2007-2016.
Reprinted by permission from Springer Nature Customer Service Centre GmbH: Nature, A comprehensive quantification of global nitrous oxide sources and sinks, Tian et al., © 2020, doi: https://doi.org/10.1038/s41586-020-2780-0.

2.1.1. IPCC methodology

The IPCC assumes that anthropogenic N_2O emissions from inland and coastal waters are indirectly caused by anthropogenic nitrogen (N) inputs from either i) managed lands (i.e. agricultural lands) following N leaching and runoffs from agricultural soils and N atmospheric deposition on water surfaces following N volatilization from land; and ii) N-rich wastewater discharge into water bodies (Figure 2). These indirect N_2O emissions are then estimated by multiplying the N loads predicted to be received with specific emission factors (EFs, see Appendix B for further details) for specific activities and/or receiving environments. The EFs are calculated based on experimental measurements of N_2O and N inputs in relevant ecosystems. There is currently no clear distinction between natural and anthropogenic N_2O emissions from freshwater lakes and reservoirs (Appendix C.1) and, to our knowledge, Tian et al. (2020) are the first authors to propose a differentiation.

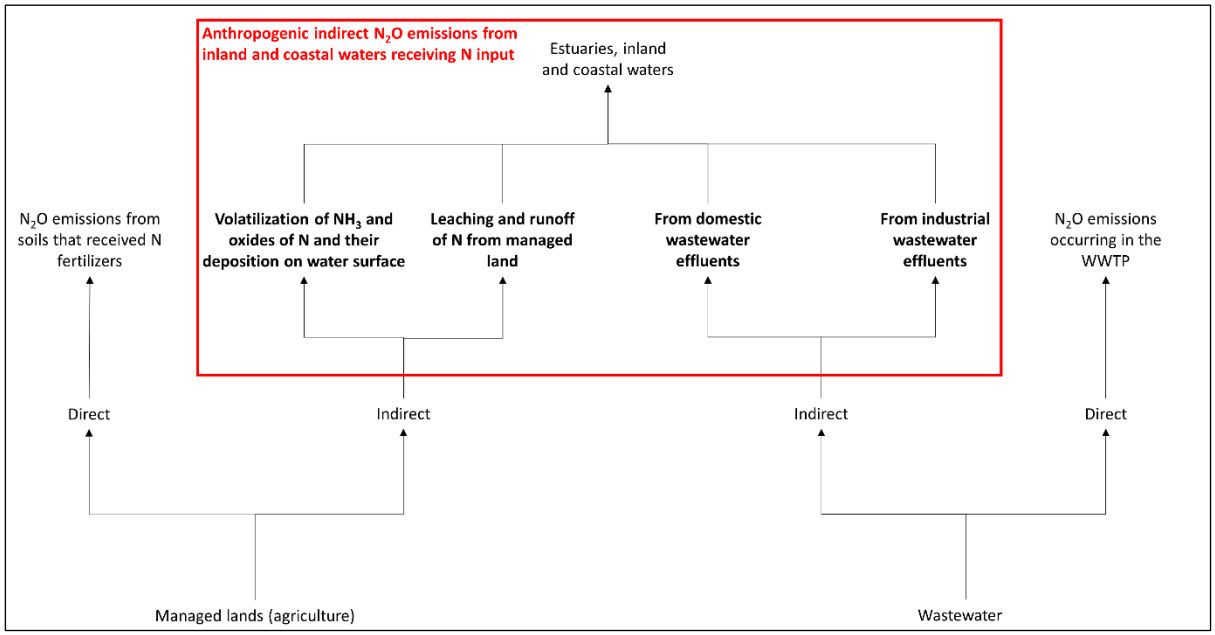

Figure 2: Anthropogenic N_2O emissions from managed lands and wastewater according to the IPCC. The four N inputs to aquatic environments categories described by the IPCC causing indirect N_2O emissions from water bodies are in bold character.

The IPCC advises to follow a three-tiered approach to calculate GHG emissions depending on the data available. The Tier 1 method enables to calculate GHG emissions using default EF values and, when applicable, default partitioning factors to estimate the N load (Appendix B). The Tier 2 method uses country-specific EFs and partitioning factors. Finally, the Tier 3 uses country-specific models and measurements (Hergoualc'h et al., 2019). For example, EF Tier 1 values of 0.01 and 0.011 kg N–N_2O·kg N input^{-1} are currently recommended to estimate indirect N_2O emissions from aquatic environments receiving N via atmospheric deposition (EF_4) and from agricultural runoff and leaching (EF_5), respectively (Hergoualc'h et al., 2019) (Figure 3). A Tier 1 EF value of 0.005 kg N–N_2O·kg N^{-1} is also

recommended to estimate indirect N_2O emissions from aquatic environments receiving N from domestic and industrial wastewater effluents, as exemplified in Box 2 (Bartram et al., 2019).

Box 2: N_2O emissions from wastewater treatment plants and wastewater effluents (Bartram et al., 2019).

Direct N_2O emissions from domestic wastewater treatment plants are calculated as:

$$N_2\text{O Plants}_{DOM} = \left[\sum_{i,j}(U_i \cdot T_{ij} \cdot EF_j)\right] \cdot TN_{DOM} \cdot \frac{44}{28}$$

Where $N_2O\ Plants_{DOM}$ represents N_2O emissions from domestic wastewater treatment plants (kg $N_2O \cdot yr^{-1}$); TN_{DOM} is the total amount of nitrogen in domestic wastewater (kg $N \cdot yr^{-1}$); U_i is the fraction of population in income group i (with i = rural, urban high income and urban low income); T_{ij} is the degree of utilization of treatment system j for each income group fraction i (with j = treatment/discharge pathway or system): EF_j is the emission factor for treatment/discharge pathway or system j (kg $N–N_2O \cdot kg\ N^{-1}$); and $\frac{44}{28}$ is the conversion factor of kg N_2O – N into kg N_2O.

Indirect N_2O emissions from wastewater effluents are calculated as a fraction of the nitrogen flux reaching the aquatic body. The removal of N from wastewater accounts for the transfer of N to sludge as well as N_2 and N_2O losses to the atmosphere due to nitrification/denitrification processes during transport and treatment. Indirect N_2O emissions from domestic wastewater effluents are therefore calculated as:

$$N_2O_{\text{EFFLUENT,DOM}} = \text{N}_{EFFLUENT,DOM} \cdot EF_{EFFLUENT} \cdot \frac{44}{28}$$

Where $N_2O_{EFFLUENT,DOM}$ represents N_2O emissions from domestic wastewater effluent (kg $N_2O \cdot yr^{-1}$); $N_{EFFLUENT,DOM}$ is the nitrogen in the effluent discharged to aquatic environments (kg $N \cdot yr^{-1}$); and $EF_{EFFLUENT}$ (default = 0.005 kg $N–N_2O \cdot kg\ N^{-1}$) is the emission factor for N_2O emissions from wastewater discharged to aquatic systems (kg $N–N_2O \cdot kg\ N^{-1}$).

$$N_{\text{EFFLUENT,DOM}} = \sum_j \left[(TN_{DOM} \cdot T_j) \cdot (1 - N_{REM,j})\right]$$

Where, T_j is the degree of utilisation of treatment system j (with j corresponding to each wastewater treatment type used) and N_{REM} is the fraction of total wastewater nitrogen removed during wastewater treatment per treatment type j.

Similar equations are used to estimate indirect N_2O emissions from industrial wastewater effluents.

2.1.2. Limitations of current EFs

Based on the methodology described above, the IPCC estimates that rivers, estuaries and coastal zones emitted 600 kt $N\text{-}N_2O \cdot year^{-1}$ in 2006 (Ciais et al., 2013). Most authors however agree there is a large uncertainty associated with the IPCC methodology due to a lack of data and many authors tested different approaches to estimate N_2O emissions from freshwater ecosystems, as further detailed in Appendix C (Hu et al., 2016; Miao et al., 2020; Tian et al., 2019; Webb et al., 2021). An additional limitation is that N_2O emissions are assumed to increase linearly with the N load and that N_2O synthesis is mostly caused by bacterial nitrification and denitrification, as further discussed below.

There is also a lack of specificity for the EFs used in different environments. For example, the same EF of 0.0026 kg N–N_2O·kg N leached and runoff^{-1} is used for reservoirs and rivers despite a significant difference, documented at 0.17 - 0.44 kg N–N_2O·kg N leached and runoff^{-1} and 0.004 - 0.005 kg N–N_2O·kg N leached and runoff^{-1} respectively (Maavara et al., 2019). The difference could be explained by different hydraulic retention time (HRT) influencing the biological processes behind N_2O production (Maavara et al., 2019). Consequently, the current IPCC estimates for N_2O emissions from rivers might be overestimated.

The same issue has been highlighted regarding the EFs used to compute N_2O emissions from groundwater and surface drainage. Webb et al. (2021) argued that indirect emissions coming from artificial agricultural surface waters (drains, ditches, canals, farm dams and farm impoundments) were overestimated when using EFs developed by the IPCC, especially because the assumption that N_2O emissions linearly increase with N concentration does not take into account the drivers of N_2O production in these ecosystems (e.g. HRT and substrate availability to support microbial activity) (Webb et al., 2021). Besides, it has been pointed out that most EFs have been calculated using data from eutrophic waters, which could lead to an overestimation for non-eutrophic waters (Tian et al., 2019). Finally, even if the EFs do not seem to be dependent on climate, most data available come from temperate regions and might not be representative of the emissions under other climates (Tian et al., 2019).

2.1.3. The IPCC acknowledges higher N_2O emissions occur in "nutrient-impacted environment".

Interestingly, the IPCC recently increased the EF associated with wastewater discharge into "nutrient-impacted waters" nearly 4-folds, from 0.005 to 0.019 kg N_2O-N·kg N^{-1} (Table 1). This change was based on "research published between 1978 and 2017 […] indicating that higher N_2O emissions occur when wastewater is discharged to nutrient-impacted (eutrophic) or hypoxic[1] aquatic receiving environments" (Bartram et al., 2019). It is however clear from the IPCC rationale for this change that the higher N_2O emissions experimentally recorded are largely due to the formation of hypoxic zones prone to N_2O emissions from bacteria. For this reason, the IPCC does not recommend to increase the EF used to compute N_2O emissions associated with N runoffs from agriculture as it states that a

[1] Oxygen-depleted condition

"combination of reducing conditions and high organic loading […] are unlikely to exist in agricultural runoff systems" (Bartram et al., 2019).

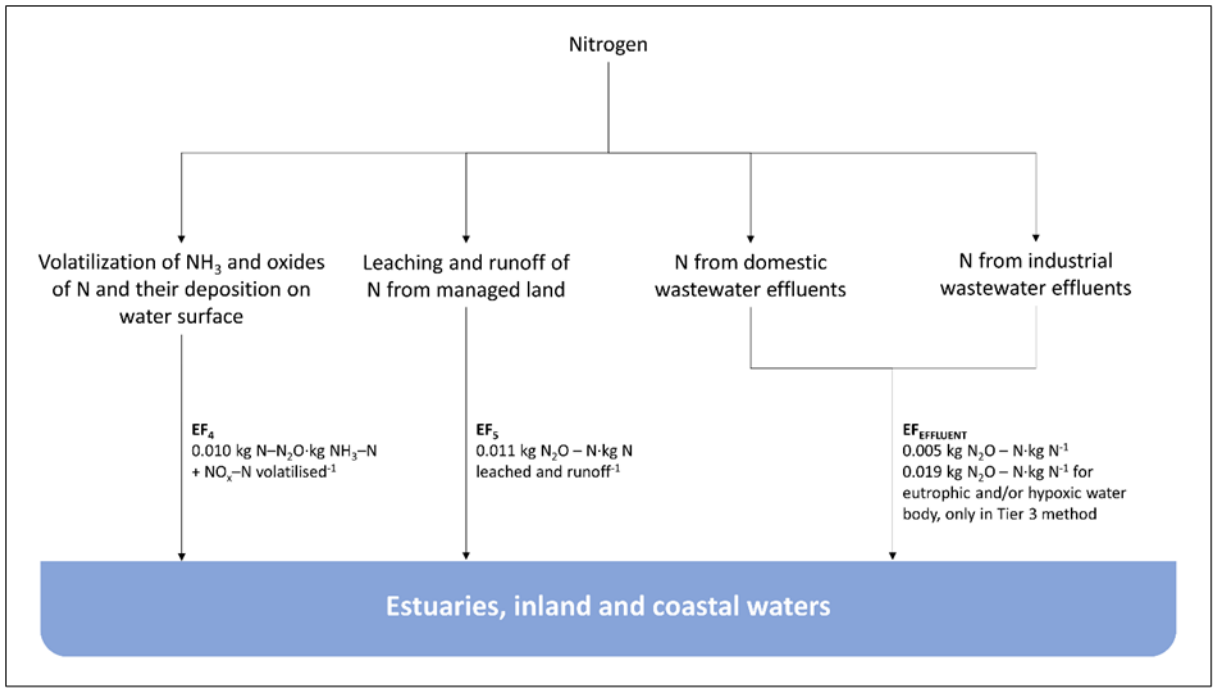

Figure 3: Current emission factors used for the different N flux causing indirect anthropogenic N_2O emissions from aquatic environments.

Table 1: Default emission factor values recommended by the IPCC (values are in kg N–N_2O·kg N^{-1}).

		1996	2006	2019
Tier 1	**EF_5**	0.025	0.0075	0.011
	EF_4	0.01	0.01	0.01
	$EF_{EFFLUENT}$	NA	0.005	0.005
Tier 3	**$EF_{EFFLUENT}$**	NA	0.005	0.005 0.019 for eutrophic waters

The IPCC considers that N_2O is mostly produced via microbial nitrification and denitrification processes. That assumption implies that mitigation strategies typically solely rely on reducing N inputs. However, microalgae have also been showed to produce N_2O (Plouviez et al., 2019a; Weathers, 1984; Weathers & Niedzielski, 1986; Guieysse et al., 2013; Burlacot et al., 2020), although their contribution to N_2O emissions from aquatic environments has barely been investigated. Besides, emissions have been recorded in oxic[2] environments that cannot always be attributed to the bacterial pathways (Table

[2] Oxygen-replete conditions

2). For example, Miao et al. (2020) observed that N_2O emissions were high under normoxia[3], especially when algae blooms occurred.

Table 2: N_2O emissions reported during published studies acknowledging algal N_2O synthesis in natural environments, simplified from Plouviez et al. (2019a).

Ecosystem	N_2O fluxes	O_2 conditions[1]	Reference
Ocean	115 nmole·m^{-2}·h^{-1}	Normoxic	Cohen & Gordon, 1978
Ocean	409 nmole·m^{-2}·h^{-1}	Hypoxic	Pierotti & Rasmussen, 1980
Coastal wetland	125 – 228 nmole·m^{-2}·h^{-1}	Anoxic and hypoxic	Smith et al., 1983
Ocean	123 – 132% saturation	Normoxic	Oudot et al., 1990
Lakes	300 – 700 nmole·m^{-2}·h^{-1}	From anoxic to normoxic	Mengis, 1997
Ocean	88 nmole·m^{-2}·h^{-1}	Not specified	Morell et al., 2001
Lake	357 – 2450 nmole·m^{-2}·h^{-1}	Not specified	Wang et al., 2006
Lakes	0 – 10,057 nmole·m^{-2}·h^{-1}	Oxic	McCrackin & Elser, 2011
Lake	12.5 – 2233 nmole·m^{-2}·h^{-1}	Normoxic and Hyperoxic	Miao et al. (2020)

[1] Anoxic conditions are assumed when the oxygen concentration ([O_2]) of the water is inferior to 3 µM, hypoxic conditions are assumed when 3 µM < [O_2] < 200 µM, normoxic conditions are assumed when 200 µM < [O_2] < 400 µM, and hyperoxic conditions are assumed when [O_2] > 400 µM in freshwater (Diaz, 2016).

Eutrophic environments are inclined to algal blooms due to their N but mostly P supply that can trigger algae proliferation (Kalff, 1983; Nalewajko & Murphy, 2001; Elser et al., 2007; Abell et al., 2010). Consequently, evidencing the role microalgae play in N_2O emissions is critical to adjust current methodologies for computing N_2O emissions from aquatic ecosystems; establish the best mitigation strategies for eutrophic environments; and generate knowledge that can be applied to further research in similar ecosystems (e.g. eutrophic marine areas).

2.2. N_2O synthesis by microorganisms

Many organisms, including phytoplankton and plants, can produce N_2O via processes such as denitrification, nitrification and nitrogen uptake from nitrates (Hahn & Junge, 1977; Hallin et al., 2018). The following section reviews these mechanisms with special emphasis on microalgae.

[3] Air-saturated conditions

2.2.1. Bacteria

N_2O can be produced by bacteria through nitrification, denitrification, coupled nitrification-denitrification, nitrifier-denitrification, and anaerobic ammonia oxidation in the benthic[4] zone of different aquatic ecosystems.

Nitrification: Autotrophic ammonia-oxidizing bacteria (AOB), such as *Nitrosomonas* and *Nitrosococcus* species, use ammonia (NH_3) as energy source under oxic conditions. AOB thus carry out the first step of nitrification, the aerobic oxidation of NH_3 into nitrite (NO_2^-) by the enzyme ammonia monooxygenase (AMO). AMOs are copper-containing membrane-associated monooxygenases encoded by the genes *amoA, amoB* and *amoC* (Hayatsu et al., 2008). During nitrification, NH_3 is oxidised into hydroxylamine (NH_2OH) by AMO and NH_2OH is then oxidised to NO_2^- by hydroxylamine oxidoreductase (HAO). During this process, N_2O can be formed from the spontaneous chemical decomposition of NH_2OH or NO_2^- as illustrated in Figure 4 (Hayatsu et al., 2008; Wrage et al., 2001; Zhu-Barker et al., 2015). Nitrite-oxidizing bacteria (NOB) such as *Nitrobacter* and *Nitrospina* genera are responsible for the final step of nitrification, the oxidation of NO_2^- into nitrate (NO_3^-) by nitrite oxidoreductase (NXR). Microorganisms capable of oxidizing NH_3 all the way to NO_3^- steps have recently been discovered and called complete ammonia oxidizer (comammox) (Daims et al., 2016). These organisms belong to the genus *Nitrospira* and can produce N_2O from the abiotic conversion of NH_2OH or NO_2- as described above (Han et al., 2021). Heterotrophic nitrifiers (e.g. *Paracoccus, Pseudomonas* and *Staphylococcus* genera) carry out heterotrophic ammonium oxidation to nitrate under normoxia or hypoxia, but urea can be used instead of ammonia (Wrage et al., 2001). AOB, NOB, heterotrophic nitrifiers and comammox can all be found in marine and freshwater ecosystems (Ward et al., 2011; Huang et al., 2020).

[4] Located at the bottom of the water body

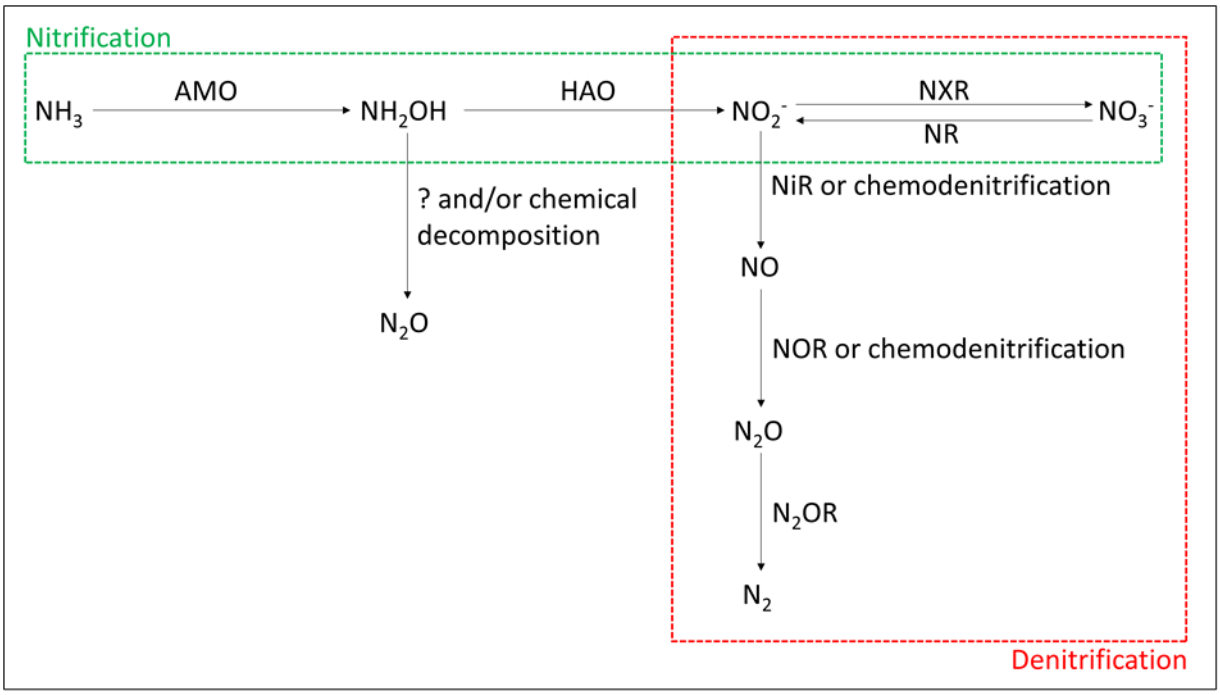

Figure 4: Nitrification and denitrification pathways in bacteria.
Abbreviations/symbols: NH_3, ammonia; NH_2OH, hydroxylamine; NO_2^-, nitrite; NO_3^-, nitrate; NO, nitric oxide; N_2O, nitrous oxide; N_2, dinitrogen; AMO, ammonia monooxygenase; HAO, hydroxylamine oxidoreductase; NXR, nitrite oxidoreductase; NR, Nitrate reductase; NiR, nitrite reductase; NOR, nitric oxide reductase; N_2OR, nitrous oxide reductase; ?, unknown enzyme.

Denitrification: Denitrifying bacteria (e.g. *Pseudomonas* and *Alcaligenes* genera) are responsible for N_2O production during partial denitrification under hypoxia or anoxia. Denitrification is a respiratory pathway during which NO_3^- is first reduced to NO_2^- by nitrate reductase (NR) and NO_2^- is then reduced to nitric oxide (NO) by nitrite reductase (NiR). NO is in turn reduced to N_2O by nitric oxide reductase (NOR) and N_2O is finally reduced to nitrogen (N_2) by nitrous oxide reductase (symbolized as either N_2OR or NOS in the literature) as illustrated in Figure 4. The genes *narG, nirS* and *nirK, norB* and *norZ,* and *nosZ* encode NR, NiR, NOR and N_2OR, respectively (Garrido-Amador et al., 2021; Ren et al., 2019). During denitrification, N_2O production increases with the presence of O_2 and at low pH as these conditions inhibit N_2OR activity. Denitrification is a widespread biological process that occur in most aquatic environments (Piña-Ochoa & Álvarez-Cobelas, 2006).

Nitrifier-denitrification: Certain AOB and methanotrophs can oxidise NH_3 until NO_2^- and then denitrify NO_2^- to N_2 via N_2O (as described above). Such coupled nitrification-denitrification process may also involve bacterial consortia where the nitrification and denitrification steps are carried out by different bacteria (Wrage et al., 2001). During nitrifier-denitrification under hypoxia, N_2O is released as an intermediate of nitrite reduction as in the case of 'classical' denitrification.

Anaerobic ammonia oxidation: Under anoxia, annamox bacteria oxidize ammonium (as energy source) using nitrite as electron acceptor. In the presence of NH_4^+ and NO_2^-, N_2O emissions have been

reported during annamox-based wastewater treatment but the pathway of N_2O synthesis by these bacteria has not yet been identified (Kampschreur et al., 2009; Ali et al., 2016). Anammox bacteria can be found in the anoxic[5] and hypoxic zones of freshwater and marine environments[6] (Ward et al., 2011). These bacteria have so far only been reported in one lake and, therefore, their significance to N_2O emissions in freshwater ecosystems is still poorly understood (Ward et al., 2011).

2.2.2. Fungi

Fungi such as *Fusarium oxysporum* can produce N_2O via denitrification and co-denitrification (Figure 5). The fungal denitrification pathway takes place under either aerobic and anaerobic conditions and is similar to the bacterial denitrification pathway described above. The fungal *nirK* gene encoding its NirK enzyme is an orthologue[7] of the bacterial *nirK* gene. The fungal NOR enzyme, called cytochrome P450 nitric oxide reductase (P450nor), is encoded by the gene *p450nor* and is a member of the CYP55 family of the P450 cytochrome superfamily. Therefore, fungi can also produce N_2O from NO_2^- and a nitrogen co-substrate (e.g. NH_4^+, amino acids, urea) in a process catalysed by the fungal NOR and known as co-denitrification (Hayatsu et al., 2008; Shoun et al., 2012; Higgins et al., 2016). Fungi are present in lentic[8] bodies' sediments and N_2O emissions from Poyang Lake, China, have been correlated with fungal biomass concentration (Liu & Xu, 2016).

[5] Severe oxygen depleted conditions
[6] i.e. sediments and oceanic OMZs
[7] An orthologous gene is a gene inherited in two species by a common ancestor and which diverged after the creation of the two species. The gene and its main function are conserved despite the divergence.
[8] Body of standing water

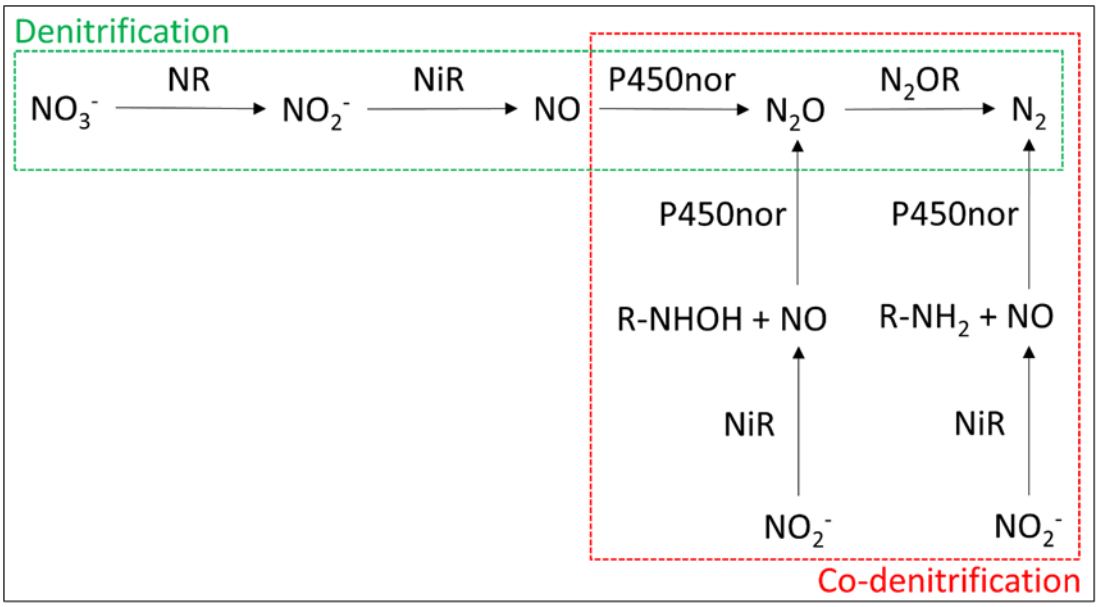

Figure 5: Denitrification and co-denitrification pathways in fungi.
Abbreviations/symbols: NO_3^-, nitrate; NO_2^-, nitrite; NO, nitric oxide; N_2O, nitrous oxide; N_2, dinitrogen; R-NHOH, imine; R-NH_2, amine; NR, Nitrate reductase; NiR, nitrite reductase; P450nor, cytochrome P450 nitric oxide reductase; N_2OR, nitrous oxide reductase.

2.2.3. Archaea

Certain ammonia-oxidizing Archaea (AOA) harbour *amo*-like genes, *amoA*, *amoB*, and *amoC* encoding the three subunits of the AMO enzyme. AOA are thus capable of catalysing the first step of nitrification following the same pathway as AOB (Hatzenpichler, 2012). AOA were found to significantly contribute to N_2O emissions from oceans (Santoro et al., 2011; Löscher et al., 2012; Qin et al., 2017). While the pathways of archaeal N_2O synthesis are still debated (Wu et al. 2020; Stein et al. 2021), Jung et al. (2019) recently suggested that a strain of AOA could synthesise N_2O enzymatically at low pH in a reaction involving NO reduction into N_2O by the cytochrome P450. Some archaea are also capable of denitrification via a pathway similar to bacteria, and this mechanism could be a potential N_2O source (Hayatsu et al., 2008). AOA are generally found in marine waters but their presence has been reported in lakes as well (Wenk et al., 2016; Prosser et al., 2020).

2.2.4. Microalgae

Photosynthetic microorganisms include prokaryotes (e.g. cyanobacteria) and eukaryotes (e.g. Chlorophyceae, diatoms, etc.), including unicellular algae (existing as individual cells or in groups) known as microalgae. While microalgae are taxonomically all eukaryotic phototrophs, cyanobacteria are often considered as microalgae members in the engineering literature: This broader definition will

be used in this review for simplicity. Microalgae are mostly found in aquatic environments (Borowitzka, 2012), and their contributions to N_2O emissions have mainly been confirmed and reported in the last decade (Plouviez et al., 2019a).

While the study of N_2O synthesis in microalgae is still at its infancy, various pathways have been proposed in the literature, especially in the green unicellular microalga *Chlamydomonas*, as summarized in Figure 6. Succinctly, microalgae N_2O synthesis is currently believed to occur via the successive reduction of nitrate into nitrite and NO. NO is thus seen as the substrate of N_2O via various putative pathways as further detailed below.

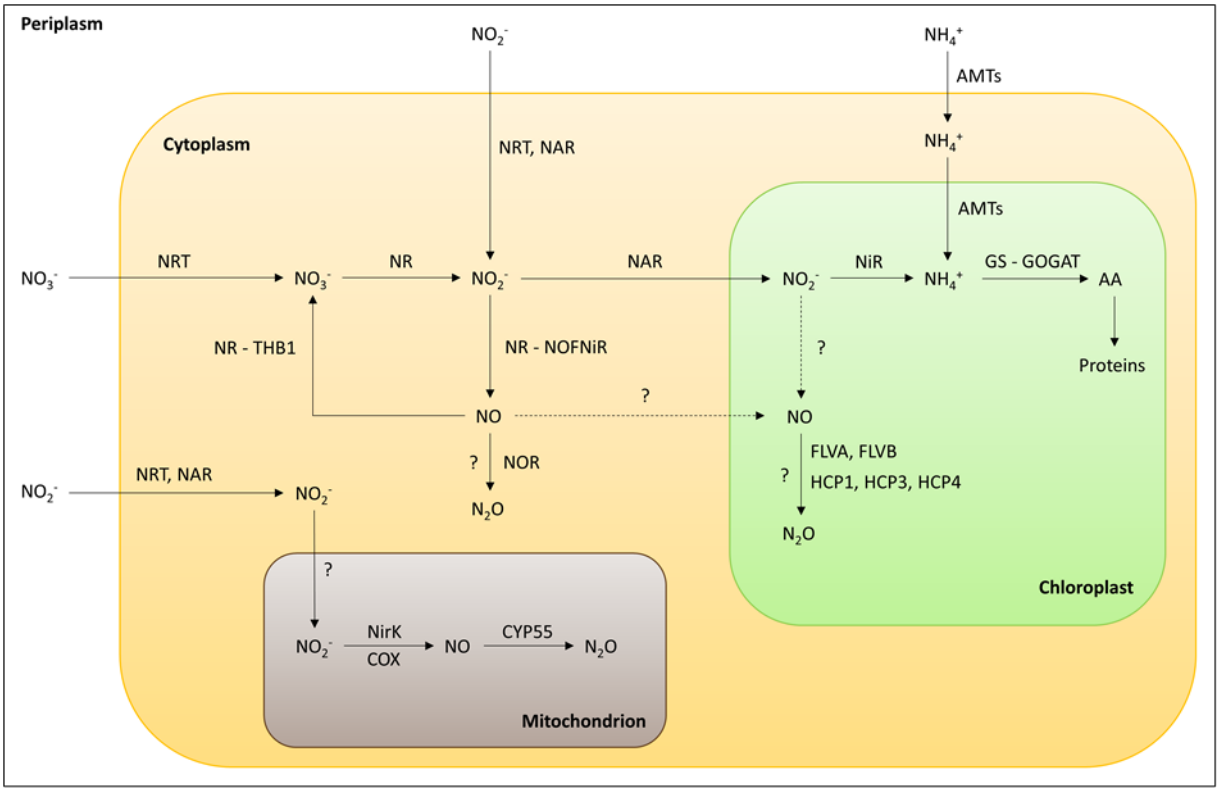

Figure 6: N_2O putative production pathways in Chlamydomonas.
Abbreviations/symbols: NH_4^+, ammonium; NO_2^-, nitrite; NO_3^-, nitrate; NO, nitric oxide; N_2O, nitrous oxide; AA, Amino acids; NRT, High-affinity nitrate transporter; NAR, Nitrite transporter; AMT, High-affinity ammonium transporter; NR, Nitrate reductase; NiR, Nitrite reductase; GS-GOGAT, Glutamate synthase - Glutamine oxoglutarate aminotransferase; NOFNiR, NO-forming nitrite reductase; THB1, Truncated hemoglobin; NirK, copper-containing nitrite reductase; COX, Cytochrome c oxidase; CYP55, Cytochrome P450 (Nitric oxide reductase); NOR, Nitric oxide reductase; FLV, Flavodiiron protein; HCP, Hybrid cluster protein.

2.2.4.1. NO synthesis

NO is an important signal molecule in plants and algae. It is also involved in nitrate assimilation and can be synthetized by the enzymes NirK and NR in *Chlamydomonas* (Sanz-Luque et al., 2015a). NR is

encoded by the gene *NIA1* in *Chlamydomonas* and is made of 2 identical subunits each containing three prosthetic groups: flavin adenine dinucleotide (FAD), b_{557} heme, and molybdenum cofactor (Sanz-Luque et al., 2015a). NR expression is repressed by NH_4^+ but induced by light and NO_3^-. NR plays a crucial role in the intracellular NO_3^-/ NO_3^- cycle as its activity changes depending on its partner protein (Figure 6): When associated with NOFNiR (NO-forming nitrite reductase), the NR-NOFNiR dual enzyme reduces NO_2^- into NO (Chamizo-Ampudia et al., 2016). In association with THB1 (Truncated Hemoglobin 1), the NR-THB1 dual enzyme catalyses NO oxidation into NO_3^- (Sanz-Luque et al., 2015b; Bellido-Pedraza et al., 2020).

NirK is not broadly conserved in eukaryotes (Kim et al., 2009) but *Chlamydomonas* harbours a gene homologous to the bacterial and fungal genes encoding the enzyme NirK involved in reducing NO_2^- into NO (Figure 7). The function of the *Chlamydomonas* enzyme, called *Cr*NiRK, has not been described yet but its presence suggests a pathway for NO synthesis from NO_2^- in the mitochondria (Figure 6). NirK is a copper-containing nitrite reductase composed of three subunits (Zumft, 1997) and NirK proteins are divided into two classes. *Cr*NIRK belongs to the class II within which all eukaryotic and some prokaryotic NirK proteins are gathered. Kim et al. (2009) suggested that eukaryotic *NirK* homologs have a common origin: the protomitochondrion[9].

[9] The ancestral bacterial endosymbiont from which all mitochondria are thought to be derived

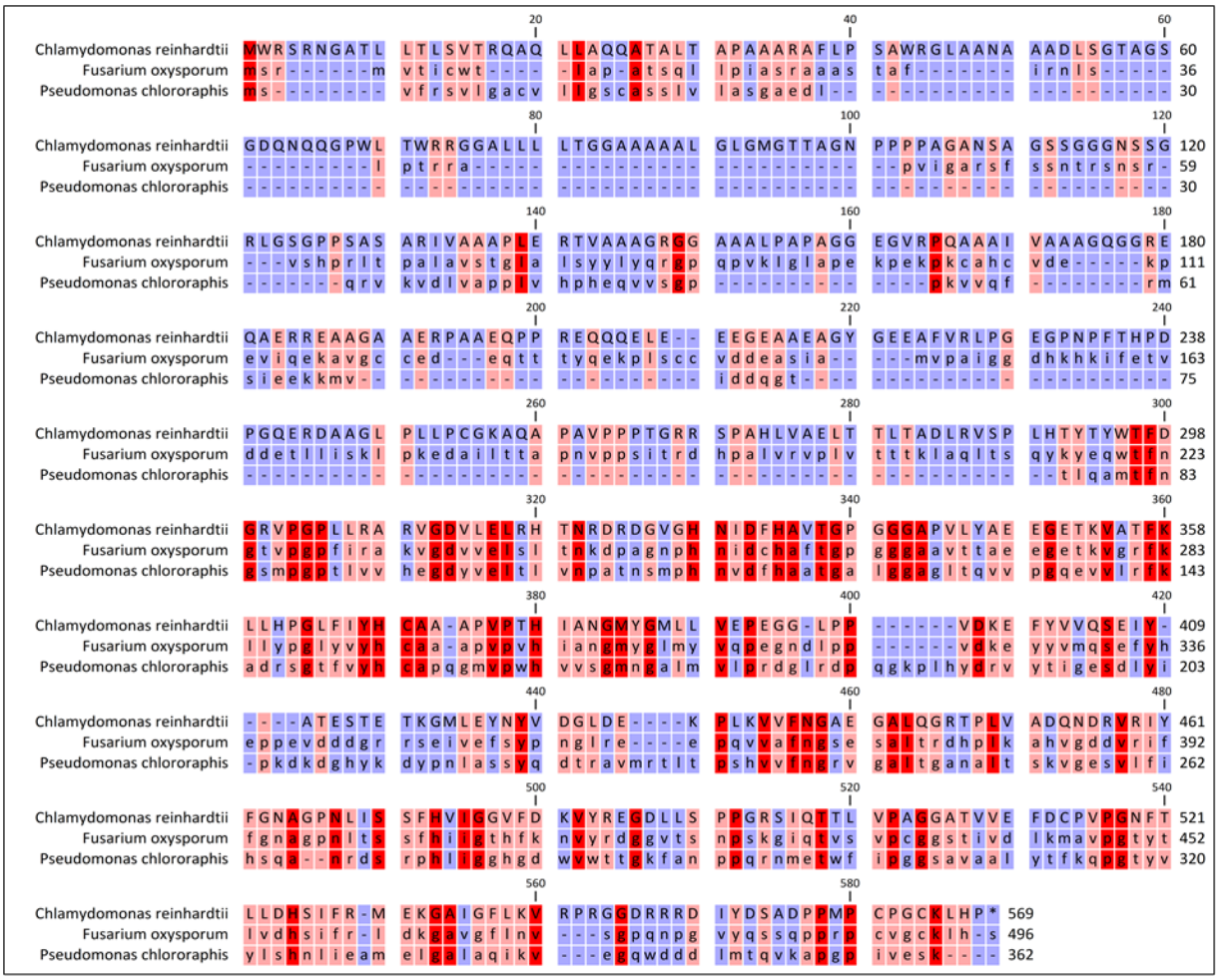

Figure 7: Peptides alignment of Nirk proteins from Chlamydomonas reinhardtii (microalga), Fusarium oxysporum (fungus) and Pseudomonas chlororaphis (bacterium) generated using the software CLC Sequence Viewer.

2.2.4.2. FLVA and FLVB

Flavodiiron proteins (FDPs) are commonly found in bacteria, archaea and many eukaryotes. Here, we focus on the class-C flavodiiron proteins which are found in photosynthetic organisms and are named FLVs (Alboresi et al., 2019). In prokaryotes, FLV2 and FLV4 are unique to β-cyanobacteria while FLV1 and FLV3 are present in all cyanobacteria (Alboresi et al., 2019). *Chlamydomonas* has two FLVs, named FLVA and FLVB, which are structurally similar to the cyanobacterial proteins. A nitric oxide and oxygen reductase activity has been reported for FLVs. In cyanobacteria, FLV1 and FLV3 have an electron sink role by reducing oxygen into water under light conditions. This reaction protects the photosystem I (PSI) during light fluctuation (Chaux et al., 2017; Jokel et al., 2015, 2018). In *Chlamydomonas*, O_2 reduction into H_2O by FLVs constitutes an alternative electron transport pathway which limits the overproduction of cell-damaging redox power and maintains ATP synthesis immediately after an increase in illumination and under constant illumination (Alboresi et al., 2019; Saroussi et al., 2019).

In *Chlamydomonas,* FLVs have recently been suggested to reduce NO into N_2O using electrons from photosynthesis under illumination (Burlacot et al., 2020). Additionally, FLVs have been reported to play a role during sulfur deprivation in *Chlamydomonas* as their activity increased when the cells were switching from aerobiosis[10] to anaerobiosis[11] to produce ATP without generating reducing power (Alboresi et al., 2019).

2.2.4.3. CYP55

Chlamydomonas harbours a gene analogous of the fungal *CYP55* gene encoding a nitric oxide reductase (NOR) and possibly localized in the mitochondria (Plouviez et al., 2017a). *CYP55* is upregulated in presence of nitrate (Gérin et al., 2010), and the use of CYP55-deficient mutants appears to indicate that CYP55 is involved in NO reduction into N_2O in the dark, as illustrated in Figure 6 (Burlacot et al., 2020; Plouviez et al., 2017a). Alternatively, Burlacot et al. (2020) proposed that CYP55 may be located in the chloroplast although reducing power can also be transferred from chloroplasts to mitochondria where mitochondrial proteins (like the alternative terminal respiratory oxidase AOX1) can help alleviate light energy excess (Kaye et al., 2019).

2.2.4.4. HCP

Chlamydomonas also possess four Hybrid Cluster Proteins (HCPs) found in a large range of prokaryote and eukaryote organisms (Almeida et al., 2006). These enzymes are metalloproteins characterized by the presence of an iron-sulfur-oxygen cluster and, while their physiological functions are still uncertain in *Chlamydomonas,* different roles have been proposed based on bacterial HCPs. In *Escherichia coli,* these proteins have a peroxidase activity (Almeida et al., 2006) and also seem to be responsible for the production of N_2O in anaerobic conditions, as shown in studies using HCP-deficient *E. coli* mutants (Wang et al., 2016). Furthermore, Van Lis et al. (2020) suggested that HCPs might exhibit a nitrate-reducing S-nitrosylase activity in *Chlamydomonas* that would catalyse NO_3^- transformation into nitrosonium (NO^+), but these authors argued that a NO-reductase role of HCP is unlikely in *Chlamydomonas*. The roles of these proteins in eukaryotic microalgae are still poorly understood and require further investigation.

[10] Growth in an environment containing oxygen.
[11] Growth in an environment devoid of oxygen.

Van Lis et al. (2020) hypothesised that *HCP* genes in *Chlamydomonas* appeared via duplication events. HCP1, 3 and 4 have been predicted to be found in chloroplasts while HCP2 was located in mitochondria. In *Chlamydomonas, HCP* transcripts were reported to be highly upregulated under dark anoxia conditions but not translated into proteins (van Lis et al., 2020). Although no physiological explanations have been formulated for this lack of translation, it could indicate that HCPs are regulated at different transcriptional and translational levels to prime cells before exposure to conditions when HCPs are required. The mRNA generated during HCPs transcription was also reported to accumulate in the presence of NO_3^- (Gérin et al., 2010).

2.2.4.5. Other mechanisms

N_2O emissions from several microalgae species have been reported in the literature (Table 3) but, to our knowledge, the molecular mechanisms involved have not been further studied for these strains. Bellido-Pedraza et al. (2020) suggested that almost 33% of microalgae contain at least one of the proteins involved in N_2O synthesis in *Chlamydomonas* (NirK, CYP55, FLVs, HCP).

Table 3: Algal species involved in N_2O emissions reported during published studies (modified from Plouviez et al. (2019a)).

Alga division	Algal species	N_2O flux	Reference
Green algae	*Chlorella vulgaris*	109 – 1480 nmole·h^{-1}·g DW^{-1}	Guieysse et al. (2013)
	Chlorella rubescens	1,200 – 2,500 nmole·h^{-1}·g DW^{-1}	Weathers (1984)
	Coelastrum sp.	560 – 1,100 nmole·h^{-1}·g DW^{-1}	Weathers (1984)
	Chlorococcum vacuolarum	150 – 290 nmole·h^{-1}·g DW^{-1}	Weathers (1984)
	Neochloris sp.	9.60 – 38,000 nmole·m^{-2}·h^{-1}	Plouviez et al. (2017b)
	Scenedesmus dimorphus	6 – 73 nmole·h^{-1}·g DW^{-1}	Bauer et al. (2016)
	Scenedesmus obliquus	0 – 1,000 nmole·h^{-1}·g DW^{-1}	Weathers (1984)
Diatoms	*Skeletonema marinoi*	0.039 – 0.31 nmole·h^{-1}·$aggregate^{-1}$	Stief et al. (2016)
	Thalassiosira weissflogii	0.087 – 0.3 nmole·L^{-1}·h^{-1}	Kamp et al. (2013)
Cyanobacteria	*Aphanocapsa 6308*	0 – 1,500 nmole·h^{-1}·g DW^{-1}	Weathers & Niedzielski (1986)
	Aphanocapsa 6714	0 – 5,700 nmole·h^{-1}·g DW^{-1}	Weathers & Niedzielski (1986)
	Nostoc sp.	0 – 1,500 nmole·h^{-1}·g DW^{-1}	Weathers & Niedzielski (1986)

To summarize the current state of the art on biological N_2O synthesis, nitrification and denitrification are the two major biological pathways involved in N_2O production. These processes have traditionally been considered to be undertaken by bacteria and archaea. However, increasing evidence suggests that other organisms, such as microalgae, might be able to carry out at least part of these processes

and be responsible for N_2O emissions from aquatic environments. The lack of knowledge on the pathways involved in microalgal N_2O synthesis could mean that current N_2O inventories are missing or misallocating significant N_2O sources. Studying algal N_2O emissions from eutrophic ecosystems is especially relevant now that the IPCC considers using a new higher EF to estimate N_2O emissions from eutrophic waters receiving N from wastewater effluents. Indeed, the ability of microalgae to synthesise N_2O combined with their ubiquity in eutrophic ecosystems suggest that microalgae play a significant role in these N_2O emissions. Besides, as wastewater effluents are commonly discharged in lakes prone to eutrophication, lakes may thus constitute potential significant N_2O sources. Finally, N_2O emissions from terrestrial plants have been reported during NO_3^- assimilation (Dean & Harper, 1986; Hakata et al., 2003; Smart & Bloom, 2001; Timilsina et al., 2020a; Timilsina et al., 2020b), which means the study of N_2O production pathways in microalgae, a higher plant ancestor, could improve our understanding of the mechanisms involved in plants.

2.3. Diversity of freshwater lakes

2.3.1. Dimension/Morphology

Freshwater lakes, rivers and reservoirs hold 0.26% of the liquid freshwater found on Earth. Freshwater lakes cover 2.7 million km^2 and hold 175,000 km^3 of water (Carpenter et al., 2011). Natural lakes are formed during events such as volcanic eruption, glacier retreat, river movement, landslides, tectonic movement, shorelines movement and the action of wind on land, and solution lakes are a specific type of natural lakes formed by dissolution and collapse of rock structures. Artificial lakes, called reservoirs or impoundments, are typically created following the damming of a river. How a lake is formed establishes the lake's morphology, especially water depth and the hydraulic retention time (HRT) of the water flowing through the lake. The depth and HRT in turn impact the biological productivity of the lake (Wetzel, 2001a) through the interactions between the water, nutrient-laden sediments, and microorganisms (Wetzel, 2001a). Generally, biological productivity increases with the HRT and the area of sediments in contact with water.

A distinction is often made between deep (> 10 m) and shallow (< 10 m) lakes in the literature: Around 40% of the volume of freshwater held in freshwater lakes is found in great lakes basins (i.e. deep) but most lakes are small and shallow (Wetzel, 2001a; Meybeck, 1995; Downing et al., 2006). Shallow lakes are characterized by the absence of sustained thermal stratification (Kar, 2013). Compared to deep lakes, shallow lakes are also characterized by a relatively low HRT, low nutrient loss to the sediments, and high sediments resuspension due to the influence of wind (Wetzel, 2001b). These characteristics lead to a high nutrient load to the aqueous phase causing shallow lakes to be more prone to eutrophication than deep lakes. As further discussed below, lakes can be classified based on different characteristics and the trophic state is often used when considering water quality (see Appendix D for further details).

2.3.2. Trophic states

Carlson (1977) developed the Trophic State Index (TSI) to facilitate communication with the public and classify lakes based on their trophic state. This index is based on the chlorophyll a concentration (Chla), the Secchi depth (SD), and the total phosphorus (TP) concentration of the lake. The Chla concentration provides an indication of the algal biomass concentration in the water and is often correlated to TP concentration when phosphorus is the limiting nutrient for algae growth (Elser et al., 2007). The Secchi depth is used to estimate water transparency by measuring the depth below which a disc of 20 cm in diameter vanishes from sight when immersed in the water. This variable is also related to the algal

biomass concentration as it defines the depth of the layer inside which photosynthesis can be performed by primary producers. In New Zealand, a similar index ranging from 0 to 7 called the Trophic Level Index (TLI) is used to better fit the lake conditions of the country as explained in Appendix E. In contrast to the TSI, the TLI includes the total nitrogen (TN) concentration in its calculations because nitrogen has also been reported to be limiting algae growth (Abell et al., 2020; White et al., 1985). The different lake trophic states according to the TLI score are described in Table 4. The trophic state of a water body can give an idea of the water quality for different water uses.

Table 4: Description of the different trophic states of a lake according to its TLI score (Lake Trophic Level Index, 2020).

Trophic states	Description	TLI Score
Microtrophic	Very low levels of nutrients and algae, the water is transparent.	0 – 2
Oligotrophic	Water is transparent, oxygen is available in all layers, the nutrient level is low, and the water is poor in phytoplankton.	2 – 3
Mesotrophic	The water has moderate levels of nutrient and algae.	3 – 4
Eutrophic	The water is less transparent, rich in nutrients and the sediments are rich in organic matter. Hypolimnial oxygen depletion and frequent algae bloom can occur during summer.	4 – 5
Supertrophic	The water is cloudy, very rich in nutrients, especially nitrogen and phosphorus, with a high risk of algae blooms.	5 – 7

2.4. Eutrophication

Eutrophication is a natural phenomenon characterized by the overgrowth of primary producers (e.g. microalgae including the prokaryotic cyanobacteria, macroalgae etc.) in an aquatic ecosystem. Over geological timescales, eutrophication can lead to the filling, and ultimately the disappearance, of the water basin. Anthropogenic activities have accelerated the rate of eutrophication due to excess N and P inputs to aquatic ecosystems leading to many environmental issues as further discussed below (Pinay et al., 2018). Natural lakes, impoundments and ponds cover more than 3% of the Earth's surface (Downing et al., 2006) and as many of 30 - 40% of these aquatic bodies are eutrophic (Yang et al., 2008). Thus, it has been estimated that 0.9 - 1.2 % of the Earth's surface is covered with eutrophic lakes, which is equivalent to 5.36 million km² or 20 times the area of New Zealand.

2.4.1. Parameters leading to eutrophication

Eutrophication is characterized by the excessive growth of primary producers. Primary producers are photosynthetic organisms using light energy to convert CO_2 into organic matter via photosynthesis. Their growth can be promoted by different parameters, as described below.

Nutrients: Eutrophication is generally linked to the excessive input of N and/or P into aquatic bodies. These nutrients can originate from point and nonpoint sources. Point sources are usually continuous and relatively easy to identify and include wastewater effluents, runoffs from waste disposal or construction sites, storm overflows and sanitary sewer outfalls. Nonpoint sources are harder to identify because of their diffuse nature and include agriculture runoffs, urban runoffs from unsewered areas, septic tank leachate, atmospheric deposition caused by fossil fuel combustion, and land activities (Carpenter et al., 1998). Carpenter et al. (1998) estimated that most of the nutrients inputs leading to eutrophication originate from nonpoint sources in the USA (*1998 National Water Quality Inventory Report to Congress*, 1998; Carpenter et al., 1998). Beusen et al. (2016) estimated that the global contribution of agriculture to N and P inputs to freshwater has increased from 19% to 51% and 35% to 56%, respectively between 1900 and 2000. As explained above, nutrient availability is higher in shallow lakes than in deep lakes, which means nutrient concentration is often non-limiting in shallow lakes. Consequently, phytoplankton growth in shallow lakes will be mainly regulated by the four factors described below (Wetzel, 2001b).

Light: Wind and water flow (i.e. turbulence) resuspend particles (e.g. silt, clay, microorganisms) that reduce light penetration in water. Thus, the growth of benthic[4] primary producers is limited to low-depth area with clear water and low turbulence (Pinay et al., 2018). In many lakes, photosynthetic activity is mainly located near the surface as the primary producers themselves shade the water column below.

Temperature: Temperature (>15°C) accelerates biological reactions and promotes microbial growth (Paerl et al., 2001). For example, Wiedner et al. (2007) observed that water temperature rise promoted the spread of the invasive tropical freshwater cyanobacterium *Cylindrospermopsis raciborskii* in lakes Langer See and Melangsee (Germany). Temperature also reduces the solubility of dissolved oxygen in the water, thereby increasing the symptoms of eutrophication during spring and summer, when temperatures are higher (Pinay et al., 2018).

Water retention and water mixing: A longer HRT means that phytoplankton suspended in water stays longer in the aquatic ecosystem before being flushed out. Thus, a longer HRT can favour nutrient exchanges between phytoplankton, sediments, and water as more time is given for these exchanges

to occur (Pinay et al., 2018). The occurrence of algal blooms can also increase in poorly mixed water and during sustained water stratification. When turbulence becomes excessive, phytoplankton growth is reduced or even stopped due to cells damage caused by shear. Turbulence can also disrupt interactions between bacteria and cyanobacteria (Paerl et al., 2001). Thermal stratification increases the risk of algal bloom because phytoplankton can be trapped in a nutrient-rich layer near the surface, where light is also available (Pinay et al., 2018).

O_2 concentration: internal eutrophication occurs when lakes become hypoxic. In aerobic conditions, the decomposition of organic matter involves redox reactions where oxygen is usually the final electron acceptor. However, in hypoxic or anoxic conditions, chemical species such as nitrate, iron (hydr)oxides and sulphate can act as final electron acceptors. As P often forms stable complexes with iron (hydr)oxides in sediments, the reduction of iron (hydr)oxides can cause the release of P to the water (Smolders et al., 2006).

2.4.2. Environmental, societal, and political implications of eutrophication

The proliferation of microalgae has critical ecological implications: Blooms increase water turbidity and, consequently, attenuate light penetration in the water column. This leads to a switch to respiratory processes leading to hypoxia/anoxia, which is accelerated by the decay of algal organic matter. Low oxygen concentration in turn impacts the biological community structure and, thus, the trophic network of the ecosystems (Glibert, 2017). For example, Roberts et al. (2009) noticed that the seasonal hypolimnetic hypoxia of Lake Erie (USA) impacted yellow perch distribution and foraging. Eutrophication can therefore have profound and long-term effects on an ecosystem (Pinay et al., 2018).

Eutrophication has also several economic and political implications. The proliferation of microalgae, and especially toxic microalgae as harmful algal bloom (HAB), can indeed impact the economy via restrictions for fisheries, industry intake, and recreational water use. HABs are a threat to human and animal health due to the toxins released by microalgae such as *Microcystis,* as it happened in Lake Rotoiti (New Zealand) in 2004 (Wood et al., 2006). When a drinking water supply is affected, the local authorities can advise the population not to drink water from the tap for safety reasons, as it happened in Toledo (Ohio) during summer 2014 (Jetoo et al., 2015).

Most governments have adopted regulations that seek to prevent or mitigate eutrophication, such as the international Convention for the Protection of the Marine Environment of the North-East Atlantic in 1998 (*Convention for the protection of the marine environment of the North-East Atlantic*, 1998)

and the National Policy Statement for Freshwater Management in New Zealand in 2020 (*National Policy Statement for Freshwater Management*, 2020). Increasing public awareness is also putting pressure on regional councils in charge of water management (Pham et al., 2019).

2.4.3. Water quality control

Monitoring lakes is of the upmost importance to ensure the safety of water users. Besides, lakes are typically found in the upstream part of the freshwater – marine continuum, meaning that an excess of nutrients or an algal bloom in a lake can propagate to rivers, estuaries and marine environments located downstream (Aubriot et al., 2020). Monitoring reservoirs is also important to efficiently manage drinking water treatment.

2.4.3.1. Parameters monitored

In recreational water, monitoring is mostly done during the swimming season (e.g. from November/December to February/March in New Zealand). Several parameters are regularly measured to evaluate water quality such as the water pH, turbidity, and the presence of pathogens (Almeida et al., 2012). The guidelines and standards used to assess microbiological water quality depend on the water use and are country-specific (see Table 5 and Table 6 for New Zealand guidelines).

The World Health Organization (WHO) recommends to monitor the presence of HAB in freshwater by i) assessing the carrying capacity of the ecosystem for cyanobacteria; ii) visually inspecting sites to detect any scum development; and iii) quantifying the algal biomass to evaluate the bloom risk (Bartram & Rees, 1999). The first step involves the quantification of the concentration of TP and TN (as these support algae growth) and, sometimes, the chemical oxygen demand (COD) (Almeida et al., 2012). The second step involves the measurement of the Secchi depth and the search for any color irregularity and scums on the water surface. Biomass quantification is done either via chlorophyll a concentration measurement or cell count under the microscope.

Considerable research efforts have aimed at developing models that predict the occurrence of algae blooms and simulate the effects of physical (light, temperature, turbulence, HRT), chemical (nutrients), biological (microbial interactions), and ecological (food network) parameters on water quality (Janssen et al., 2019). These models could be used later in this project to make predictions on water quality and, thus, algae proliferation in water bodies.

Table 5: New Zealand guidelines for cyanobacteria in recreational fresh waters (Wood et al., 2009)

Mode	Trigger level for potentially toxic cyanobacteria		Management response
	Benthic	Planktonic	
Surveillance	Up to 20% coverage of potentially toxigenic cyanobacteria attached to substrate.	Total cyanobacteria cell count < 500 cells/mL; or The biovolume equivalent for the combined total of all cyanobacteria does not exceed 0.5 mm^3/L.	Routine monitoring.
Alert	20–50% coverage of potentially toxigenic cyanobacteria attached to substrate.	Biovolume equivalent of potentially toxic cyanobacteria between 0.5 and 1.8 mm^3/L; or Total biovolume of all cyanobacterial material between 0.5 and 10 mm^3/L.	Notify public, erect signs with information on appearance of mats and potential risks. Increase monitoring and consider toxin testing.
Action	Greater than 50% coverage of potentially toxigenic cyanobacteria attached to substrate; or Up to 50% where potentially toxigenic cyanobacteria are visibly detaching from the substrate, accumulating as scums along the river's edge or becoming exposed on the river's edge as the river level drops.	More than 12 µg/L total microcystins; or Biovolume equivalent greeter than 1.8 mm^3/L of potentially toxic cyanobacteria; or Total biovolume of all cyanobacterial material greeter than 10 mm^3/L; or Cyanobacterial scums consistently present.	Notify public, erect signs with information on appearance of mats and potential risks, notify the public of potential risk to health. Increase monitoring and consider toxin testing.

Table 6: Microbiological water quality guidelines for marine and freshwater recreational areas (New Zealand & Ministry for the Environment, 2003)

Mode	Trigger level for faecal indicator bacteria (per 100 mL)		Management response
	Beach	River/Lake	
Surveillance	Enterococci ≤ 140	*E. coli* ≤ 260	Routine monitoring
Alert	140 < Enterococci < 280	260 < *E. coli* < 550	Increase monitoring and investigation of contaminant source
Action	Enterococci > 280	*E. coli*> 550	Public warnings if required, increased monitoring and investigation of contaminant source

2.4.3.2. Limiting nutrients in lakes

Phosphorus availability can limit microalgae growth in lakes. Consequently, it has been suggested that many algal blooms can be prevented by reducing phosphate inputs. Schindler et al. (2008) studied the trophic state of oligotrophic Lake 227 (Canada) under 3 different nutrient loading regimes: 1) N and P supply with a high N:P ratio (around 12) for 6 years; 2) N and P supply with a low N:P ratio (around 5) for 15 years; and 3) No N supply for 16 years without changing the P supply. When both N and P were supplied during the first 21 years of the study, the lake became highly eutrophic. When only P was supplied for the 16 following years, no significant change in the biomass of phytoplankton was observed. These results suggested that N input had little impact on eutrophication and that, therefore, P input was always limiting algae growth. The authors then extrapolated their results to freshwater

lakes and law-salinity estuaries under the assumption that N shortage is mitigated by N_2 fixation from cyanobacteria, causing P to remain the limiting nutrient. The same authors also pointed out the lack of whole-ecosystem data to attempt to prevent eutrophication by reducing N input (Schindler & Hecky, 2009). While this study is one of the most cited in the literature and has been a reference for years for mitigation strategies in regulatory frameworks, the "P limitation paradigm" has been challenged by several authors (Glibert, 2017; Howarth & Marino, 2006; Paerl, 2009; Conley et al., 2009; Xu et al., 2010; Paerl et al., 2011, 2016; Smith et al., 2016) who argued that only controlling P supply is not always sufficient to prevent HABs, and that a dual control of P and N must instead be established:

- Despite efforts to reduce P inputs, Lake Taihu (China) still regularly undergoes HABs during summer. Bioassays performed on lake samples showed phytoplankton growth[12] was limited by N input during summer (Paerl et al., 2011; Xu et al., 2010). As toxin production by non N_2-fixing cyanobacteria (e.g. *Microcystis*) can be promoted by N supply (Paerl et al., 2016), reducing N input could have the double effect of decreasing the occurrence of blooms and reducing the hazard associated with HABs.
- P was shown to not be the limiting nutrient in tropical lakes in the study of Sterner (2008).
- The claim that N_2 fixers can alleviate N paucity has been strongly contested because N_2 fixation is an anaerobic process that can only be performed by certain species under oxia when the water is stratified. Also, N_2 fixation is seasonal and unlikely to supply enough N for algal growth (Paerl, 2009). As *Microcystis* have the capacity to move through the water column and, therefore, consume P directly at the sediment layer and bloom at the surface, reducing P loading might not be enough to prevent algae growth in lakes that accumulate P in sediments.
- Controlling only one nutrient can change the nutrient stoichiometry of the water, which can lead to undesirable effects on the biogeochemical cycles and algal biodiversity (Glibert, 2017) as observed in the San Francisco Estuary (USA) and in Lake Taihu in China (Glibert et al., 2011; Glibert et al., 2014).

As noted above, Schindler et al. (2008) extrapolated their results on the impact of P control to all freshwater lakes and law-salinity estuaries. However, these extrapolations have been challenged because of the differences in chemical and physical characteristics of the ecosystems compared. Indeed, N is lost via ammonification and denitrification along the freshwater to marine continuum. As P is not lost, the P:N ratio increases, which causes N limitation to increase along the continuum (Paerl,

[12] especially the non-N_2 fixing cyanobacteria *Microcystis* spp often responsible for HABs

2009). Another important consequence of only limiting P input in lakes is that all the N that could have been consumed (at high P input) at the start of the freshwater - marine continuum, will now be consumed in estuarine and coastal waters, increasing eutrophication at the end of the freshwater - marine continuum. There is therefore a need to evaluate the full impact of nutrient management on the entire continuum (Conley et al., 2009; Paerl, 2009). This issue will not be further discussed as it is outside the scope of this study.

2.4.3.3. Preventing/mitigating eutrophication in lakes

Strategies to fight HABs and their symptoms include artificial oxygenation to reduce hypoxia or the addition of chemicals (e.g. lime, aluminium salts, ferrous sulfates or ferric chloride) to precipitate P (Pinay et al., 2018). The use of algicides can be efficient in small lakes not used for recreational activities. In small lakes, disturbing the thermal stratification by mechanical mixing or air bubbling can also be an alternative (Paerl et al., 2001). Biomanipulation via, e.g., the removal of planktivorous fishes to promote the growth of zooplankton can also be efficient to reduce eutrophication and restore biodiversity (Mehner et al., 2002; Pinay et al., 2018). Regardless the successes of these strategies, the main approach to prevent or mitigate eutrophication in lakes remains to reduce P and/or N inputs. This involves the identification of any point-source pollution that would directly increase the nutrient loads to the water. Nonpoint-source pollution, especially those from agricultural runoffs, needs to be well monitored and, when possible, reduced. However, Duarte et al. (2009) argued that a reduction of nutrient input does not necessarily lead to a cessation of eutrophication because of a delay in algal production response due to internal nutrient storage/recycling within the ecosystem (e.g. polyphosphate, (Plouviez et al., 2021)). Consequently, the objectives behind mitigation strategies should be carefully selected and a return to a historical lower trophic state might not be feasible in case of significant baseline shifts (e.g. increased CO_2 concentration, global warming, sea level rise, habitat loss etc.). To better understand how N and P impact algae growth and, by extension, algal N_2O synthesis, it is therefore important to understand N and P metabolism in algae.

2.5. Algae cell biology

Algae are a polyphyletic group including photosynthetic prokaryotes and eukaryotes (Table 7). This section focuses on the N and P metabolisms of microalgae (unicellular algae) because these nutrients trigger algae blooms and their combined impact on algal N_2O synthesis is still unknown.

Table 7 : Main features of recognized algae divisions (simplified from Borowitzka (2012)).

Alga division	Cell forms	Habitats	Selected genera
Prokaryotic algae			
Cyanophyta (Cyanobacteria), 2 classes: 'blue-green algae' and 'prochlorophytes'	Unicellular, filaments and colonial	Freshwater, marine and terrestrial	*Microcystis, Spirulina, Prochloron*
Eukaryotic algae			
Glaucophyta (Glaucophytes)	Unicellular, flagellates	Freshwater	*Cyanophora*
Rhodophyta 'red algae', 2 classes	Unicellular, filamentous or thalloid	Marine and freshwater	*Bangia, Ceramium*
Cryptophyta	Mainly unicellular, one filamentous genus, flagellates	Marine and freshwater	*Cryptomonas*
Heterokontophyta, 7 classes			
- Class Phaeophyceae 'brown algae'	Multicellular	Marine	*Ascophyllum*
- Class Bacillariophyceae 'diatoms'	Unicellular and colonial	Freshwater and marine	*Navicula*
Dynophyta 'dinoflagellates'	Predominately unicellular, some coccoid filamentous, flagellates	Mainly marine	*Alexandrium*
Haptophyta, 2 classes	Unicellular, flagellates	Mainly marine	*Emiliana*
Euglenophyta 'euglenoids'	Unicellular with single flagellum	Mainly freshwater	*Euglena*
Chlorophyta 'green algae', 10 classes			
- Class Chlorophyceae	Coccoid, unicellular, or colonial flagellates, multicellular or multinucleate filaments.	Mainly freshwater	*Chlamydomonas, Chlorella*

2.5.1. Nitrogen metabolism

2.5.1.1. N cycle

N is an essential macronutrient often limiting primary production in aquatic environments (Elser et al., 2007). N is especially needed for the synthesis of amino acids, which are the building blocks of proteins, and nucleotides, which compose nucleic acids (Deoxyribonucleic Acid, DNA; Ribonucleic Acid, RNA). In aquatic environments, N can be found as dissolved inorganics (NH_4^+, NO_3^-, NO_2^-), particulate organic matter, and dissolved gases (N_2, N_2O). Although the main N reservoir is the atmosphere, N_2 can only be assimilated by specialized N_2-fixing bacteria and archaea. These microorganisms convert N_2 into inorganic N (NH_3) in a process that can generate the inorganic N used by other organisms (Kuypers et al., 2018). The industrial production of N fertilizer from N_2 via the Haber-Bosch process has considerably increased the flux of N from the atmosphere to the biosphere (Erisman et al., 2008) (Figure 8).

The total nitrogen (TN) concentration in freshwater lakes is highly variable and can range from 0.1 to 8 $mg \cdot L^{-1}$ during summer in temperate lakes (Guildford & Hecky, 2000; Jin et al., 2005; McCauley et al., 1989). A high variability is also reported in tropical-subtropical lakes (Huszar et al., 2006). Seasonal

fluctuation in dissolved N concentration can be observed due to changes in the microorganisms populations involved in ammonification, nitrification and denitrification processes in lakes (Domogalla et al., 1926).

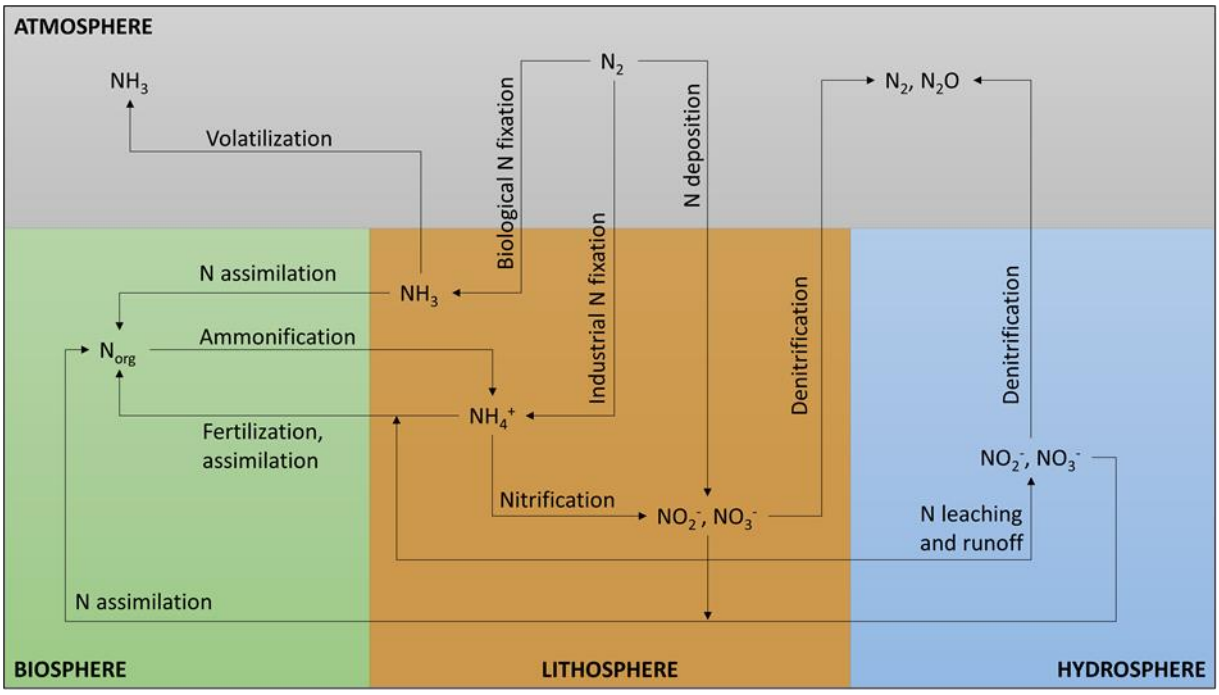

Figure 8: Nitrogen biogeochemical cycle.
Abbreviations/symbols: NH_3, ammonia; NH_4^+, ammonium; NO_2^-, nitrite; NO_3^-, nitrate; N_2, dinitrogen; N_2O, nitrous oxide; N_{org}, organic nitrogen.

2.5.1.2. Microalgae N metabolism

Microalgae can assimilate different forms of N from the environment. For example, *Chlamydomonas* species can assimilate both inorganic (e.g. NO_2^-, NO_3^-, NH_4^+) and organic (e.g. urea, purines, L-amino acids) N (Calatrava, 2018). Ammonium and nitrate are the two main sources of N for algae, with a preference for NH_4^+ in *Chlamydomonas* and other microalgae that repress NO_3^- assimilation in the presence of ammonium (Gonzalez-Ballester et al., 2004). *Chlamydomonas* genome encodes eight ammonium transporters (AMTs) with different regulation patterns (Gonzalez-Ballester et al., 2004). Some of these transporters are induced under deprivation, suggesting a putative role as high-affinity transporters, whereas other transporters are mainly expressed in N-rich media, indicating a possible role as low-affinity transporters (Gonzalez-Ballester et al., 2004). Once inside the cell, ammonium is transported into the chloroplast where it is incorporated into amino acids through the GS-GOGAT cycle (**G**lutamine **S**ynthetase – **G**utamine **O**xo**G**lutarate **A**mino **T**ransferase).

When NH_4^+ supply is insufficient to sustain growth, microalgae can also assimilate NO_3^-. NO_3^- first enters the cell cytosol via NO_3^- transporters (NRTs and NARs) where it is then reduced into NO_2^- by

nitrate reductase (NR). Cytosolic NO_2^- is transported to the chloroplast where it is further reduced into NH_4^+ and NH_4^+ is then incorporated into amino acids as described above. Under specific conditions, some NO_2^- can be reduced into NO and this NO is then either reduced into N_2O or converted to NO_3^- by truncated haemoglobins (e.g. THB1) associated to reductases (e.g. NR) (see Figure 6 in section 2.2) (Bellido-Pedraza et al., 2020; Calatrava et al., 2017; Kuypers et al., 2018).

2.5.2. Phosphorus metabolism

2.5.2.1. P cycle

P is an essential macronutrient used in the synthesis of genetic material (DNA, RNA) and intracellular energy carriers in cells (Adenosine Triphosphate, ATP). It is also involved in cellular signalling through phosphorylation and it is a constituent of lipids in cells membranes (Ruttenberg, 2014).

In nature, P is mainly stored as orthophosphate (PO_4^{3-}) in rock sediments. Weathering causes the introduction of this mineral P in soils and rivers from where it is transported to lakes and oceans. There, P can be adsorbed to mineral matter and/or integrated in organic matter until it finally builds up at the bottom of water basins and forms sedimentary rocks under the action of pressure. Over time, the uplifting and exposure of the rock formation reintroduces P into the environment (Figure 9) (Ruttenberg, 2014). The flux of PO_4^{3-} to the biosphere has however recently increased due to P mining and use as P fertilizers. The spreading of these fertilizers leads to P run-offs and leaching to lakes, streams and coastal waters, which in turns can cause eutrophication as explained in section 2.4 (Ciais et al., 2013).

Microalgae can assimilate P under the form of dissolved inorganic PO_4^{3-} (Ruttenberg, 2014) but phytoplankton can synthetise alkaline phosphatases also enabling the use of dissolved organic PO_4^{3-} (Li et al., 2015). Following desorption from sediments or leaching from crops fertilization, particulate P can be a source of dissolved P, especially in the case of internal eutrophication as explained in section 2.4 (Paerl et al., 2001).

The total P (TP) concentration is usually around 100 $\mu g \cdot L^{-1}$ in eutrophic lakes (Canfield & Bachmann, 1981; Jacoby et al., 1982; Jin et al., 2005), which is more than twice the typical concentration found in mesotrophic lakes (Jin et al., 2005; Schindler, 1977). The soluble reactive P concentration found in mesotrophic and eutrophic lakes, which is comprised of PO_4^{3-}, polyphosphate (PolyP) and organic P compounds, ranges from 1 – 80 $\mu g \cdot L^{-1}$ and varies seasonally (Jin et al., 2005; Zhu et al., 2007). Different PO_4^{3-} concentrations can be reported with different analysis methods and chromatographic analyses, which are usually used for routine analyses, have been reported to overestimate PO_4^{3-} concentration

(Hudson et al., 2000; Rigler, 1966). Using radiobioassays, Hudson et al. (2000) measured the PO_4^{3-} concentrations in 53 North American lakes with different trophic status and reported PO_4^{3-} at picomolar concentrations (0.003 and 0.084 $\mu g \cdot L^{-1}$).

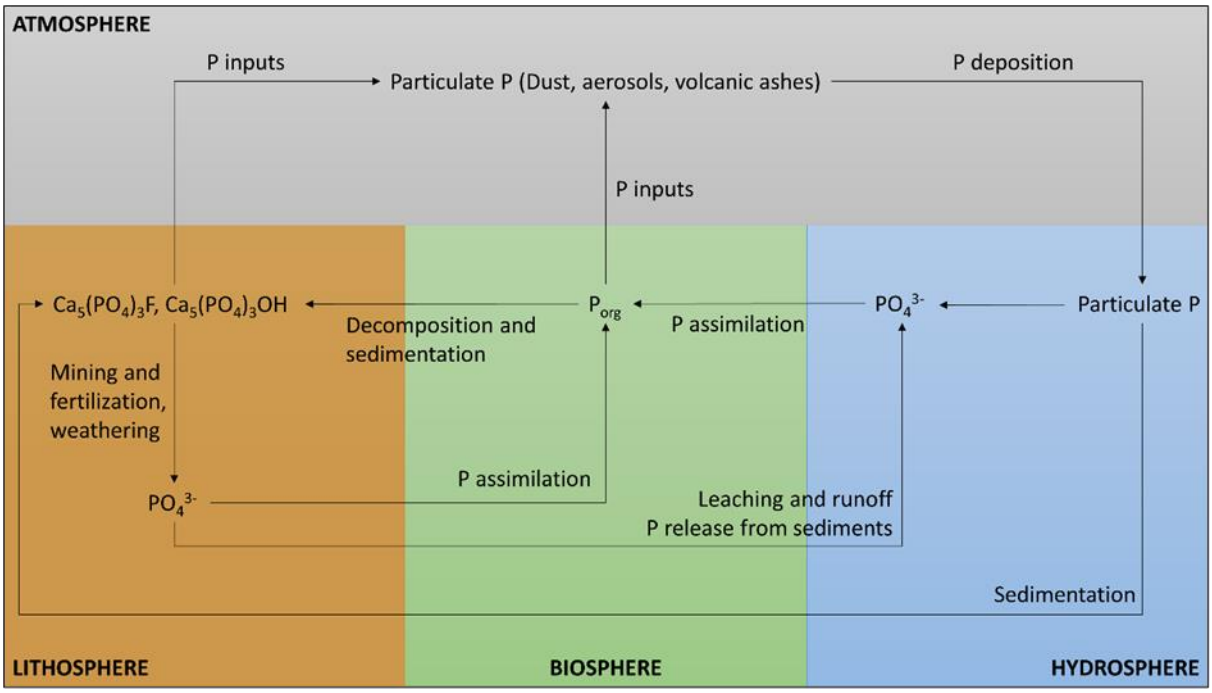

Figure 9: Phosphorus biogeochemical cycle.
Abbreviations/symbols: $Ca_5(PO_4)_3F$, fluorapatite; $Ca_5(PO_4)_3OH$, hydroxyapatite; PO_4^{3-}, phosphate; P_{org}, organic P.

2.5.2.2. Microalgae P metabolism

As discussed earlier, P is one of the main nutrients limiting microalgae growth in aquatic ecosystems (Kalff, 1983; Nalewajko & Murphy, 2001; Elser et al., 2007; Abell et al., 2010). Wang et al. (2020) identified 25 putative PHTs (phosphate transporters) in *Chlamydomonas* which are divided into four subfamilies: CrPTA, crPTB, CrPHT3 and CrPHT4. Using four algorithms predicting subcellular localization of the CrPHTs via the detection of targeting motifs in their N-terminal peptides, the PTA family proteins were predicted to be located in the plasma membrane. PTB proteins were thus predicted to target either the secretory pathway or the plasma membrane; PHT3 was predicted to target to mitochondria; and most of the PHT4 family proteins were predicted to be located in chloroplasts. Wang et al. (2020) also identified two transport systems that could be represented by PTB proteins in green algae Na^+/PO_4^{3-} symporters (Reid et al., 2000), and H^+/PO_4^{3-} symporters (Cauthier & Turpin, 1994) that could correspond to PTA proteins. Following the qRT-PCR (quantitative Reverse Transcription-Polymerase Chain Reaction) analyses of CrPHT genes under P depletion, these authors suggested that PTA1 and PTA3 may be low-affinity PHTs while CrPTB2, CrPTB3, CrPTB4, CrPTB5, CrPTB6, CrPTB7, and CrPTB8 were candidates for high-affinity PHTs. Wykoff et al. (1999) suggested

that CrPHT genes may be regulated by the transcription factor *CrPSR1* (phosphate starvation regulator 1) in P-limited medium. Another putative low-affinity transporter encoded by *PTC1* and similar to the yeast *Saccharomyces cerevisiae* has been identified in *Chlamydomonas* but its location and function have not yet been confirmed (Grossman & Aksoy, 2015).

Microalgae can accumulate PO_4^{3-} under the form of polyphosphates (polyPs), which are chains of tens to hundreds of PO_4^{3-} groups linked by anhydrous orthophosphate bonds (P-O-P). ATP is the PO_4^{3-} donor in this reaction and, therefore, polyP synthesis requires energy (Sanz-Luque et al., 2020a; Smith, 1966). In prokaryotes, polyP is synthetised by the enzyme PolyP kinase (PPK) encoded by the gene *ppk* and regulated by the *pho* regulon (Santos-Beneit, 2015; Sanz-Luque et al., 2020a). In cyanobacteria, polyP is degraded by polyphosphatase encoded by the gene *ppx* (Sanz-Luque et al., 2020a). In most eukaryotes, polyP is synthetised by the VTC4 subunit of the Vacuolar Transporter Chaperone (VTC) complex, a transmembrane protein that also translocates the growing polyP into the vacuole where they are stored (Plouviez et al., 2021; Sanz-Luque et al., 2020a). The regulation of polyP synthesis is linked to the inositol phosphate metabolism in eukaryotes (Plouviez et al., 2021; Sanz-Luque et al., 2020a). If phytoplankton is cultivated in a medium deprived of P and is then transferred to a P-rich medium, cells synthesize and accumulate polyP via a mechanism called overcompensation uptake (Aitchison & Butt, 1973). Algae also store polyP without previous deprivation and this accumulation is called luxury uptake (Powell et al., 2011). Luxury uptake has been suggested to be a protective process to prevent future P limitations in ecological niches where strong fluctuations in P availability may occur (Sanz-Luque et al., 2020a). PolyP accumulation has also been observed in microalgae during nutrient (sulfur and nitrogen) deprivation (Sanz-Luque et al., 2020a; 2020b).

To conclude, N metabolism is responsible for N_2O synthesis and N is often limiting primary producers' growth. Thus, it would be tempting to only link algal N_2O emission to N supply in eutrophic ecosystems, as currently done by the IPCC for bacterial N_2O production. However, P is also a critical nutrient often limiting microalgae growth in natural ecosystems. The fluctuations in the availability/supply of N and P together with the algae's capacity to manage their internal N and P cellular pools have a significant ecological impact on the eutrophication of lakes. As P supply can support eutrophication (sometimes synergistically with N supply), simplifying N_2O emissions as only an output of N supply may lead to erroneous prediction of N_2O emissions from eutrophic ecosystems. Understanding the impact of P supply on algal N_2O emissions is, thus, critical to estimate these N_2O emissions accurately.

2.6. Conclusions from the literature review

The IPCC currently estimates N_2O emissions from aquatic environments by assuming that bacterial nitrification and denitrification processes leading to N_2O synthesis are linearly related to the N inputs received by the aquatic body assessed. Thus, the N_2O emissions are calculated as a fraction of the N flux reaching the aquatic body defined as emission factors (EFs). However, this 'bacteria-centric' assumption that N_2O emissions only depends on the N input received by an aquatic system may be challenged by the ability of algae to bloom in response to P inputs (or combined N and P inputs) and produce N_2O. Eutrophic aquatic environments are already known to be a higher source of N_2O than mesotrophic environments and the IPCC recently acknowledged this fact by increasing the Tier 3 factor used to compute indirect N_2O emissions from wastewater discharge into eutrophic and nutrient-impacted aquatic environments from 0.005 to 0.019 kg N_2O-N emitted per kg of N received. However, the higher emissions from eutrophic environment are only considered at a Tier 3 level for wastewater discharge and is not considered in the case of indirect N_2O emissions from eutrophic aquatic ecosystems receiving N inputs from agricultural N leaching and runoff. In addition, microalgae are still not considered as the potential cause of these N_2O emissions and therefore, emissions are still only computed from N inputs. Thus, we hypothesize that microalgae could significantly contribute to N_2O emissions in eutrophic aquatic environments and that it may be necessary to also consider P input to accurately estimate N_2O emissions from these systems.

Understanding the exact source of the N_2O emissions in eutrophic aquatic environments is critical for two main reasons:

1. 'microalgal-N_2O' emissions can vary greatly and are affected by very specific parameters (e.g. light). This means that past monitoring based on 'bacteria-centric' methodologies may have missed the contribution of microalgal metabolism.

2. while 'bacterial N_2O' is typically directly related to the N load received by a specific environment, 'microalgal-N_2O activity' could be boosted by P (phosphorus supply) triggering eutrophication, meaning that N_2O emissions from affected ecosystems could no longer be based solely on N-loadings (as currently done).

3. Research plan

3.1. Research objectives

This thesis seeks to answer the following questions: 1) Do eutrophic ecosystems generate significant N_2O emissions and what are the conditions potentially triggering these emissions? 2) Do microalgae contribute to these emissions and, if they do, what are the main chemical (especially the combination of nitrogen and phosphorous supply), environmental (e.g. light, temperature) and biological (associated microorganisms) parameters influencing microalgal N_2O emissions in eutrophic ecosystems? To reduce the scope of the research, emphasis will be given to the study of eutrophic lakes as a 'worse-case environment' due to occurrence of 'hyper-eutrophication' in New Zealand lakes receiving agricultural runoffs (e.g. Lake Horowhenua), the high potential relevance on these ecosystems (Plouviez et al., 2019a), and practical reasons (site accessibility, health and safety, existing monitoring data). We nevertheless expect that the knowledge generated will be of broader relevance as it may, for example, suggests that other eutrophic environments should be better studied. Besides, this thesis may also improve the accuracy of natural N_2O emissions estimates, which is important for policy. Finally, the work will ultimately improve our ability to monitor, predict, and mitigate N_2O emissions from aquatic environments.

To answer the questions listed above, it will be necessary to achieve two main objectives divided in 5 sub-objectives (Figure 10):

Objective 1: Assess the magnitude of N_2O emissions from eutrophic lakes

Sub-objective 1.1: Field monitoring

N_2O emissions from selected New Zealand eutrophic and control 'clean' lakes will be determined using a bespoke high-temporal resolution monitoring strategy. This activity will also provide lake microcosms for laboratory assays and inform on possible correlations between water quality and N_2O emissions to guide the design of sub-objectives 1.2 and 2.1.

Sub-objective 1.2: Assess the impact of N and P supply in laboratory assays

The influence of nitrogen and phosphate supply regimes on microalgal N_2O synthesis will be evaluated using lake microcosms as well as representative model microalgae species *C. reinhardtii*. This will inform us on the potential impact of N and P supply on N_2O emissions, better inform field monitoring (Sub-objective 1.1) and provide evidence as of the biological origin of these emissions (Objective 2).

These laboratory assays will also provide sample to study the impact of these nutrients on the expression of key genes associated with N_2O synthesis in *C. reinhardtii* for sub-objective 2.2.

Sub-objective 1.3: Assess the potential global significance N_2O emissions from eutrophic lakes

Together, sub-objectives 1.1 and 1.2 will provide the experimental data needed to establish the potential of N_2O emissions from eutrophic lakes from water quality data.

Objective 2: Assess the significance of microalgal N_2O synthesis in eutrophic lakes

Sub-objective 2.1: Assess the role of microalgae synthesis on N_2O emissions in laboratory assays

Lake microcosms assays using specific inhibitors as well as assays using knockout and/or knockdown mutants of *C. reinhardtii* will be performed to evaluate the microalgal contribution to N_2O emissions at a laboratory scale. This preliminary activity will enable us to develop the methods that will then be used to 'isolate' algal production from artificial consortia (with focus on *C. reinhardtii*) and 'natural' lake microcosms. The results from these tests will also inform us on the genes that are more likely to be expressed in field samples (Sub-objective 2.2).

Sub-objective 2.2: Confirm the expression of key genes in selected field samples

Following the identification of key enzymes and molecules involved in the algal N_2O production pathway (from past and ongoing research with our collaborators), quantitative PCR analyses will be performed on selected field samples to confirm if algae are indeed actively synthesising N_2O in the monitored ecosystems and/or if other microorganisms significantly contribute to these emissions (Sub-objective 2.1). Using the data gathered before, the potential global environmental significance of N_2O emissions from eutrophic lakes will be assessed and a "refine" methodology to estimate N_2O emissions from eutrophic lakes and guidance for mitigation strategies will be proposed (Sub-objective 1.3).

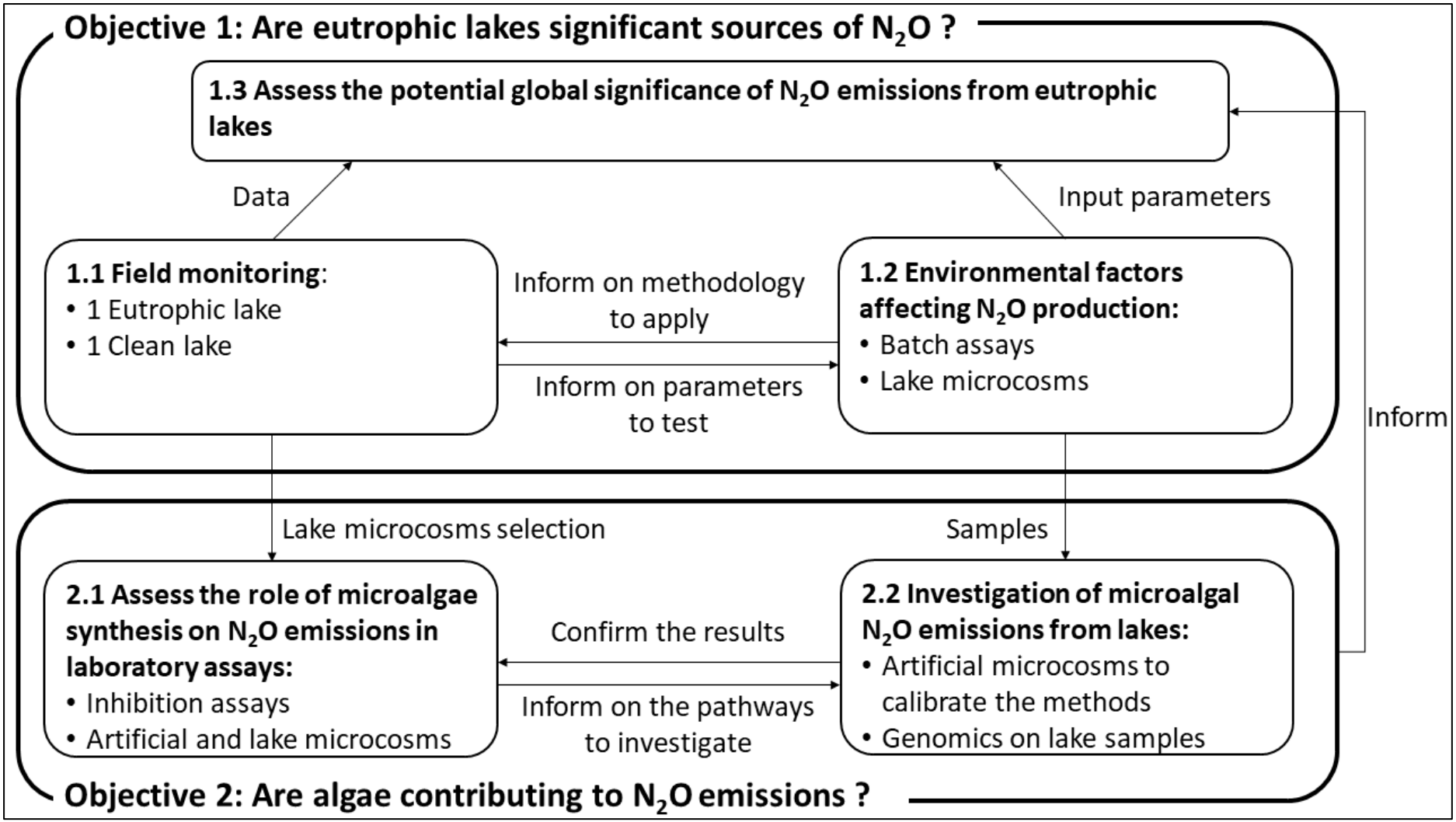

Figure 10: Thesis framework.

3.2. Adaptation to the circumstance of the COVID-19 pandemic

Due to the COVID-19 pandemic, I had to start my research in the Department of Biochemistry and Molecular Biology at Cordoba University in Spain for 7 months, where I was hosted by my co-supervisor Dr Emanuel Sanz-Luque. Consequently, I started by conducting experiments on axenic *Chlamydomonas* cultures to train in the laboratory and acquire a better understanding of the molecular pathways involved in N_2O production under varying conditions and obtain preliminary data (Sub-objective 2.1). The analytical equipment (G2508 gas concentration analyser (PICARRO)) used to measure N_2O emissions being the property of another department (Department of Botanic, Plant Ecology and Physiology), access to this equipment was limited. I was also able to conduct my literature review while I was there. Once in New Zealand, I started working on building more field knowledge (Sub-objective 1.1) and the influence of environmental factors on microalgal N_2O emissions (Sub-objective 1.2). However, due to unforeseen circumstances, the PhD thesis was converted into a Master thesis.

Consequently, I could not extend the monitoring and laboratory activities initially scheduled. The following thesis therefore focuses on the presentation of approximately 5 months of field monitoring data with one associated bioassay done in New Zealand, as well as the laboratory data on axenic *Chlamydomonas* cultures done in Spain. While this limited dataset limits my ability to conclude if microalgae indeed contribute to the N_2O emissions from eutrophic aquatic ecosystems, it provides evidence on how to best direct future research as discussed below.

4. Proposed methodology

4.1. Significance of N_2O emissions from eutrophic ecosystems

4.1.1. Assessing the magnitude of N_2O emissions from New Zealand eutrophic lakes

Sampling sites (n= 2) were selected depending on their trophic state history using data from Horizons Regional Council (https://www.lawa.org.nz) and the Ministry for the Environment (https://data.mfe.govt.nz), the literature (Wood et al., 2017), and the availability of local water quality and weather data. Accessibility and distance to Palmerston North (Appendix F) were also taken into consideration for health and safety reasons. Lake Horowhenua had thus been selected to be our main case study as it was supertrophic, only 48 km away from Massey University, easy to access, and most importantly, because we were working in collaboration with members of the Lake Horowhenua Trust (members of the Trust have worked hard to develop restauration solutions for the lake and they were interested in the proposed work). Five easily accessible potential back-up locations for field sampling were identified (oligotrophic: Lake Tarawera; mesotrophic: Lake Rotoiti (Tasman), Lake Okareka; eutrophic: Lake Horowhenua, Lake Wiritoa, Lake Dudding). Lake Horowhenua was sampled once per week during Autumn and Winter (when algae growth is typically low) and at least twice per week during Spring and Summer (when algae growth is typically the fastest). The Turitea drinking water reservoir has been selected to be our “clean” control lake as it is considered mesotrophic, only 8 km away from Massey University and easy to access. Access to the reservoir has been allowed by Palmerston North City Council. For each lake, pH, dissolved oxygen and conductivity were measured on site and chlorophyll a, nutrients (e.g. nitrite, nitrate, phosphate) and total suspended solid were quantified from water sampled and N_2O was quantified using the head space method (Table 8). Methods for routine sampling and analysis were tested during Winter using samples from Lake Horowhenua.

Table 8: Rationale behind the selected parameters to monitor.

Parameter	Rationale	Reference
pH	Influence biological N_2O synthesis by influencing enzymatic activity. N_2O solubility is also influenced by pH.	Section 2.2
Dissolved oxygen		Section 2.2, Appendix C
Water temperature	Impact N_2O solubility and biological reactions.	Paerl et al. (2001)
Conductivity	Impact the nutrients form (ions concentration of the water) and thus inform on nutrient availability which impacts the water trophic state.	García-Lledó et al. (2011)
Chlorophyll a	Proxy for algae biomass concentration which impacts the water trophic state and was shown to be positively correlated to N_2O emissions	Bartram & Rees (1999), DelSontro et al. (2018)
Total suspended solid	Information on water turbidity which impacts the water trophic state and light availability.	Almeida et al. (2012)
Nutrient concentration	Support algal growth, evaluation of the trophic state.	Almeida et al. (2012)
Radiant energy	Influence enzymatic activity and was shown to influence N_2O emissions.	Plouviez et al. (2017b)
Wind speed	Influence the average transfer velocity of N_2O.	Miao et al. (2020)

This field monitoring enabled us to gather data regarding the water quality of the lakes and their N_2O emissions. These data will be used to establish correlations between the nutrient load of the lake and the N_2O emissions in future study. They will also inform us on what are the important parameters to look for during further laboratory work (Sub-objective 1.2). These data will also be used in future study to understand what inputs (e.g. TN concentration, temperature) could be needed to model N_2O emissions (Sub-objective 1.3).

4.1.2. Identification of environmental factors affecting N_2O production

Chlamydomonas reinhardtii wild type (WT) and mutants were cultivated in batch assays to determine how environmental parameters influence N_2O synthesis. Because parameters influencing microalgae growth have been extensively investigated (Carpenter et al., 1998; Smith et al., 1999; Pinay et al., 2018), this first task was achieved by testing varying nutrient (N and P) concentrations, nutrition modes (mixotrophic[13] or autotrophic[14]) and light conditions. Once the triggers and their thresholds are determined, the experiments will be extended to selected lake samples (microcosms) and seek to systematically evaluate the impact of P load under various conditions known to cause/repress N_2O

[13] Combination of two different modes of nutrition to acquire carbon by microorganisms: photosynthesis for inorganic carbon (CO_2) fixation and use of organic sources.
[14] Assimilation of inorganic carbon via photosynthesis.

synthesis during future work. These experiments also provided samples to perform qPCR to study the impact of N and P supply on the expression of key genes involved in N_2O synthesis.

Overall, these laboratory assays partially enabled us to understand and demonstrate the interactions between P and N supply on N_2O emissions. Further research is still needed to achieve this Sub-objective. These data informed us on the parameters to consider and monitor during our field work (Sub-objective 1.1). If needed, this information will also serve to establish how P supply should be considered to estimate N_2O emissions (Sub-objective 1.3).

4.1.3. Determination of the potential global environmental significance of N_2O emission from eutrophic lakes

Based on the data obtained during the previous tasks, future work will aim at determining the key parameters (e.g light, nutrients) needed to estimate N_2O emissions from lakes. Using the field data and new knowledge, and especially if future study demonstrate microalgae are playing an important role in these emissions (Sub-objectives 2.1 and 2.2), a specific methodology for N_2O emissions from eutrophic lakes will be proposed. This method will finally be applied during further study to estimate the global significance of N_2O emissions from eutrophic lakes and explore how these new tools and data could guide new strategy for monitoring and mitigation.

4.2. Microalgal contribution to N_2O emissions from eutrophic lakes

4.2.1. Evaluation of the microalgal contribution to N_2O emissions in the lab

The key pathways and parameters influencing algal N_2O synthesis were partially confirmed using *Chlamydomonas* parent mutants' strains as positive and negative controls to calibrate the methods for further work. New candidate proteins involved in the N_2O synthesis pathways were also investigated using specific *Chlamydomonas* mutants and chemical inhibitors. It is important to note that due to the need to express a strong N_2O synthesis in these assays, the nutrient concentrations tested may be irrelevantly high in comparison to the concentrations found in natural lakes. This means that the N_2O emissions rates reported should not be directly extrapolated to estimate field conditions without extensive verification. Negative controls (i.e. killed cells or sterile media supplied with NO_2^-) were used to confirm that N_2O is biologically produced by the microalgae and not via abiotic reactions.

To identify the 'microalgal contribution' to N_2O emissions within diverse microcosms, N_2O emissions from artificial algal-bacterial microcosms and selected lake samples will be tested during future work

under a range of conditions selected to enhance or repress a specific activity (e.g. light vs darkness, anoxia vs hyperoxia etc). This will also include the testing of various substrate and inhibitor, which will be challenging given the similarities in the biological pathways involved (see Section 2.2). Wild type *Chlamydomonas* and knockout mutants unable to produce N_2O will therefore be cultured with various N_2O-producing model bacteria (e.g. the nitrifier *Nitrosomonas europaea* (Arp et al., 2003)). The comparison of the N_2O production between the microcosms with WT and mutants and between pure and mixed culture will make it possible to quantify the contribution of algae to N_2O emissions while also assessing the potential ecological interaction effects between these organisms (e.g. are algal and bacterial N_2O activities complementary or competitive?). Batch assays will also investigate the effect of different inhibitors on N_2O emissions from algal-bacterial artificial co-cultures. Methods using specific inhibitors which could be then applied to real lake samples will thus be developed.

Overall, this second objective will provide new fundamental knowledge on the direct and/or indirect role of microalgae in N_2O emissions from eutrophic ecosystems and inform us on the N_2O synthesis pathways that should be investigated during the field work (Sub-objective 2.2). The biological origins of N_2O emissions will thus be identified and these emissions will be quantified more accurately (Sub-objective 1.3) during future work.

4.2.2. Investigation of microalgal N_2O emissions from lakes

To evaluate the microalgal contribution to N_2O emissions from lakes, qPCR will be used during future research to estimate the relative abundance of N_2O-specific bacterial (*nirS, nirK, Nos*), archaeal (*AmoA*), fungal (*p450nor*) and algal (*NR, Cyp55 and potentially FLVs*) genes over reference genes (e.g. 16S rRNA, ITS and 18S rRNA) in selected samples (Table 9). This work will aim at identifying the microbial community present in our samples and identifying their potential biochemical functions.

Table 9: Molecular biology principles

Method	Principle	Critical point to consider	Reference
qPCR	Measure the amount of PCR products (i.e. specific genes) in a DNA sample detected by fluorescence using a DNA binding dye as it accumulates during PCR cycles.	Long process Selection of controls Requires optimization (DNA extraction)	Smith & Osborn, 2009

To circumvent the inherent limitations potentially occurring when dealing with environmental DNA[15] (eDNA) (Buxton et al., 2017; Goldberg et al., 2016; Taberlet et al., 2018) and/or RNA (Ritalahti et al., 2010), guidelines recently developed by an international expert panel will be followed during future work (Goldberg et al., 2016). In order to design the eDNA study, a pilot study should be conducted first using pure *Chlamydomonas* cultures and artifical microcosms to assess the suitability of the methods for water collection, sample preservation, extraction, and analysis.

While the evidence obtained during this work is necessary to identify the microorganisms present in our samples, it is not sufficient to discriminate the organisms responsible for N_2O emissions in complex microcosms. This is why these data will be complemented with specific inhibition assays (Sub-objective 2.1) to target the putative microorganisms producing N_2O.

[15] Complex mixture of genomic DNA from many different organisms found in an environmental sample such as water or soil (Taberlet et al., 2018).

5. Material and methods

5.1. Lake sampling

In this work, the water quality and the N_2O concentration of the samples were quantified to determine the magnitude of N_2O emissions and gather data to study the interaction between selected parameters (e.g. N and P load) and N_2O emissions as described in section 4.1.1 (Sub-objective 1.1).

Lakes monitoring for GHGs have increased in the last decades. Various methods have been used to measure N_2O emissions as further described in Table 10 and Table 11 below.

Table 10: Methods for sampling to measure N_2O emissions from water bodies.

Sampling technique	Principle	Advantages	Limits	Reference
Floating chamber	N_2O flux is calculated by measuring the gaseous concentration of N_2O in a closed chamber floating at the surface of the water	Easy to deploy, cheap, suitable for large area (chamber size up to 150 m^3)	Causes disturbance such as shading, water turbulence	Stow et al. (2005), Rapson & Dacres (2014), Wang et al. (2020)
Headspace	Dissolved N_2O concentration is estimated by measuring the gaseous concentration of N_2O in an airtight container headspace assuming the dissolved N_2O concentration in the aqueous phase is in equilibrium with the gas phase	Easy, non-disturbing, cheap	Sampling intensive to estimate the N_2O flux	Butler & Elkins, (1991), Mengis, (1997), Reay et al. (2003)
Micrometeorological techniques	N_2O flux is measured from a large area based on N_2O measurements from a gas sensor and meteorological data (e.g. wind speed, temperature)	Non-disturbing, suitable for large area (1 – 10 km^2)	Expensive and require fast and sensitive gas analyzers	Rapson & Dacres (2014)

The headspace sampling technique has been selected for our study because this method is easy to deploy, cheap and, contrary to floating chamber, this technique does not cause disturbance such as shading. This is critical for the study of algal N_2O emissions because algae N_2O synthesis was shown to be influenced by light (Plouviez et al., 2017b).

Table 11: Methods for analysis of N_2O in gas and liquid samples, simplified from Rapson & Dacres (2014).

Analytical technique		Sensitivity	Advantages	Limits
Chromatography	Gas chromatography equipped with an electron capture detector (ECD)	Limit of detection: 30 ppb Precision: 0.18–0.4 ppb	Low operational cost, widely used	Non-continuous measurements, standard needs to be run every 3 samples, long run time
Optical	Fourier-transform infrared spectroscopy (FTIR)	Limit of detection: <1 ppb Precision: 0.03-0.1 ppb	Continuous, portable	High capital costs
	Laser absorption spectroscopy: Lead Salt Lasers	Precision: <1 ppb	Rapid and highly sensitive, low interference from other trace gases	High capital and operational costs (e.g. require cryogenic cooling)
	Laser absorption spectroscopy: Quantum Cascade Lasers (QCLs)	Precision: 0.05 ppb	Fast, portable	High capital costs
Amperometric	Microsensor	Limit of detection: 22 ppb	Low capital costs, portable	Sensor drift over long-term use, fragile

The chromatographic analysis method has been selected because our laboratory has extensive experience using this technique which is cheap, easy to maintain and to operate (Hamilton & Lewis, 2006).

Superficial water samples of 500 mL were taken weekly at 5 m and 15 m from the edge of lake Horowhenua and immediately put on ice in darkness to preserve the chlorophyll. For N_2O quantification, 6 mL of water samples were injected in triplicates using 12 mL vials (Labco Exetainer® 12ml Vial, Lampeter, UK) previously flushed with dinitrogen gas as described by Plouviez et al. (2019b). 200 µL of zinc chloride (50% w/v) were added to the vials to inhibit the metabolism of the present organisms (Kamp et al., 2013). Two aquatic environments were selected for this research:

Lake Horowhenua, the largest natural lake in the Manawatū-Whanganui region, was selected as our main case study. It is located at 2 km west of Levin and 7 km east of the coast of the Tasman Sea (Latitude: 40° 36′ 36.301′′ S; Longitude: 175° 15′ 19.718′ E). The lake is a polymictic aeolian shallow lake measuring 304 ha with a maximum depth of 2 m and considered supertrophic. The lake used to receive the treated sewage waters from Levin, which participated in its nutrients' enrichment. Access to the lake was kindly allowed by Jonathan Procter who is in close collaboration with the Lake Horowhenua Trust.

The Turitea drinking water reservoir was selected as a control "clean" lake. This is an artificial lake formed following the damming of the Turitea stream and located at 8 km from Massey University. The reservoir measures 12 ha with a maximum depth of 10 m and is considered mesotrophic. It constitutes the main water supply of Palmerston North which is why access to the reservoir is restricted. Access to the reservoir was kindly allowed by Steve Langevad who was the Water Treatment Supervisor from Palmerston North City Council.

5.2. Strains selection and maintenance

5.2.1. Strains used

The model unicellular green alga *Chlamydomonas reinhardtii* was selected to study N_2O production pathways because this microorganism has already been extensively studied, its genome has been sequenced (https://phytozome.jgi.doe.gov), there are numerous molecular techniques optimized for this organism to create mutants, and mutants libraries are readily available (relevant strain have already been selected and tested (Table 12)). All strains were maintained on a sterilised solid Tris-Acetate-Phosphate (TAP) medium containing 16 $g \cdot L^{-1}$ of agar.

Table 12: Strains used in that study.

Strain	Genetic background	Gene common name	Notes	Source
M3	nii1$^-$	NiR (Cre09.g410950)	Originate from the cross between G1 and 04-1	Navarro et al., 2000
CC-4533 (CMJ030)	Wild type (cw15, mt$^-$)	cw15	Originate from the cross between D66+ and 4A-. It cannot grow in nitrate.	Zhang et al., 2014
LMJ.RY0402.052321	cw15, flvb$^-$, mt$^-$	FLVB (Cre16.g691800)	Background strain: CC-4533	Li et al., 2019
LMJ.RY0402.177695	cw15, cyp55$^-$, mt$^-$	CYP55 (Cre01.g007950)	Background strain: CC-4533	Li et al., 2019
6145c	Wild type		CC-2895 mt -: derivative of Ruth Sager's strain 6145 (see CC-1691)	Chlamycollection.org
CC-1691	Wild type		mt- equivalent to Sager's basic wild type strain (see CC-1690). It has the wild type alleles at the NIT1 and NIT2 loci and can grow on nitrate. Phenotype: yellow in the dark.	Chlamycollection.org
CC-1690 mt + (21gr)	Wild type		Sager's basic wild type strain. It has the wild type alleles at the NIT1 and NIT2 loci and should be green in the dark.	Chlamycollection.org

5.2.2. Microalgae cultivation

The protocols for *Chlamydomonas* culture and maintenance are well established (Harris, 2009). An E-flask of 100 mL filled with 40 mL of buffered TAP medium was inoculated with axenic cultures of the chosen strain. The cultures were then incubated for 2 days under continuous agitation (100 rpm), constant illumination (54 µmol photons·m^{-2}·s^{-1}) and a temperature of 24°C. The cultures were then transferred into a 1 L E-flask to which buffered TAP medium was added up to 400 mL and the cultures were then incubated in the same conditions as the inoculum culture for 2 days. The cultures were then refreshed daily and used as the inoculum culture for the experiments for a maximum of 5 days.

5.3. Batch assays

During these assays, the N_2O production of the cultures were quantified to determine the impact of environmental factors (e.g. N and P supply) on microalgal N_2O emissions as described in section 4.1.2 (Sub-objective 1.2).

As described by Harris (2009), axenic *Chlamydomonas* cultures were previously grown in buffered TAP medium under light in a 1 L E-flask. For experiments in High Salt Medium (HSM) or minimal medium (MM), cells were induced for 6 h in the chosen medium: around 200 mL of cells in exponential phase were taken and put in 50 mL sterile falcon tubes to be centrifuged for 3 minutes at 1,200 x g. The supernatant was discarded, and the cells were then cleaned twice with the final medium. The cells were then grown in this medium under light for 6 h in a 1 L E-flask.

The cultures were diluted at the beginning of each experiments to obtain a chlorophyll concentration of 10 µg·mL^{-1} (equivalent to 0.25 g DCW·L^{-1}, see Appendix G). To get N-free algae culture, the cells growing in ammonium were cleaned twice with N-free medium.

5.3.1. Experimental set-up in Spain

For N_2O quantification, cells were resuspended in 250 mL of medium supplied with nitrite and put in a 1 L Duran bottle. N_2O emissions were measured from the cultures for 24 h using cavity ring-down spectroscopy (CRDS) in the G2508 gas concentration analyser (PICARRO).

Note: This equipment belongs to another Department of the University of Cordoba (Department of Botanic, Plant Ecology and Physiology) where it is used to measure N_2O emissions from agricultural soils. Therefore, its coupling to bottles containing axenic cultures of *Chlamydomonas* required optimization.

During the experiment, cells were grown in an incubator (Versatile Environmental Test Chamber MLR-351, Sanyo) at 25°C with continuous agitation at 100 rpm (Rotamax 120, Heidolph, Schwabach, Germany) and under continuous illumination using fluorescent lamps and a light irradiance around 130 µmol photons·m^{-2}·s^{-1}. A summary of the conditions tested can be found in Table 13.

Table 13: Summary of the conditions tested in the batch assays conducted in Spain.

Strain	Medium	Conditions	Nutrient addition	Number of replicates
M3	HSM without nitrogen	Light	10 mM NO_2^-	3
	TAP medium without nitrogen	Light	0.01 mM NO_2^-	1
			0.1 mM NO_2^-	1
6145c	HSM without nitrogen	Light	10 mM NO_2^-	3
				1
	HSM without nitrogen + DCMU	Light	10 mM NO_2^-	4
	HSM without nitrogen + DMSO	Light	10 mM NO_2	1
cc-4533 (CMJ030)	HSM without nitrogen	Light	10 mM NO_2^-	8
				1
052321 (*flvb* mutant)	HSM without nitrogen	Light	10 mM NO_2^-	3
177695 (*cyp55* mutant)	HSM without nitrogen	Light	10 mM NO_2^-	3
21gr	HSM without nitrogen	Light	10 mM NO_2^-	1
No cells	HSM without nitrogen	Light		1

5.3.2. Experimental set-up in New Zealand

While the actual conditions changed depending on the purpose of the experiment, the following protocol developed by Plouviez et al. (2017a) was used to study N_2O synthesis in pure cultures: Cells were resuspended at 10 µg chlorophyll·mL^{-1} in the treatment medium supplied with the chosen concentration of nitrite and put in serum flasks sealed with rubber septa. Cells were incubated in a Multitrom (Infors HT) at 25°C under continuous agitation and either under continuous illumination (120 µmol photons·m^{-2}·s^{-1}) or in the dark. Cell concentration was assessed by measuring both chlorophyll concentration and the dry cell weight.

5.4. Inhibition assays

In these inhibition assays, the N_2O production from axenic microalgal culture and lake samples were quantified to evaluate the contribution of each type of microorganisms (especially bacteria and algae) as described in section 4.2.1 (Sub-objective 2.1).

The experiments were performed using the protocol described above but DCMU (3-(3,4-dichlorophenyl)-1,1-dimethylurea), an inhibitor of the photosystem II, was added to the medium after 15 h to investigate the contribution of the photosynthetic transport electron chain to N_2O production. Other inhibitors (especially bacterial inhibitors) were planned to be used in similar assays conducted with artificial microcosms and lake samples (Table 14). Experiments will be conducted during future work to check the inhibition efficiency and the specificity of each inhibitor on the microbial cultures. The use of microalgae mutants that are not producing N_2O will be preferred to the use of microalgae inhibitors because inhibitors are not always specific and could thus affect the growth of other organisms.

Table 14: Inhibition assays.
[1] essential posttranslational modification of the translation initiation factor 5A that stimulates ribosomal peptidyltransferase in archaea.
[2] Cell damage due to the oxidation of proteins, lipids, and DNA.

Organism	Inhibitor	Main effect	Reference
Fungi	Carbendazim Thiophanate-methyl Benomyl	Inhibit the microtubule polymerization, disrupting cell division	Mahan et al. (2005)
Archaea	N1-guanyl-1, 7- diaminoheptane	Hypusination[1] inhibitor	Jansson et al. (2000)
Bacteria	Penicillin G potassium Streptomycin sulfate	Affects bacterial cell wall synthesis Affects bacterial ribosomes	Guieysse et al. (2013)
Microalgae	Hydrogen peroxide (cyanobacteria) Copper sulfate	Induce a severe oxidative stress[2] Interacts with proteins, nucleic acids and metabolites	Hanson & Stefan (1984) Zhou et al. (2020)

5.5. Primers design and optimisation

In selected experiments, the expression of key genes was quantified to determine the impact of test conditions (e.g. P supply, presence of inhibitor as described in sections 4.1.2 and 4.2.1) on N_2O synthesis regulation (Sub-objectives 1.2 and 2.1) .

The expression of genes encoding putative proteins involved in N_2O production in *Chlamydomonas* (*FLVA*, *FLVB*, *NIRK*, *HCP1*, *HCP2*, *HCP3*, *HCP4 and CYP55)* was measured using qPCR. Primers for these genes have been designed using QuantPrime online tool (https://quantprime.mpimp-golm.mpg.de/) and the efficiency of the PCR using these primers was checked (Table 15).

Based on the kinetics of N_2O production from the axenic *Chlamydomonas* cultures, gene expression was measured at 6 different times (0 h, 1 h, 3 h, 6 h, 17 h and 24 h) in M3 and CMJ030 cultures in HSM-N (control) and HSM-N + 10 mM NO_2^- (treatment).

Table 15: Sequence of the designed primers.
** This gene had been designed and the efficiency of the PCR had been checked before this study.*

Gene	Transcript identifier	Primer forward sequence	Primer forward length	Primer forward Tm	Primer forward GC	Amplicon length
FLVA 2	Cre12.g531900.t1.1	ACTGCAGGCAATCGCTCCTTTG	22	64,315	54,545	62
FLVB	Cre16.g691800.t1.1	GCATGAGCGATGTGGTCATGTG	22	62,788	54,545	130
*CYP55**	Cre01.g007950.t1.1	GATGGCCGCTTCTCCAAGGTC	21			
HCP1	Cre09.g391450.t1.1	TCGCATTCCAGAAGAGCACTGG	22	63,232	54,545	119
HCP2	Cre02.g129550.t1.1	CGAATGGCATACGGTGACTAAGGC	24	64,186	54,167	68
HCP3	Cre02.g129500.t1.1	CGCGATGCCTCTATTAAGGCCAAG	24	64,254	54,167	72
HCP4	Cre09.g391650.t1.1	CAATAAAGAGGCAGGCGCGTAG	22	62,28	54,545	80
NIRK	Cre08.g360550.t1.1	AGGAGTTCTACGTGGTGCAGTC	22	62,33	54,545	70

Lyophilised primers (obtained from Invitrogen) were resuspended in ultrapure distilled water at 100 µM. Primer stock solution was prepared by mixing forward and reverse primers at a final concentration of 10 µM of each in distilled water.

Primer efficiency was assessed by PCR, using a serial dilution of a mix of cDNA previously obtained as template. The log copy number (or log dilution times) against the number of PCR cycle (Ct) was plotted to calculate the slope, which was used to calculate the efficiency according to the following Equation 1:

$$Efficiency\ (\%) = 10^{-\frac{1}{slope}} - 1 \qquad \text{Equation 1}$$

Briefly, the PCR mix was prepared with 0.8 µM of primer stock solution, cDNA, ultrapure water and 10 µL of reagent (SsoFast™ EvaGreen® Supermix); for a total of 20 µL per well as indicated in the manufacturer's instructions. Two replicates per dilution were run. As internal control for relative quantification (housekeeping genes) we used *CBLP*, *UBI* or *ACT1* genes, whose expressions remained unchanged upon different nitrogen sources. The PCR protocol entailed one cycle at 96 °C for 2 minutes followed by 40 cycles of 10 seconds at 96°C and 30 seconds at 60°C.
For relative quantification we used the ΔCt method to compare the level of changes in gene expression. To do so, the fold difference was used and calculated using Equation 2.

$$Fold\ difference = 2^{(\overline{\mathrm{Ct}}_{\text{reference gene}} - \overline{\mathrm{Ct}}_{\text{gene of interest}})} \qquad \text{Equation 2}$$

Where the fold difference (ΔCt) is the relative expression of the gene of interest compared to the reference gene; $\overline{\mathrm{Ct}}_{\text{gene of interest}}$ is the mean threshold cycle value of the two replicates of the gene of interest and $\overline{\mathrm{Ct}}_{\text{reference gene}}$ is the mean threshold cycle value of the two replicates of the reference gene.

5.6. Analysis

5.6.1. Algal cell quantification

5.6.1.1. Chlorophyll measurement

The total chlorophyll concentration in pure cultures and artificial microcosms was determined by spectrophotometry (DU® 800 UV/Visible Spectrophotometer, Beckman Coulter, Brea, California, USA) from triplicate samples as described by Wintermans & De Mots (1965). A sample of 750 µL of culture was transferred in a 1.5 mL Eppendorf and centrifuged for 75 seconds at 12,000 x g. The supernatant was discarded and 750 µL of ethanol was added to the pellet. The mixture was then mixed using a vortexer and centrifuged for 75 seconds at 12,000 x g. The absorption of the supernatant at 649 nm (A_{649}) and 665 nm (A_{665}) was then measured and the total chlorophyll concentration was calculated by Equation 3:

$$\text{Chlorophyll concentration } (\mu g \cdot mL^{-1}) = 6.1 \times A_{665} + 20.04 \times A_{649} \quad \text{Equation 3}$$

In lake samples, the total chlorophyll concentration was also determined using Equation 3 but to extract chlorophyll, a known volume was first filtered by vacuum suction through a 2.7 µm glass microfiber filter (47 mm, MicroScience MS GC filters, Australia) in triplicates as described by Papista et al. (2002) and Sartory & Grobbelaar (1984). The filters were then immersed in a solution of ethanol at 90% and left in a cold room at 4°C for 24 h. The extract was then centrifuged for 2 min at 3,000 x g and the supernatant was transferred to a 15 mL clean Falcon tube. The colour of the pellet was checked to be sure that no visible chlorophyll remained in it. The optical density of the clarified extract at 649 nm (chlorophyll b) and 665 nm (chlorophyll a) was then measured using a UV-1800 spectrophotometer (Shimadzu, Japan).

5.6.1.2. Dry cell weight and Total suspended solid

As described by Béchet et al. (2015), 2.7 µm glass microfiber filters (47 mm, MicroScience MS GC filters, Australia) previously dried at 105°C for 24 h were weighted, then a known volume of cells were filtered and rinsed with the same volume of distilled water to remove any dissolved salts. The filters were then dried for 1h at 105°C and weighted. The mass concentration was then calculated using Equation 4:

$$Mass\ concentration = \frac{Weight_{Filter\ with\ cells} - Weight_{Filter}}{Volume\ of\ cells} \quad \text{Equation 4}$$

5.6.1.3. Cell counting

As described by Guillard & Sieracki (2005), the number of cells in the culture were counted using a Bürker pattern counting chamber. For this purpose, a sample of 10 µL of culture were put on the counting chamber and photos of the cells inside 12 squares diagonally arranged on the counting chamber using the microscope's magnification 40X were taken. The cells inside each square and on the upper and right edges were counted. The Mesurim software was used to count the cells when the number of cells per square exceeded 10. The final concentration was calculated using Equation 5:

$$Cell\ concentration = \frac{N_{cells}}{N_{squares} \times V} \times DF \qquad \text{Equation 5}$$

Where N_{cells} is the total number of cells counted, $N_{squares}$ is the number of squares in which cells were counted, V is the liquid volume in one square and DF is the dilution factor.

5.6.1.4. Optical density

The culture optical density was determined from triplicates by measuring the absorbance at 683 nm and 750 nm of 1 mL of culture. The blank was previously done using the same medium as the culture.

5.6.2. pH, Dissolved oxygen, and Conductivity

The dissolved oxygen (DO) concentration, conductivity and pH were monitored using a multimeter (Orion™ Star A329, Thermo Scientific) equipped with the relevant probes (Orion™ 4-Electrode Conductivity Cell, Thermo Scientific; Orion™ RDO™ Dissolved Oxygen Probe, Thermo Scientific; Orion™ ROSS Ultra™ Low Maintenance Triode™ pH/ATC electrode, Thermo Scientific). The calibration of the probes was checked before each sampling.

5.6.3. Nutrients

The concentrations of PO_4^{3-}, NO_2^-, NO_3^- and NH_3 in filtered samples (0.2 µm, Sartorius Minisart filters, Gottingen, Germany) were quantified using a Lachat Quikchem 8500 Series 2 Flow Injection Analysis System (Lachat Instruments, Loveland, Colorado, USA). In the case that the equipment broke down,

well-described methods that we have experience with were used to measure NO_2^- i.e. the substrate of N_2O [16].

A Dionex ICS-2000 Ion Chromatograph (Dionex Corporation, Sunnyvale, California, USA) that was used to measure the concentration of chloride and sulphate in filtered samples could also be used as back-up to measure concentrations of NO_3^-, NO_2^- and PO_4^{3-}.

The dissolved carbon and dissolved nitrogen concentrations will be determined using a Total Organic Carbon Analyser (TOC-L, Shimadzu, Japan) during future work.

5.6.4. Light intensity

The light intensity in the incubators was measured using a PAR meter taking the mean of 9 measurements inside the incubators. During lake sampling, meteorological data (solar irradiance, air temperature, wind velocity and direction, and relative humidity) were taken from a close weather station (Levin Electronic Weather Station, 1.2 km away from the Horowhenua lake; Palmerston North Electronic Weather Station, 7.4 km away from the Turitea reservoir). The data from the National Climate Database collected by the National Institute of Water and Atmospheric Research (NIWA) and MetService were accessed using the CliFlo web system (https://cliflo.niwa.co.nz/). An example of how data can be extracted and used is provided by the CliFlo web system.

5.6.5. N_2O measurement

N_2O was quantified using either a G2508 gas concentration analyser (Spain) or an ECD-gas chromatograph (New Zealand).

G2508 analyser: The N_2O concentration in the gas phase of a Duran bottle in which the algal culture was growing was continuously (at least one measure per minute) measured by Cavity Ring-Down Spectroscopy (G2508 Gas Concentration Analyzer (Picarro), Santa Clara, California, USA). The accuracy

[16] The nitrite concentrations in the culture supernatants were determined by a colorimetric assay based on Griess reaction. A sample of 750 µL of algal culture was put in a 1.5 mL Eppendorf and centrifuged for 75 seconds at 12,000 x g. The cell-free supernatant was kept in the freezer. A working reagent mixture was prepared mixing equal volumes of 10 $g \cdot L^{-1}$ sulfanilamide with 200 mL of HCl 12 N and 200 $mg \cdot L^{-1}$ N-(1-naphthyl)ethylenediamine dihydrochloride. A volume of 150 µL of the prepared working reagent mixture was put in a flat-bottom 96-wells microtiter plates and 75 µL of supernatant was added to the wells. The mixture was incubated for 2 minutes and the absorbance at 540 nm was then measured using a microplate reader (iMark, Bio-Rad). Samples were diluted as needed and the nitrite concentration was calculated using previously made calibration curves containing seven points of known concentrations ranging from 0 to 4 mM KNO_2.

of the equipment was verified by measuring a standard mix of gas (499.5 ppm CO_2, 0.498 ppm N_2O, 1.99 ppm CH_4). In this protocol, the gas entering the analyser first went through a desiccator and a filter to avoid the accumulation of water or particles inside the equipment and the gas coming from the pump was filtered with a hydrophilic PVDF 0.22 µm filter (Millipore Millex GV) before entering the Duran bottle to avoid any contamination.

GC-ECD: In the serum flasks, gaseous N_2O concentration was measured by sampling 5 mL of the gas phase with a gas-tight syringe and a needle. This sample was then injected onto a ECD-gas-chromatography (Shimadzu GC-2010, Shimadzu, Japan) using a 1000 µL sample loop (380°C), a Alltech Porapak QS 80/100 column (70°C, Sigma-Aldrich, USA) and an electron conductivity detector (315°C) as described by Guieysse et al., (2013). Calibration was achieved using a 100 ppm N_2O standard in N_2 (neutral gas).

Computation and key assumptions: In both serum flasks and Duran bottles, we assumed the gas and the liquid phase N_2O concentrations were at equilibrium at the time of sampling. The concentration of N_2O dissolved in the liquid phase was therefore calculated using Henry's law at 25°C and the total amount of N_2O produced was then calculated by summing up the amount of N_2O that was present in the gas and liquid phase as (Equation 6):

$$n^t_{N_2O_{total}} = x^t_{N_2O} \cdot P^t \cdot \left(\frac{V_g}{R \cdot T} + H_{N_2O} \cdot V_l\right) \quad \text{Equation 6}$$

Where $n^t_{N_2O_{total}}$ is the total amount of N_2O produced in the Duran bottle at time t (moles N_2O); $x^t_{N_2O}$ is the molar fraction of N_2O in the gas phase at time t (mol N_2O·mol gas^{-1}); P^t is the pressure in the gas headspace at time t (typically 101325 Pa unless otherwise stated); V_g is the volume of gas in the bottle/serum flask (mL); V_l is the volume of liquid in the bottle/serum flask (mL); R is the ideal gas constant (8.314 J·mol^{-1}·K^{-1}); T is the temperature inside the bottle (298.15 K); and H_{N_2O} is the Henry law constant of N_2O at T ($2.5 \cdot 10^{-7}$ mol·L^{-1}·Pa^{-1}). The pressure changes and the N_2O losses caused by sampling were accounted for as described by Guieysse et al. (2013) and Plouviez (2017).

Emissions were computed as described by Plouviez et al. (2019b) using Equation 7:

$$\Phi_{N_2O} = ([N_2O]^* - [N_2O]) \cdot Kl_{N_2O} \quad \text{Equation 7}$$

Where Φ_{N_2O} represents the N_2O flux (mol·m^{-2}·d^{-1}), $[N_2O]^*$ represents the dissolved N_2O concentration at equilibrium with earth atmosphere ($1.3 \cdot 10^{-8}$ mol·L_{water}^{-1}), $[N_2O]$ is the mean dissolved N_2O concentration in our samples (mol·L_{water}^{-1}) and Kl_{N_2O} is the N_2O mass transfer coefficient (m·d^{-1}).

The field value of Kl_{N_2O} was estimated from the mass transfer coefficient for oxygen at 20 °C and corrected for temperature based on the diffusivities of these gases and a temperature correction factor of 1.024 (Equation 8):

$$Kl_{N_2O} = 1.024^{T-20} \cdot Kl_{O_2} \cdot \sqrt{\frac{DF_{N_2O}}{DF_{O_2}}} \quad \text{Equation 8}$$

Where Kl_{N_2O} is the N_2O mass transfer coefficient ($m \cdot d^{-1}$), T is the temperature of the liquid (°C), Kl_{O_2} is the O_2 mass transfer coefficient ($m \cdot d^{-1}$), DF_{N_2O} and DF_{O_2} are the molecular diffusion coefficients in water at 20°C of N_2O and O_2 ($1.98 \cdot 10^{-9}$ $m^{-2} \cdot s^{-1}$ and $1.84 \cdot 10^{-9}$ $m^{-2} \cdot s^{-1}$, respectively).

The field value of Kl_{O_2} was calculated according to Schwarzenbach et al. (2005) calculations as (Equation 9):

$$Kl_{O_2} = (4 \cdot 10^{-4} + u^2 \cdot 4 \cdot 10^{-5}) \cdot 86{,}400 \cdot 0.01 \quad \text{Equation 9}$$

Where Kl_{O_2} is the O_2 mass transfer coefficient ($m \cdot d^{-1}$), u ($m \cdot s^{-1}$) is the average surface wind speed, 86,400 is used to convert the secondly rate into daily values ($s \cdot d^{-1}$) and 0.01 is used to convert the values from cm to m ($m \cdot cm^{-1}$).

5.6.6. RNA extraction from axenic *Chlamydomonas* cultures and qPCR

Cells were harvested and concentrated prior to extracting RNA from the samples. Four different harvest methods were tested to optimise the cell extract preparation protocol (Appendix H). This step is crucial as it determines the RNA concentration of the sample: RNA must be preserved, and sampling volume must be kept low enough to avoid large volume changes over time.

RNA extraction from axenic *Chlamydomonas* cultures was done following the protocol proposed by Sanz-Luque & Montaigu (2018). Briefly, RNA was extracted from the cells sample using a phenol (pH 4.5):chloroform:isoamyl alcohol solution and precipitated using a solution of lithium chloride (8 M). The contaminating genomic DNA was removed from the RNA extract using a kit of DNase I recombinant, RNase-free (Roche, Mannheim, Germany) according to the manufacturer's instructions. Once the RNA was purified, cDNA was synthesised from our RNA extract by RT-qPCR using the iScript™ cDNA Synthesis Kit (Biorad, Hercules, California, USA) following the manufacturer's instructions. The real time qPCR was then carried out using the reagent SsoFast™ EvaGreen® Supermix (Biorad, Hercules, California, USA) as stated in the manufacturer's manual. Genes *CBLP, UBIQUITIN* and *ACT1* were used as reference genes. The quality of the RNA sample was estimated by calculating the ratio

of the absorbance at 260 nm and 280 nm (260/280). Using this protocol, gene expression was quantified under various conditions and times (e.g. cells grown in HSM – N and in HSM – N + 10 mM NO_2^- after 0 h, 1 h, 3 h, 6 h, 17 h and 24 h of experiment).

5.6.7. Electrophoresis and DNA sequencing

Electrophoresis was used to verify RNA integrity after extraction and separate the DNA produced during primers optimisation. DNA sequencing was used to check that amplification worked properly (no unspecific amplifications).

The nucleic acids were separated using agarose gels containing 1%-2% agarose (w/v) in TAE buffer (4.84 $g \cdot L^{-1}$ Tris; 1.1 $mL \cdot L^{-1}$ acetic acid; 1 mM EDTA pH 8.0). Ethidium bromide at 0.5 $\mu g \cdot mL^{-1}$ was added to the gel to dye the nucleic acids and allow detection using a UV-transilluminator. Prior to loading the samples in the gel, 2 µL of loading buffer (50% glycerol; 0.25% bromophenol blue; 0.25% xylene cyanol) was added to the samples and the wells were then filled with 15 µL of the mixture. As molecular weight marker, 10 µL of Invitrogen 1 kb Ladder Plus marker (ThermoFisher Scientific) was used in the first and the last well of the gel.

Once the migrations on the gel were over, nucleic acids were visualized using UV light and data analysed with the image system Gel Doc 2000 (BioRad). For the RNA, two discrete bands of ribosomal RNA were indicative of no significant degradation. For the DNA, the observed bands corresponding to DNA fragments of interest were extracted and purified from the gel by cutting the gel with a scalpel and then using the Ultrafree®-DA (Millipore) centrifugal filter units according to the manufacturer instructions. The DNA samples were sequenced using Sanger technology by the centralized research support service SCAI (Servicio Central de Apoyo a la Investigacion) at the University of Cordoba (Spain).

6. Results and discussion

6.1. N_2O emissions from New Zealand lakes

Due to COVID-19, the New Zealand border was closed which delayed my arrival in NZ (March 2021). As a consequence, weekly sampling at Lake Horowhenua and Turitea reservoir only started in April and October 2021, respectively. As shown in Figure 11, algal blooms still occurred during autumn in lake Horowhenua.

Figure 11: Lake Horowhenua in June 2021 (left) and January 2018 (right).

Table 16 summarizes the experimental evidence gathered between April and October 2021. At this time, there is no clear relationship between chlorophyll concentration and dissolved N_2O concentration. N_2O was however synthesized in the presence of O_2.

Based on the average of the mean values of chlorophyll, dissolved nitrite, dissolved nitrate and phosphate (dissolved phosphorus) concentrations, we calculated a TLI score of 7.5 for lake Horowhenua and 4.8 for the Turitea reservoir. Based on longer monitoring performed by the team in New Zealand, the value have been recalculated and indicate that Lake Horowhenua (12 months of data) is eutrophic (TLI score of 5.0) and the Turitea reservoir (6 months of data) is oligrotrophic (TLI score of 2.2). The latter results correspond to historical data for lake Horowhenua provided in LAWA (*Lake Horowhenua Water Quality*, 2021).

The N_2O emissions were estimated at 0.4 – 8.7 g $N\text{-}N_2O \cdot ha^{-1} \cdot yr^{-1}$ (n = 29 sampling events) between April and October 2021 for lake Horowhenua, which is low and can be explained by a lower biological activity due to lower temperature and light during winter. However, data from lake Horowhenua were already gathered in 2018 and presented at the IWA Conference of 2019 on Algal Technologies and

Stabilization Ponds for Wastewater Treatment and Resource Recovery. N_2O emissions of Lake Horowhenua during Summer 2018 were thus estimated at 0.6 – 24.2 g $N\text{-}N_2O \cdot ha^{-1} \cdot yr^{-1}$ (n = 3 sampling events). The N_2O emissions from the Turitea reservoir were estimated at 0.3 – 1.0 g $N\text{-}N_2O \cdot ha^{-1} \cdot yr^{-1}$ (n = 3 sampling events) between August and October 2021. These results show that the N_2O emissions were higher at the eutrophic lake compared to the oligotrophic reservoir, which is consistent with our hypothesis. Also, these results tally with the observation from the IPCC that nutrient-impacted waters emit more N_2O than clean waters. Besides, the recorded emissions between April and October 2021 (0 – 3.5 $nmole \cdot m^{-2} \cdot h^{-1}$) are in the lower range of the fluxes reported in the literature for lakes (Table 2, fluxes ranged from 0 to 10,057 $nmole \cdot m^{-2} \cdot h^{-1}$).

Lakes represent around 1.3% of New Zealand area (*Land Cover*, 2021) and around half of New Zealand monitored lakes are eutrophic or worse (Ministry for the Environment & Stats NZ, 2020), meaning that 167,500 ha of lakes are eutrophic. Based on our data from lake Horowhenua, we estimated that national N_2O emissions from New Zealand eutrophic lakes represent 0.07 to 4.1 t $N\text{-}N_2O \cdot yr^{-1}$. This corresponds to 0.0004 – 0.02% of New Zealand agricultural N_2O emissions in 2020 (Ministry for the Environment, 2022) which is the main sector responsible for N_2O emissions in New Zealand. Thus, emissions from eutrophic lakes represent a small portion of New Zealand N_2O emissions.

Based on the data from lake Horowhenua, global N_2O emissions from eutrophic lakes and reservoirs, which represent 126,000,000 ha, were estimated at 25 – 1,500 t $N\text{-}N_2O \cdot yr^{-1}$. These emissions represent 0.008 to 0.3% of global anthropogenic N_2O emissions from inland and coastal waters (Tian et al., 2020). The global contribution of eutrophic lakes to N_2O emissions is thus low.

To conclude, the N_2O emissions from eutrophic lakes reported in this study are low and therefore the national and global significances are low. However, the measured fluxes in this study were in the lower range of fluxes reported in the literature. Thus further research is required to understand which parameters (e.g. type of lake, nutrients, etc.) could explain the variability of fluxes reported in different studies.

Table 16: First sampling data from Lake Horowhenua (LH) and Turitea reservoir (TR).
The mean values are based on triplicates.

Lake	Date	Time	Radiation ($MJ \cdot m^{-2}$)	Distance from the lake edge (m)	Water temperature	Air temperature (°C)	Conductivity ($\mu S \cdot cm^{-1}$)	Dissolved oxygen ($mg \cdot L^{-1}$)	pH	Chlorophyll ($mg \cdot L^{-1}$)		Total suspended solid ($g \cdot L^{-1}$)		N_2O (nmol $N_2O \cdot L$ water^{-1})		NO_2^- ($\mu g \cdot L^{-1}$)	NO_3^- ($mg \cdot L^{-1}$)	PO_4^{3-} ($\mu g \cdot L^{-1}$)		Chloride ($mg \cdot L^{-1}$)		Sulfate ($mg \cdot L^{-1}$)	
										Mean	Error	Mean	Error	Mean	Error			Mean	Error	Mean	Error	Mean	Error
LH	27/04/2021	10:10	1.09	15		15	220.4		7.88	1.38	0.10	0.23	0.01					520.0	22.9	27.8		8.5	
LH	06/05/2021	10:30	0.725	15	17.3	17	234.3	9.98	8														
				2	17.7		239.7	5.34	8.1	3.83	0.09	1.39	0.01					228.6	1.0	26.6		9.3	
LH	13/05/2021	10:40	1.48	15	12.1	12	246.4	6.39	7.41	0.05	0.03	0.01	0.00					208.7	2.0	24.6		7.1	
				5	12.9		250.3	7.03	7.56	0.47	0.04	0.21	0.02					120.6	1.5	26.7		7.2	
LH	19/05/2021	10:30	1.13	15	13.5	16	239.1	10.01	7.93	0.05	0.01	0.03	0.00			52.7	2.0	89.5	1.1	26.4		10.1	
				5	14.2		238.5	10.5	8.09	0.03	0.01	0.03	0.00			109.5	1.3	57.6	2.2	24.5		7.1	
LH	27/05/2021	10:30	1.095	15		12	262.3	10.78	7.58	0.06	0.00	0.09	0.01			23.6	1.2	66.8	1.2	26.5		10.8	
				5			255.2	12.65	7.65	0.20	0.01	0.16	0.01			59.6	1.2	88.9	0.7	28.1		13.2	
LH	03/06/2021	10:30	0.695	15	10.5	10	252.5	10.93	7.4	0.12	0.01	0.07	0.00			128.3	2.9	48.3	9.8	28.4		17.2	
				5	10.5		259.6	11.62	8.06	0.83	0.02	0.25	0.04			47.2	0.9	34.8	0.7	30.0		18.3	
LH	10/06/2021	10:30	0.535	15	12.6	14	235.7	10.81	7.54	0.11	0.00	0.02	0.00	25.6	2.7	86.9	2.0	34.9	5.4	28.7		21.2	
				5	12.6		242.4	15.42	8.53	2.75	0.05	0.55	0.02	16.3	5.2	61.0	1.1	57.6	2.2	29.4		20.2	
LH	16/06/2021	10:30	0.525	15	14.4	15	0.215	4.94	7.17	0.02	0.00	0.01	0.00	10.7	2.1	50.7	1.0	47.4	2.6	30.1	0.2	19.7	0.2
				5	14.5		284.5	7.19	7.14	0.08	0.01	0.04	0.01	4.7	0.5	54.8	0.4	54.8	5.3	34.4	0.2	18.6	0.1
LH	23/06/2021	10:30	0.72	15	7.6	7	235.4	8.75	6.83	0.03	0.00	0.01	0.00	7.7	0.5	16.4	1.1	28.5	0.4	27.1	0.1	20.3	0.1
				5	7.9		240.3	9.3	7.09	0.08	0.00	0.07	0.01	7.1	10.3	39.5	1.7	23.7	2.0	27.8	0.0	20.3	0.0
LH	01/07/2021	10:30	0.945	15	7.7	9	223.7	9.62	7.89					15.2	0.7	69.1	3.3	54.0	7.1	25.9	0.0	20.6	0.0
				5	7.9		222	9.77	7.74					18.1	3.2	10.4	3.2	52.2	1.5	25.7	0.1	20.1	0.1
LH	09/07/2021	10:30	0.975	15	7.6	9	228.4	9.58	6.73	0.04	0.00	0.02	0.00	22.5	0.3	39.3	4.4	40.1	0.8	26.0	0.1	22.9	0.0
				5	7.6		226.7	9.72	7.18	0.05	0.00	0.02	0.00	12.2	7.9	41.9	5.2	30.8	0.8	26.3	0.2	23.1	0.2
LH	14/07/2021	10:30	0.625	15	6.1	6	240.6	10.71	6.6	0.08	0.00	0.08	0.00	23.4	2.1	36.6	6.2	41.7	0.2	27.4	0.1	25.8	0.1
				5	6		243.4	11.52	7.07	0.13	0.00	0.14	0.00	17.3	1.8	43.6	5.8	46.0	0.3	28.1	0.1	25.5	0.1
LH	22/07/2021	10:30	0.44	15	11.9	13	227.5	8.87	8	0.01	0.00	0.02	0.00	12.2	1	106.6	2.4			29.7	0.1	19.3	0.1
				5	12		211.9	8.85	7.57	0.02	0.00	0.03	0.01	12.8	0.7	17.5	1.4			28.5	0.0	18.0	0.1
LH	30/07/2021	10:30	0.965	15	11.4	14	226.6	8.69	6.7	0.01	0.00	0.01	0.00	32.4	6.2	94.2	7.3			27.0	0.0	24.1	0.0
				5	11.9		228.2	8.59	6.82	0.02	0.00	0.01	0.00	37.2	2.9	56.7	6.9			27.1	0.0	23.8	0.1
LH	05/08/2021	13:00	1.02	15		10	226.8	10.9	6.89	0.04	0.00	0.07	0.01	25.8	1.7	25.6	9.7			27.6	0.0	23.7	0.0
				5			238.3	10.23	6.75	0.07	0.00	0.19	0.00	34.8	2.2	93.0	10.1			29.4	0.0	23.6	0.1
LH	12/08/2021	10:30	0.47	15	10.8	13	219.7	9.82	7.73	0.03	0.00	0.04	0.00	69.5	4.3	46.0	9.8			27.6	0.1	23.9	0.0
				5	10.4		227.8	9.78	8.07	0.03	0.00	0.01	0.00	65.5	4.5	37.3	9.2			27.3	0.0	23.7	0.0
TR	16/08/2021	10:00	1.19	5	9	12	93.4	11.2	6.15	0.02	0.00	0.00	0.00	7.1	1.8	16.7	1.0			17.9	0.0	4.2	0.0
LH	15/10/2021	11:00	1.51	15	15.5	14.2	215.2		7.1	0.03	0.00	0.01	0.00	16.2	2	37.8	9.7						
				5	15.2		225.3		7.28	0.04	0.00	0.04	0.01	14.4	0.8	146.1	4.5						
TR	15/10/2021	12:40	1.69	5	13	14.5	88.15		6.1	0.01	0.00	0.00	0.00	6.3	1	19.8	0.4						
LH	21/10/2021	11:00	1.77	15	17.5	15.8	212.3	10.24	7.28	0.02	0.00	0.01	0.00	12.5	1.4	59.3	6.8						
				5	17.3		214.5	10.62	7.35	0.02	0.00	0.01	0.00	13.8	0.8	86.1	5.8						
LH	27/10/2021	10:30	2.05	15	21.2	17.5	212.7	9.8	7.04	0.03	0.00	0.01	0.00	7.3	1.6	256.8	5.4						
				5	22.1		212.8	10.59	7.3	0.03	0.00	0.01	0.00	7.4	0.2	62.9	3.2						
TR	27/10/2021	12:30	2.15	5	17.8	19	87.5	10.4	6.73	0.01	0.00	0.00	0.00	3.2	0.4	8.1	0.0						

6.2. Physiological conditions leading to N_2O synthesis in *Chlamydomonas*.

CYP55 has been proposed as the main enzyme involved in N_2O production by *Chlamydomonas* in the dark (Plouviez et al., 2017a; Burlacot et al., 2020) while FLVs could be responsible for N_2O production in the light (Burlacot et al., 2020). HCPs, have been evidenced to catalyze N_2O synthesis in *E. coli* (a bacterium) under anaerobic conditions (Wang et al., 2016) but their putative N_2O producing roles in *Chlamydomonas* have not been investigated yet.

The physiological conditions associated with the production of N_2O by the model organism *Chlamydomonas reinhardtii* are still not well known. Nitrite has been identified as a precursor of N_2O production as nitrite can be reduced into nitric oxide (NO) intracellularly, and NO is in turn reduced to N_2O. Laboratory-scale experiments were therefore conducted to study the N_2O synthesis by different axenic cultures of *Chlamydomonas* under different nutrient and light conditions.

Because the accumulation of NADPH and ATP blocks the electron flow and leads to the production of reactive oxygen species with detrimental effects when cells cannot use excess light; we hypothesised that *Chlamydomonas* cells produce N_2O to maintain the electron flow and protect cells against the impact of light excess. Specifically, we believe that the production of N_2O from NO is a mechanism to divert energy excess, possibly supported by FLVs (A and B) (Figure 12). To validate this hypothesis, we chemically inhibited the photosynthetic electron flow coming from PSII (using DCMU) in *Chlamydomonas* wildtype. In addition, FLV-deficient mutants were used to assess the role of FLVs in N_2O production.

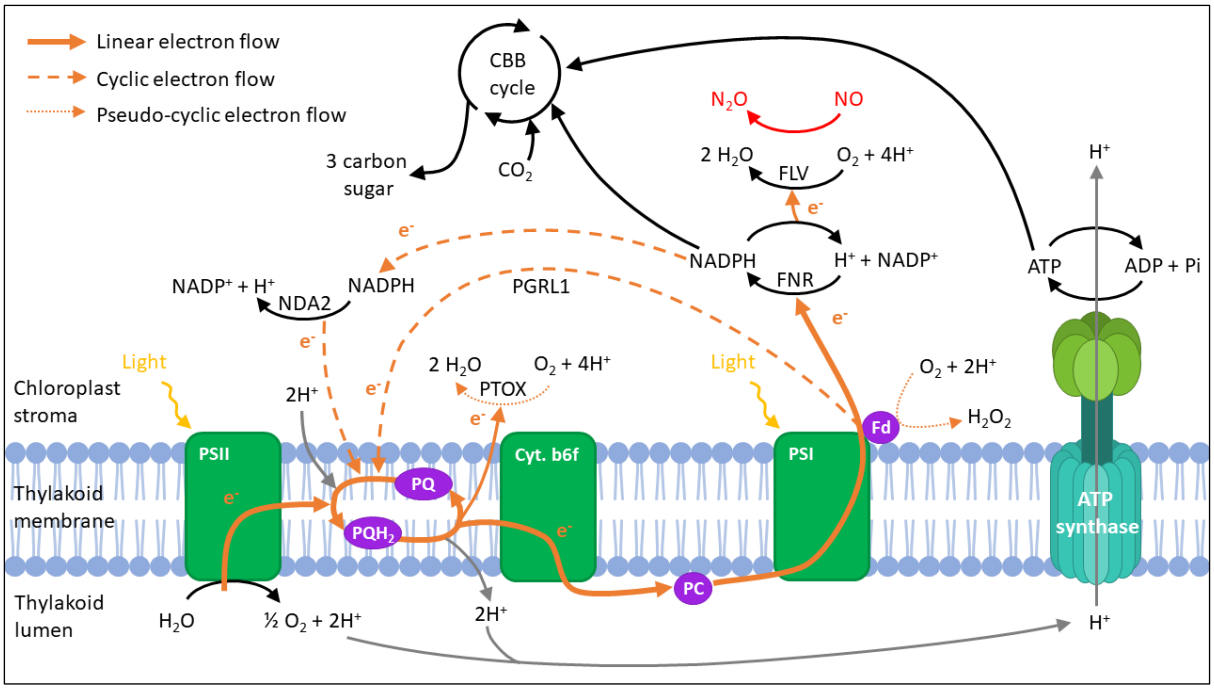

Figure 12: Oxygenic photosynthesis pathway in Chlamydomonas reinhardtii.
Photosynthesis enables the conversion of light energy into chemical energy to fix carbon. The photolysis of water releases electrons that are transported through the thylakoid membrane and used to generate reducing power (NADPH) and high-energy orthophosphate bonds (ATP). This energy drives the fixation of CO_2 in the Calvin-Benson-Bassham cycle. Environmental light and/or nutrient fluctuations can trigger the production of reactive oxygen species which are detrimental to the photosynthetic apparatus. To acclimate to these fluctuations, photosynthetic organisms possess different alternative electrons routes to dissipate the excess energy (e.g. NDA2, PTOX). Here, we conjecture that the reduction of NO into N_2O by the FLVs (in red) could be an alternative pathway to divert the excess energy received by the microalga. Abbreviations/symbols: H_2O, water; O_2, dioxygen; H_2O_2, hydrogen peroxide; NO, nitric oxide; N_2O, nitrous oxide; CO_2, carbon dioxide; H^+, hydron; e^-, electron; PSII, photosystem II; PQ, plastoquinone; PQH_2, plastoquinol; Cyt. b6f, cytochrome b6f; PC, plastocyanine; PSI, photosystem I; Fd, ferredoxine; ATP, adenosine triphosphate; ADP, adenosine diphosphate; Pi, inorganic phosphate; NADP+/NADPH, nicotinamide adenine dinucleotide phosphate; FNR, ferredoxin NADP+ reductase; FLV, flavodiiron protein; PGRL1, proton gradient regulation 5-like photosynthetic phenotype 1; PTOX, plastid terminal oxidase; NDA2, type II NADPH dehydrogenase; CBB cycle, Calvin-Benson-Bassham cycle.

The wild type strain 6145c was used as a control as it is the parental strain of the M3 mutant. The M3 mutant, which is deficient in nitrite reductase, was selected because it produces more N_2O than the parental strain 6145c (Plouviez et al., 2017a). This strain cannot convert nitrite into ammonium and, therefore, secretes most of the nitrite to the medium. This nitrite is being continuously taken up and excreted and can also be constantly reduced into NO, the substrate for N_2O synthesis, allowing us to use this mutant as a tool to investigate and enhance the impact of different conditions and molecular players on the N_2O production. We also used the "WT" strain CMJ030 (cc-4533) as a control because it is the parental strain for the *flv* and *cyp55* mutants.

6.2.1. N_2O synthesis by the wild type *Chlamydomonas 6145c*

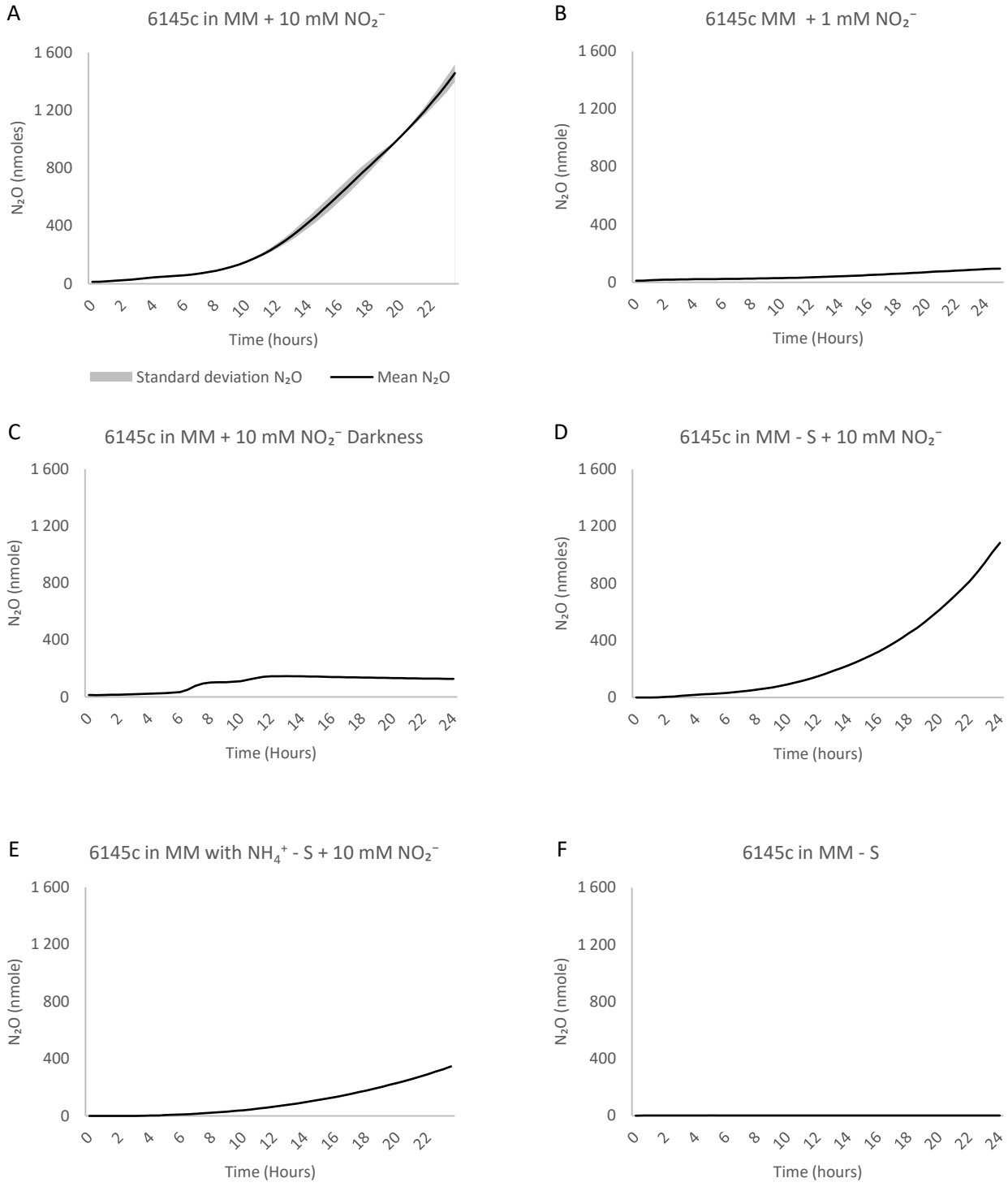

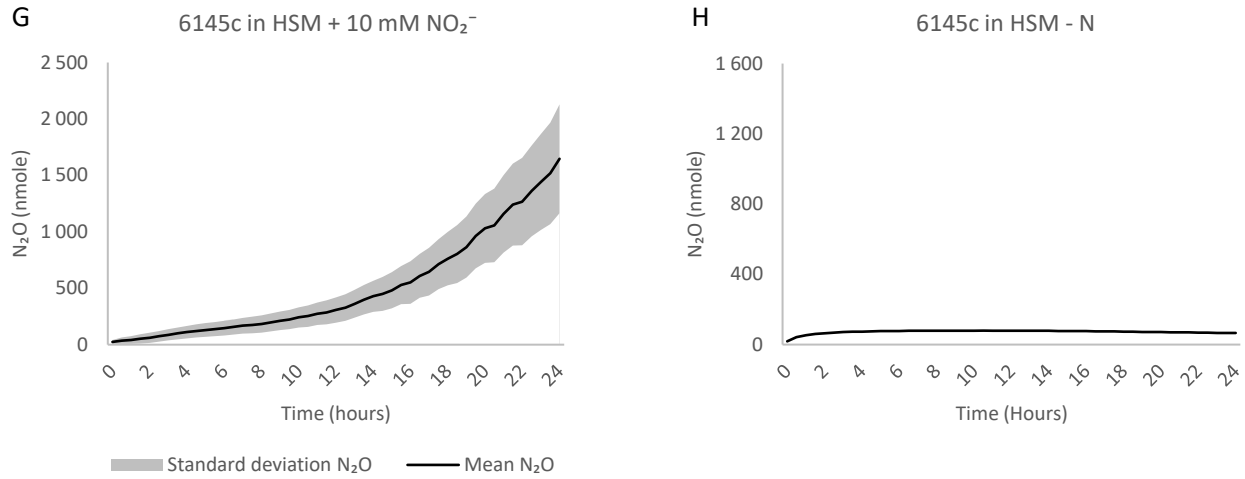

Figure 13: N_2O batch test with C. reinhardtii 6145c (10 mg chlorophyll·L^{-1} ~ 0.25 g DCW·L^{-1}). 6145c in MM + 10 mM NO_2^-, triplicate (A); 6145c MM + 1 mM NO_2^- (B); 6145c in MM + 10 mM NO_2^- in the dark (C); 6145c in MM - S + 10 mM NO_2^- (D); 6145c in MM - S + 10 mM NO_2^- (E); 6145c in MM – S (F); 6145c in HSM + 10 mM NO_2^-, triplicate (G); 6145c in HSM – N, control (H). The graphs A to F come from another set-up in which the cells were grown in a temperate room without windows at 25°C under continuous light provided by four 300×300×40 mm LED panels of 30 W, with warm white light (3200 K) at a light irradiance around 145 µmol photons.s^{-1}.m^{-2}.

First, results from an initial batch assay experiments confirmed that N_2O emissions had a biological origin in our set-up and required nitrite to be significant (see abiotic controls in Appendix I). These results, presented in Figure 13, also showed that axenic cultures of *Chlamydomonas* 6145c synthesised N_2O mainly under illumination when supplied NO_2^- in autotrophic conditions. N_2O total production over 24 h was lower when NO_2^- supply was decreased (Figure 13 A and B). We thus recorded a production of 31.5 ± 10.7 µmole N_2O·g DW^{-1} after 24 h when cells were grown autotrophically and supplied with 10 mM NO_2^-. The N_2O specific production rate between 4 and 24 h after nitrogen addition was 1215 nmol N_2O· g DW^{-1}·h^{-1}. These values are similar to *Chlorella vulgaris* production of 37.9 µmole N_2O·g DW^{-1} reported under similar conditions by Weathers (1984) , who also recorded a production rate of 1580 nmol N_2O·g DW^{-1}·h^{-1} when supplying 33 mM NO_2^- (Weathers, 1984). However, our production rate was one order of magnitude higher than *C. vulgaris* production of 109 nmol N_2O·g DW^{-1}·h^{-1} when supplying 12 mM NO_2^- under similar conditions (Guieysse et al., 2013). The discrepancy between the results from Weathers (1984) and Guieysse et al. (2013) might be due to a difference of light intensity during these experiments and/or a difference in the genetic background of the *C. vulgaris* strains used. There is therefore a possibility that the genetic background plays an important role in N_2O production as we can observe a high variation of the production in our experiments between the different *Chlamydomonas* wild type strains (6145c, CMJ030 and 21gr) cultured in the same conditions (see sections 6.2.1, 6.2.3 and 6.2.4).

As can be seen in Figure 13 A and C, N_2O production was significantly lower in the dark than in the light. An opposite trend was observed when other green algae species were grown mixotrophically (Weathers, 1984). This could be explained by a variation in oxygen level when a carbon source is available. We also suggest that in autotrophic conditions N_2O production is triggered to get rid of the excess energy received when no carbon source is available.

To assess if a different nutrient stress could trigger similar N_2O production, we also cultured the cells in a medium deprived of sulphur under autotrophic conditions in the light. As seen in Figure 13 D, E and F, in the absence of a usable N source (ammonium), the N_2O total production after 24 h was slightly lower when cells were deprived S than when this nutrient was supplied. However, N_2O production was much lower when NH_4^+ was available (Figure 13 E) than when this N source was added (Figure 13 D). This difference could be explained by the fact that NO_3^- and NO_2^- assimilation are inhibited in presence of NH_4^+ in *Chlamydomonas* (Sanz-Luque et al., 2015a).

For each experiment conducted in the light, the CO_2 present in the bottle was totally consumed after 2 to 3 h of experiments. Under CO_2 depletion, the light energy cannot be used for CO_2 fixation and the cells need to get rid of the excess NADPH by activating alternative pathways. N_2O production, which consumes NADPH (Burlacot et al., 2020), could be one of the strategies used under these conditions.

6.2.2. N_2O synthesis by a *Chlamydomonas* NiR knockout mutant (M3)

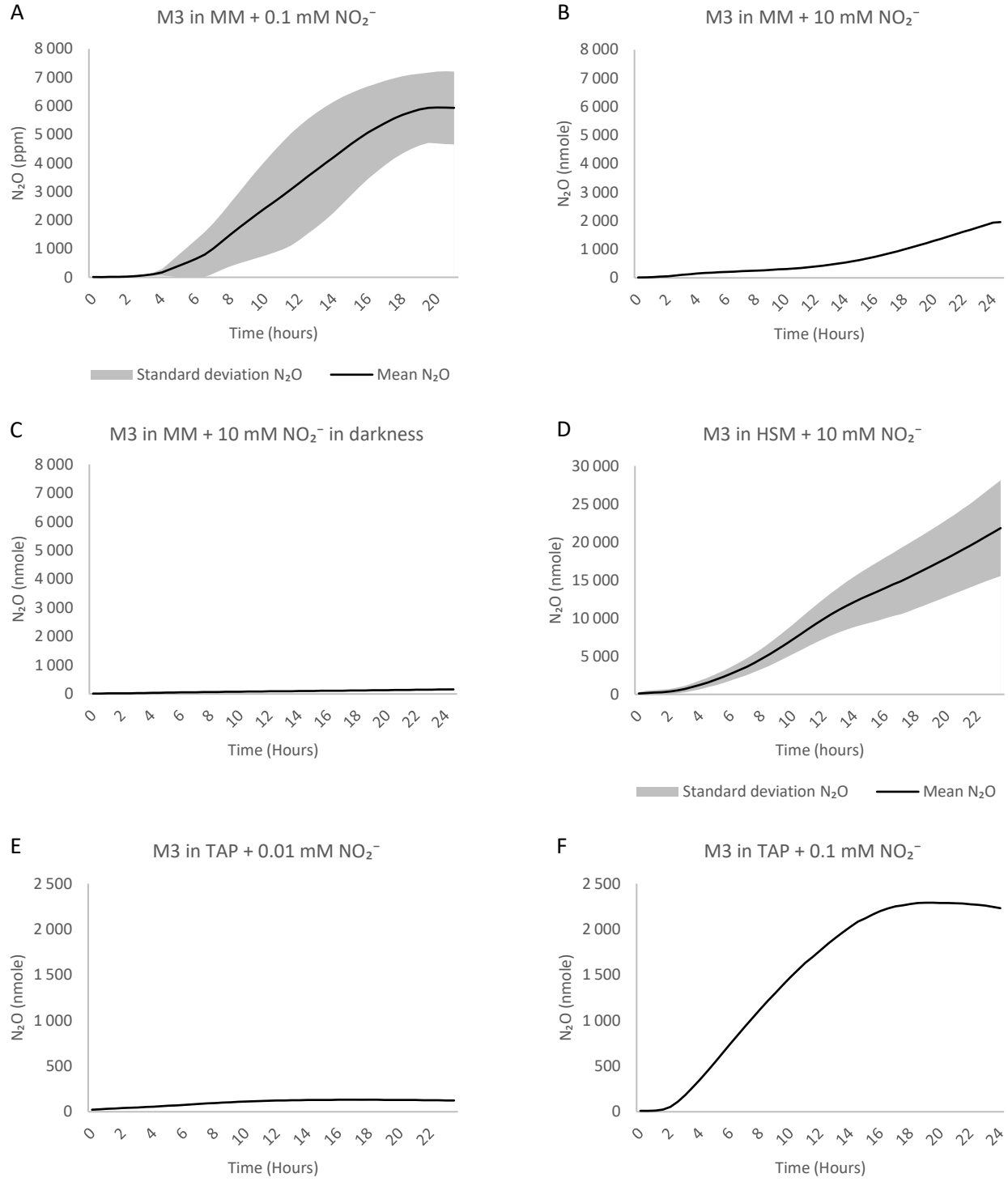

Figure 14: N_2O batch test with C. reinhardtii M3 (10 mg chlorophyll·L^{-1} ~ 0.25 g DCW·L^{-1}). M3 in MM + 0.1 mM NO_2^-, triplicate (A); M3 in MM + 10 mM NO_2^- (B); M3 in MM + 10 mM NO_2^- in the dark (C); M3 in HSM + 10 mM NO_2^-, triplicate (D); M3 in TAP + 0.01 mM NO_2^- (E); M3 in TAP + 0.1 mM NO_2^- (F). The graphs A to C come from another set-up in which the cells were grown in a temperate room without windows at 25°C under continuous light provided by four 300×300×40 mm LED panels of 30 W, with warm white light (3200 K) at a light irradiance around 145 µmol photons.s^{-1}.m^{-2}.

The M3 *Chlamydomonas* strain is a NiR deficient mutant that cannot reduce NO_2^-. Thus, nitrite supply to the medium causes this substrate to be continuously taken and secreted by M3 cells. As NO_2^-, a key precursor to N_2O, accumulates intracellularly, N_2O production is higher in the nitrite-accumulating M3 than in the nitrite-reducing wild type strain (Figure 14 D) under illumination. In darkness however, N_2O production in M3 was similar to the wild type (Figure 14 C). This was expected as nitrite reduction into NO and the subsequent synthesis of N_2O is much lower in the dark than in the light (Figure 14 B and C), as reported by Plouviez et al. (2017a).

We can observe a high variability in the production of N_2O when supplying 10 mM NO_2^-. However, our results must be analysed with care considering that the spectroscope loses accuracy when the production is higher than 8,000 nmoles of N_2O. It was nevertheless necessary to verify that the variability was not due to experimental error. During our experiments, we switched from minimal medium (MM) to high salt medium (HSM) because the use of MM frequently caused the formation of precipitates after autoclaving. The only difference between the MM and HSM media is the calcium concentration which is five times lower in HSM compared to MM. A potential biological explanation to the lower production in MM (Figure 14 B and D) could therefore be that calcium is an inducer of non-photochemical quenching (i.e. the loss of excess energy via heat) (Petroutsos et al., 2011). Under conditions of low Ca^{2+} supply, cells may need to quench more energy through pathways such as N_2O synthesis, explaining the high emission recorded in HSM.

With these experiments, we showed that microalgal N_2O synthesis varied with physiological conditions of the cell. In addition to the mixotrophic conditions leading to N_2O synthesis in the light and in the dark (Weathers, 1984; Guieysse et al., 2013; Plouviez, 2017), we showed that *Chlamydomonas* produced N_2O in autotrophic conditions under illumination. These results are consistent with the results obtained by Guieysse et al. (2013) with *Chlorella vulgaris*.

Once we identified the conditions under which *Chlamydomonas* was consistently producing N_2O, we could further investigate the N_2O synthesis pathways in this microalga.

6.2.3. N_2O synthesis in CMJ030, *flvb*, and *cyp55* strains

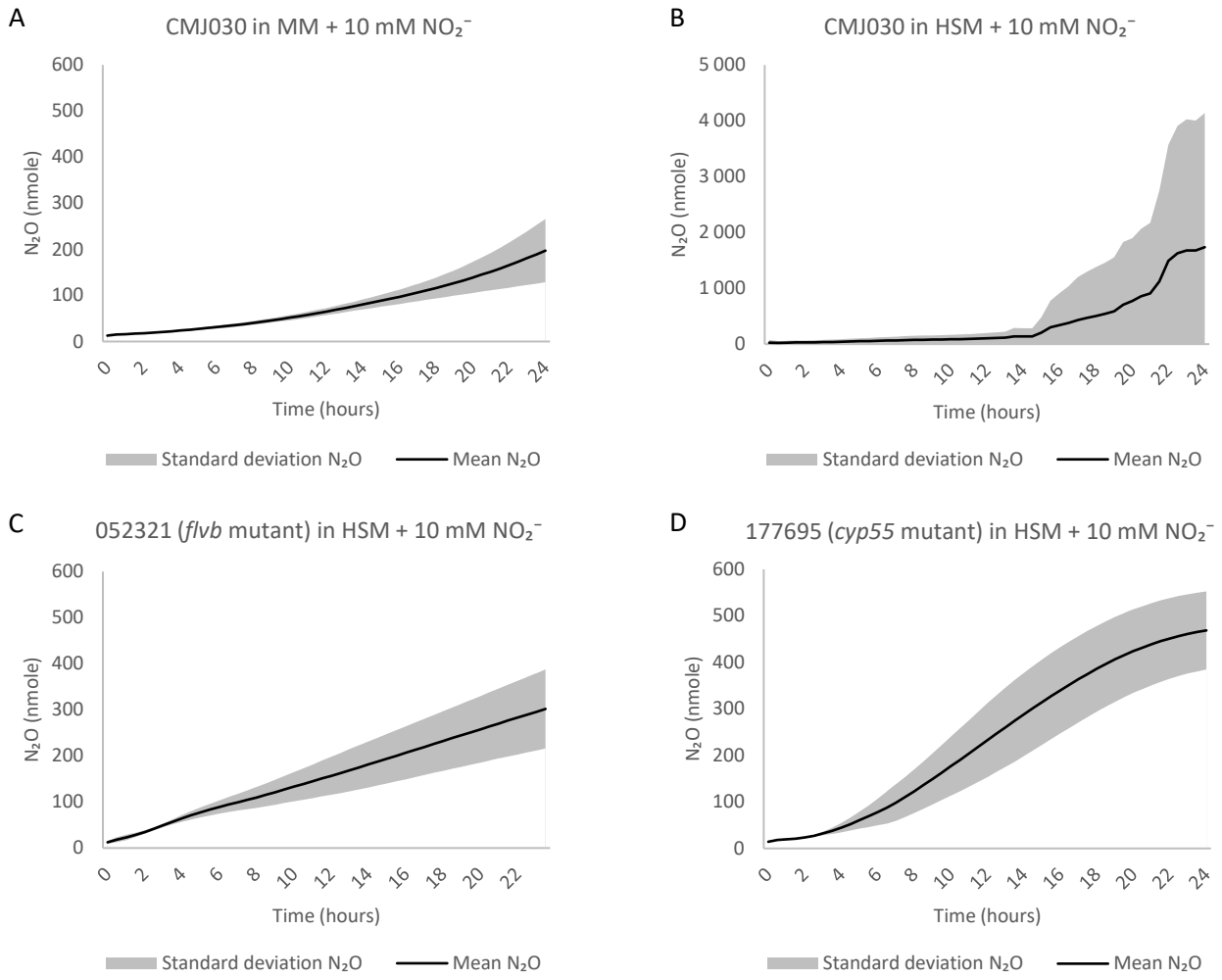

Figure 15: N_2O batch test with C. reinhardtii CMJ030, LMJ.RY0402.052321 and LMJ.RY0402.177695 (10 mg chlorophyll·L^{-1} ~ 0.25 g DCW·L^{-1}). CMJ030 in MM + 10 mM NO_2^-, triplicate (A); CMJ030 in HSM + 10 mM NO_2^-, triplicate (B); LMJ.RY0402.052321 in HSM + 10 mM NO_2^-, triplicate (C); LMJ.RY0402.177695 in HSM + 10 mM NO_2^-, triplicate (D). The graph A comes from another set-up in which the cells were grown in a temperate room without windows at 25°C under continuous light provided by four 300×300×40 mm LED panels of 30 W, with warm white light (3200 K) at a light irradiance around 145 µmol photons.s^{-1}.m^{-2}.

In order to confirm the known conditions during which FLV and CYP55 are involved in N_2O production (i.e. light and dark conditions, respectively), we obtained the previously described *flvb* and *cyp55* mutants (Burlacot et al., 2020) from the *Chlamydomonas* resource center (www.chlamycollection.org). The strain CMJ030 was used as control because this wildtype has the same genetic background as the *flvb* and *cyp55* mutants. Unfortunately, as shown in Figure 15 B, N_2O production by CMJ030 was highly variable and the experiments were not reproducible in HSM. Optimization is therefore required to determine why we are observing such variability. Nevertheless, the FLVs-deficient mutant produced a significant amount of N_2O when NO_2^- was supplied to the medium in autotrophic conditions (Figure 15 C). This production evidences that other proteins than

FLVs were involved in N_2O production in this strain under the conditions tested. This challenges the conclusions of Burlacot et al. (2020) who proposed that FLVs were the main enzymes involved in N_2O production in the light in *Chlamydomonas* (Burlacot et al., 2020).

Because CYP55 has been associated with N_2O production in the dark, we tested the production of N_2O from the *cyp55*-deficient mutant under illumination. As can be seen in Figure 15 D, this strain produced N_2O in these conditions which confirms that CYP55 is not or poorly involved in N_2O production in the light. This result requires to be confirmed by comparing the production with an adequate control strain. The production in darkness needs to be checked to confirm that no N_2O is produced as previously suggested in the literature (Plouviez et al., 2017a; Burlacot et al., 2020). If these results are confirmed, the *cyp55*-deficient mutant could be a suitable strain to use during our microcosm assays in the dark.

6.2.4. N_2O synthesis in the *Chlamydomonas* wild type strain 21gr

Considering the lack of reproducibility observed with CMJ030, another suitable parental strain was investigated. The 21gr strain is the mt+ equivalent of 6145c which reproducibly produces N_2O and whose genetic background is known. Besides, 21gr has been widely used to perform crossing and create double mutants. Thus, this strain has been selected to do a crossing between *flvb* and *cyp55* mutants to get the mutations in the 21gr background. As can be seen in Figure 16, this strain produced significant amounts of N_2O.

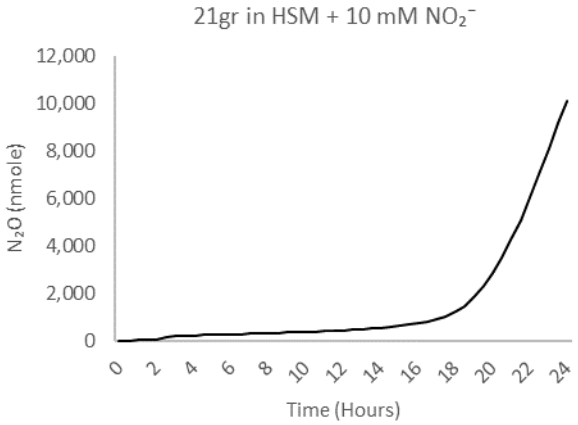

Figure 16: N_2O batch test with C. reinhardtii 21gr (10 mg chlorophyll·L^{-1} ~ 0.25 g DCW·L^{-1}).

6.3. Inhibition assays

6.3.1. Inhibition assay using the wild type Chlamydomonas 6145c

Exposure to excess light energy can lead to the degradation of the photosynthetic apparatus due to the generation of reactive oxygen species via the electron flow in the thylakoid membrane (Saroussi et al., 2019). Alternative pathways re-routing excess electrons are involved in the acclimation of *Chlamydomonas* to fluctuating environmental parameters such as light energy. We therefore conducted inhibition experiments using DCMU on wild type cells to investigate the contribution of the photosynthetic electron flow to N_2O production.

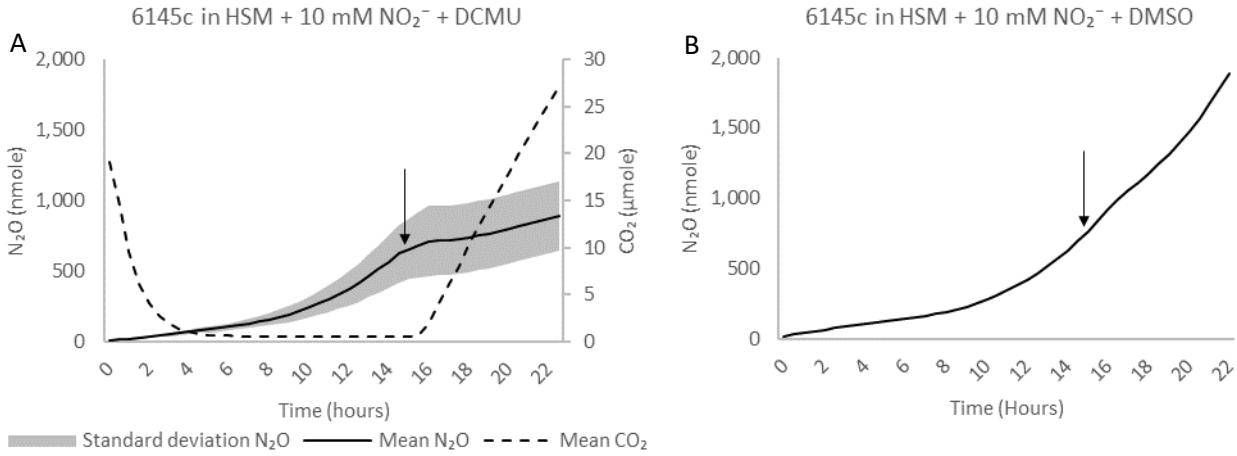

Figure 17: Inhibition assay with C. reinhardtii 6145c (10 mg chlorophyll·L^{-1} ~ 0.25 g DCW·L^{-1}). After 15 h of experiment, 10 µM DCMU (left) or DMSO (right) was added to the medium (arrow).

For this purpose, we also added DMSO (dimethyl sulfoxide) after 15 h in our control because the DCMU was diluted in DMSO. As shown in Figure 17 A, N_2O production significantly decreased when DCMU is added to the medium whereas DMSO addition had not impact on the control. As DCMU blocks the electron flow coming from the photosystem II, the experimental evidence herein shown suggest that at least part of the N_2O production depends on the photosynthetic electron flow.

6.3.2. Inhibition test using lake samples

In order to study the biological source of N_2O in lake Horowhenua, we performed inhibition assays on lake samples rich in microalgae (samples withdrawn during a bloom on 12/08/2021). Penicillin G potassium was selected because it has been previously shown to inhibit bacterial activity without inhibiting microalgal activity during N_2O synthesis.

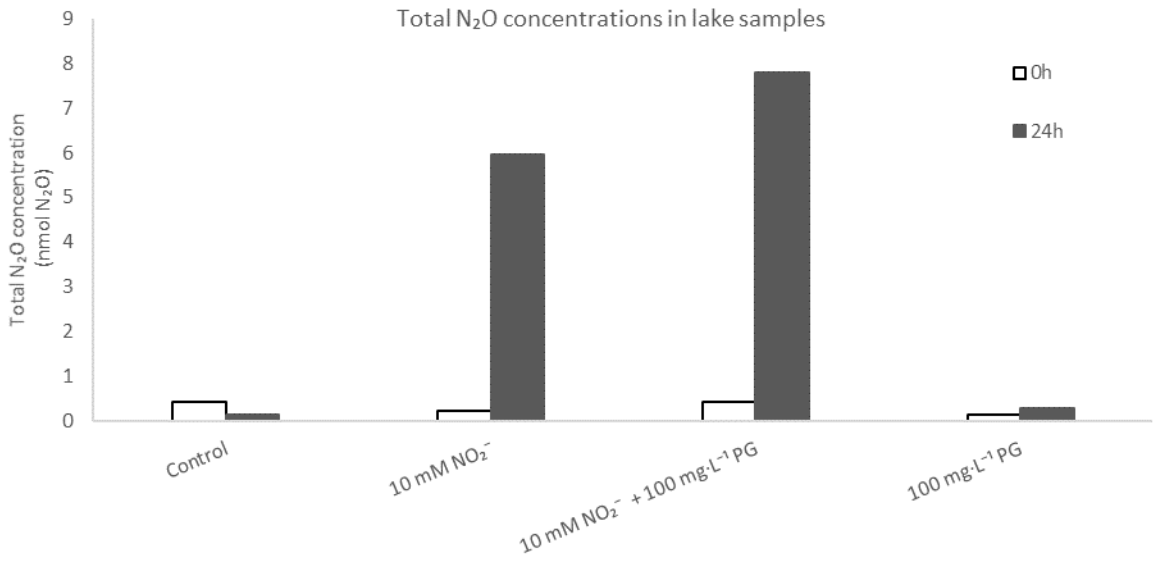

Figure 18: Inhibition assays using superficial samples from lake Horowhenua visibly rich in algae (28 µg chlorophyll·L^{-1}). At time 0h, either 10 mM NO_2^-, 10 mM NO_2^- + 100 mg·L^{-1} Penicillin G potassium (PG), or 100 mg·L^{-1} Penicillin G potassium was added to the sample.

As shown in Figure 18, N_2O production increased when nitrite was added to the medium compared to the control after 24h of cultivation. This was expected as we observed the same trend during batch assays with pure algae cultures supplied with nitrite (see section 6.2). When the medium was supplied with Penicillin G potassium, a broad bacterial inhibitor, N_2O production was similar to the production recorded in the control culture after 24h. We even obtained the highest N_2O production when both nitrite and Penicillin G potassium were added to the culture medium, which suggests that bacteria are not the main producers of N_2O.

However, these results need to be confirmed with further experiments performed on lake samples in triplicates.

6.4. qPCR

6.4.1. RNA extraction

Following RNA extraction from culture aliquots, 260/280 ratio values of around 2, which is expected for good quality samples, were measured for most samples (Appendix J). The shape of the absorbance curve of each sample was also checked as it informs on the quality of the sample.

6.4.2. qPCR results

As a first step, we decided to focus on the expression of *FLVA*, *FLVB*, *NIRK* and *CYP55* genes because the involvement of these genes in N_2O production had already been demonstrated.

Following on primers optimization and efficiency tests, we performed qPCR on samples from M3 and CMJ030 cultures in HSM-N (control) and HSM-N + 10 mM NO_2^- (treatment). The melting peak charts at different primer dilutions was compared to our samples to verify that the peak occurred at the expected temperature and, thus, that no unspecific amplification was performed during PCR (see Appendix K).

The qPCR results are not shown here because the expressions of our reference genes were highly variable both in the control and the treatment. Further optimization is therefore required. However, while we could not normalize the expression of *FLVA*, *FLVB*, *NIRK* and *CYP55,* their transcript numbers were similar in the controls and treatment. While these results are preliminary and specific to the conditions studied, the similarity between treatment and controls could mean that the proteins targeted were already present and active in the cells and/or that nitrite did not impact their expressions. If confirmed, these results could mean that RT-qPCR may not be suitable to identify the microalgae genes directly responsible for N_2O synthesis following nitrite supply, but the technology may still be suitable to confirm the biological source of N_2O in microcosms.

7. Conclusions

Preliminary data gathered from Lake Horowhenua show that the lake is a source of N_2O (0.4 – 8.7 g $N\text{-}N_2O \cdot ha^{-1} \cdot yr^{-1}$, n = 29 sampling events) and is eutrophic but no relationship between the algal biomass concentration and the N_2O production could be evidenced at this stage. Based on our data, the national significance of N_2O emissions from New Zealand eutrophic lakes is low compared to the fluxes reported in the literature. Further research is thus required to determine which parameters affect these emissions. Preliminary inhibition assays under illumination performed on lake samples supplied 10 mM NO_2^- and 100 $mg \cdot L^{-1}$ Penicillin G potassium suggest that bacteria are not the main producers of N_2O in the lake.

While the ability of microalgae to produce N_2O has been demonstrated in the laboratory and 2 pathways have been determined, new evidence suggest that other enzymes could be involved in N_2O production: CYP55, which catalyses the reduction of NO to N_2O, has thus been proposed as the main enzyme involved in *Chlamydomonas* in the dark (Plouviez et al., 2017a), while flavodiiron proteins (FLVs) have been suggested to be responsible for N_2O production in the light (Burlacot et al., 2020). In additions, hybrid cluster proteins (HCPs) present in both bacteria and *Chlamydomonas* are producing N_2O in *E. coli* in anaerobic conditions and could be involved in N_2O production in *Chlamydomonas*. Consequently, investigating the different putative N_2O production pathways in the laboratory is still needed to confirm the enzymes involved during microalgal N_2O synthesis and thus select the right genes in our field samples.

Preliminary batch assays under illumination demonstrated that wild type *Chlamydomonas reinhardtii* produced N_2O up to 31.5 ± 10.7 µmole $N_2O \cdot g\ DW^{-1}$ over 24 hours in autotrophic conditions and when supplied 10 mM NO_2^-. Inhibiting the electron flow coming from PSII in the same conditions suggests that the electron transport chain is involved in N_2O production. Mutant deficient in FLVs were however still synthesizing N_2O when supplied with NO_2^- under illumination, showing that the FLVs were not the only enzymes involved in N_2O production in autotrophic conditions, which challenges conclusions from the literature. These results were presented at the Plant Science Central conference (6-8 July 2021; Massey University, Palmerston North, New Zealand; New Zealand Institute of Agricultural and Horticultural Science (NZIAHS), New Zealand Branch of the International Association of Plant Biotechnology (NZIAPB), New Zealand Society of Plant Biologists (NZSPB)) and at the Physiomar & Australia New Zealand Biotechnology Society (ANZMBS) 2021 Conference held online virtually (7-9 September 2021).

My research has therefore demonstrated:

1. The suitability of pure algae bioassays aiming at determining the pathways (e.g. use of mutants and inhibitor). This preliminary research has however evidenced a knowledge gap regarding the pathways, and we have not yet been able to identify clear conditions repressing algae N_2O synthesis. Future research should finalize a crossing over of mutants that should be repressed in their ability to produce N_2O under the 'standard conditions' of production. Our results also showed that the genetic background plays an important role in N_2O production. These are important to consider for designing future assays.

2. The suitability of protocols for studying gene expression. The RNA extraction protocol is satisfactory but the qPCR still requires optimization.

3. The suitability of protocols for field analysis.

Thus, all the methods required to achieve Objective 1 are suited and the methods for Objective 2 are being optimized. Based on the literature (Hanson & Stefan, 1984; Jansson et al., 2000; Mahan et al., 2005; Guieysse et al., 2013; Zhou et al., 2020), it should be possible to use inhibitors such as antibiotics to distinguish algal from bacterial N_2O emissions and thereby study the production from pure algal and/or bacterial cultures and lake samples. In future work, the potential ecological interactions between algal and bacterial N_2O synthesis could also be assessed, although this still requires the identification of suitable mutants as noted above.

The next steps to achieve this project would be to:

- Continue field monitoring at lake Horowhenua and the Turitea reservoir
- Test the influence of P supply on N_2O emissions from axenic *Chlamydomonas* cultures
- Identify and acquire pure nitrifiers and facultative denitrifiers and test N_2O emissions from these species.
- Identify and test inhibitors on pure bacteria and artificial algae-bacteria consortium
- Test the impact of different N and P supply on N_2O synthesis in microcosms and compare the N_2O production from pure algae culture, pure bacteria culture, artificial algae and bacteria cultures and lake samples.

8. References

1998 National Water Quality Inventory Report to Congress. (1998). 631.

Abell, J. M., Özkundakci, D., & Hamilton, D. P. (2010). Nitrogen and Phosphorus Limitation of Phytoplankton Growth in New Zealand Lakes : Implications for Eutrophication Control. *Ecosystems*, *13*(7), 966-977. https://doi.org/10.1007/s10021-010-9367-9

Abell, J. M., van Dam-Bates, P., Özkundakci, D., & Hamilton, D. P. (2020). Reference and current Trophic Level Index of New Zealand lakes : Benchmarks to inform lake management and assessment. *New Zealand Journal of Marine and Freshwater Research*, *54*(4), 636-657. https://doi.org/10.1080/00288330.2020.1726974

Air-Water Exchange. (2005). In R. P. Schwarzenbach, P. M. Gschwend, & D. M. Imboden, *Environmental Organic Chemistry* (2nd ed., p. 887-943). John Wiley & Sons, Inc. https://doi.org/10.1002/0471649643.ch20

Aitchison, P. A., & Butt, V. S. (1973). The Relation between the Synthesis of Inorganic Polyphosphate and Phosphate Uptake by *Chlorella vulgaris*. *Journal of Experimental Botany*, *24*(3), 497-510. https://doi.org/10.1093/jxb/24.3.497

Alboresi, A., Storti, M., Cendron, L., & Morosinotto, T. (2019). Role and regulation of class-C flavodiiron proteins in photosynthetic organisms. *Biochemical Journal*, *476*(17), 2487-2498. https://doi.org/10.1042/BCJ20180648

Ali, M., Rathnayake, R. M. L. D., Zhang, L., Ishii, S., Kindaichi, T., Satoh, H., Toyoda, S., Yoshida, N., & Okabe, S. (2016). Source identification of nitrous oxide emission pathways from a single-stage nitritation-anammox granular reactor. *Water Research*, *102*, 147-157. https://doi.org/10.1016/j.watres.2016.06.034

Almeida, C. C., Romão, C. V., Lindley, P. F., Teixeira, M., & Saraiva, L. M. (2006). The Role of the Hybrid Cluster Protein in Oxidative Stress Defense. *Journal of Biological Chemistry*, *281*(43), 32445-32450. https://doi.org/10.1074/jbc.M605888200

Almeida, C., González, S. O., Mallea, M., & González, P. (2012). A recreational water quality index using chemical, physical and microbiological parameters. *Environmental Science and Pollution Research*, *19*(8), 3400-3411. https://doi.org/10.1007/s11356-012-0865-5

Arévalo-Martínez, D. L., Kock, A., Löscher, C. R., Schmitz, R. A., & Bange, H. W. (2015a). Massive nitrous oxide emissions from the tropical South Pacific Ocean. *Nature Geoscience*, *8*(7), 530-533. https://doi.org/10.1038/ngeo2469

Arévalo-Martínez, D. L., Kock, A., Löscher, C. R., Schmitz, R. A., Stramma, L., & Bange, H. W. (2015b). Influence of mesoscale eddies on the distribution of nitrous oxide in the eastern tropical South Pacific. *Biogeosciences Discussions*, *12*(12), 9243-9273. https://doi.org/10.5194/bgd-12-9243-2015

Arp, D., Whittaker, M., Hommes, N., Arciero, D., Sayavedra-Soto, L., Norton, J., Klotz, M., Hooper, A., Hauser, L., Land, M., Lao, V., Regala, W., Larimer, F., Lamerdin, J., &

Chain, P. (2003). Complete Genome Sequence of the Ammonia-Oxidizing Bacterium and Obligate Chemolithoautotroph Nitrosomonas europaea. *J. BACTERIOL.*, *185*, 15.

Assessment of the eutrophication susceptibility of New Zealand's estuaries. (2019, May 1). Ministry for the Environment. https://environment.govt.nz/publications/assessment-of-the-eutrophication-susceptibility-of-new-zealands-estuaries/

Aubriot, L., Zabaleta, B., Bordet, F., Sienra, D., Risso, J., Achkar, M., & Somma, A. (2020). Assessing the origin of a massive cyanobacterial bloom in the Río de la Plata (2019) : Towards an early warning system. *Water Research*, *181*, 115944. https://doi.org/10.1016/j.watres.2020.115944

Bartram, D., Short, M. D., & Ebie, Y. (2019). *2019 Refinement to the 2006 IPCC Guidelines for National Greenhouse Gas Inventories—Volume 5 Waste—Chapter 6 : Wastewater Treatment and Discharge*. Intergovernmental Panel on Climate Change.

Bartram, J., & Rees, G. (Eds.). (1999). *Monitoring Bathing Waters : A Practical Guide to the Design and Implementation of Assessments and Monitoring Programmes*. CRC Press. https://doi.org/10.4324/9780203478264

Bauer, S. K., Grotz, L. S., Connelly, E. B., & Colosi, L. M. (2016). Reevaluation of the global warming impacts of algae-derived biofuels to account for possible contributions of nitrous oxide. *Bioresource Technology*, *218*, 196-201. https://doi.org/10.1016/j.biortech.2016.06.058

Béchet, Q., Chambonnière, P., Shilton, A., Guizard, G., & Guieysse, B. (2015). Algal productivity modeling : A step toward accurate assessments of full-scale algal cultivation: Toward Accurate Algal Productivity Predictions. *Biotechnology and Bioengineering*, *112*(5), 987-996. https://doi.org/10.1002/bit.25517

Bellido-Pedraza, C. M., Calatrava, V., Sanz-Luque, E., Tejada-Jiménez, M., Llamas, Á., Plouviez, M., Guieysse, B., Fernández, E., & Galván, A. (2020). Chlamydomonas reinhardtii, an Algal Model in the Nitrogen Cycle. *Plants*, *9*(7), 903. https://doi.org/10.3390/plants9070903

Beusen, A. H. W., Bouwman, A. F., Van Beek, L. P. H., Mogollón, J. M., & Middelburg, J. J. (2016). Global riverine N and P transport to ocean increased during the 20th century despite increased retention along the aquatic continuum. *Biogeosciences*, *13*(8), 2441-2451. https://doi.org/10.5194/bg-13-2441-2016

Borowitzka, M. A. (2012). Phycology. In John Wiley & Sons, Ltd (Ed.), *ELS* (p. a0000334.pub3). John Wiley & Sons, Ltd. https://doi.org/10.1002/9780470015902.a0000334.pub3

Burlacot, A., Richaud, P., Gosset, A., Li-Beisson, Y., & Peltier, G. (2020). Algal photosynthesis converts nitric oxide into nitrous oxide. *Proceedings of the National Academy of Sciences*, *117*(5), 2704-2709. https://doi.org/10.1073/pnas.1915276117

Burns, N., Graham, B., & Eddie, B. (2000). *Protocol for Monitoring Trophic Levels of New Zealand Lakes and Reservoirs* (p. 130). Ministry for the Environment.

Butler, J. H., & Elkins, J. W. (1991). An automated technique for the measurement of dissolved N20 in natural waters. *Marine Chemistry, 34*, 47-61.

Buxton, A. S., Groombridge, J. J., & Griffiths, R. A. (2017). Is the detection of aquatic environmental DNA influenced by substrate type? *PLOS ONE, 12*(8), e0183371. https://doi.org/10.1371/journal.pone.0183371

Calatrava, V. (2018). *Nitrogen Nutrition in Algae : Unraveling Pieces of the Nitrogen Assimilation Puzzle and its Regulation in the Model Alga Chlamydomonas reinhardtii*. University of Cordoba.

Calatrava, V., Chamizo-Ampudia, A., Sanz-Luque, E., Ocaña-Calahorro, F., Llamas, A., Fernandez, E., & Galvan, A. (2017). How Chlamydomonas handles nitrate and the nitric oxide cycle. *Journal of Experimental Botany, 68*(10), 2593-2602. https://doi.org/10.1093/jxb/erw507

Canfield Jr., D. E., & Bachmann, R. W. (1981). Prediction of Total Phosphorus Concentrations, Chlorophyll *a*, and Secchi Depths in Natural and Artificial Lakes. *Canadian Journal of Fisheries and Aquatic Sciences, 38*(4), 414-423. https://doi.org/10.1139/f81-058

Carlson, R. E. (1977). A trophic state index for lakes. *Limnology and Oceanography*, *22*(2), 361-369. https://doi.org/10.4319/lo.1977.22.2.0361

Carpenter, S. R., Caraco, N. F., Correll, D. L., Howarth, R. W., Sharpley, A. N., & Smith, V. H. (1998). Nonpoint pollution of surface waters with phosphorous and nitrogen. *Ecological Applications, 8*, 559-568.

Carpenter, S. R., Stanley, E. H., & Vander Zanden, M. J. (2011). State of the World's Freshwater Ecosystems : Physical, Chemical, and Biological Changes. *Annual Review of Environment and Resources, 36*(1), 75-99. https://doi.org/10.1146/annurev-environ-021810-094524

Cauthier, D. A., & Turpin, D. H. (1994). *Lnorganic Phosphate (Pi) Enhancement of Dark Respiration in the Pi-Limited Green Alga Selenastrum minufum'. 104*, 9.

Chamizo-Ampudia, A., Sanz-Luque, E., Llamas, Á., Ocaña-Calahorro, F., Mariscal, V., Carreras, A., Barroso, J. B., Galván, A., & Fernández, E. (2016). A dual system formed by the ARC and NR molybdoenzymes mediates nitrite-dependent NO production in *Chlamydomonas* : *Chlamydomonas* ARC and NR in NO production. *Plant, Cell & Environment, 39*(10), 2097-2107. https://doi.org/10.1111/pce.12739

Chapra, S. C., & Dobson, H. F. H. (1981). Quantification of the Lake Trophic Typologies of Naumann (Surface Quality) and Thienemann (Oxygen) with Special Reference to the Great Lakes. *Journal of Great Lakes Research, 7*(2), 182-193. https://doi.org/10.1016/S0380-1330(81)72044-6

Chaux, F., Burlacot, A., Mekhalfi, M., Auroy, P., Blangy, S., Richaud, P., & Peltier, G. (2017). Flavodiiron Proteins Promote Fast and Transient O_2 Photoreduction in *Chlamydomonas*. *Plant Physiology, 174*(3), 1825-1836. https://doi.org/10.1104/pp.17.00421

Chislock, M. F., Doster, E., Zitomer, R. A., & Wilson, A. E. (2013). Eutrophication : Causes, Consequences, and Controls in Aquatic Ecosystems. *Nature Education Knowledge*, *4*(4). https://www.nature.com/scitable/knowledge/library/eutrophication-causes-consequences-and-controls-in-aquatic-102364466/

Ciais, P., Sabine, C., Bala, G., Bopp, L., Brovkin, V., Canadell, A. J., Chhabra, R., DeFries, J., Galloway, J., Heimann, M., Jones, C., Le Quéré, C., Myneni, R. B., Piao, S., & Thornton, P. (2013). Carbon and Other Biogeochemical Cycles. In *Climate Change 2013 : The Physical Science Basis. Contribution of Working Group I to the Fifth Assessment Report of the Intergovernmental Panel on Climate Change.* (Cambridge University Press).

Cohen, Y., & Gordon, L. I. (1978). Nitrous oxide in the oxygen minimum of the eastern tropical North Pacific : Evidence for its consumption during denitrification and possible mechanisms for its production. *Deep Sea Research*, *25*(6), 509-524. https://doi.org/10.1016/0146-6291(78)90640-9

Conley, D. J., Paerl, H. W., Howarth, R. W., Boesch, D. F., Seitzinger, S. P., Havens, K. E., Lancelot, C., & Likens, G. E. (2009). Controlling Eutrophication : Nitrogen and Phosphorus. *Science*, *323*(5917), 1014-1015. https://doi.org/10.1126/science.1167755

Convention for the protection of the marine environment of the North-East Atlantic, (1998).

Daims, H., Lücker, S., & Wagner, M. (2016). A New Perspective on Microbes Formerly Known as Nitrite-Oxidizing Bacteria. *Trends in Microbiology*, *24*(9), 699-712. http://dx.doi.org/10.1016/j.tim.2016.05.004

Davies-Colley, R., Vant, W., & Smith, D. (1993). *Colour and clarity of natural waters : Science and management of optical water quality* (Ellis Horwood Ltd).

De Klein, C., Novoa, R. S. A., Ogle, S., Smith, K. A., Rochette, P., Wirth, T. C., McConkey, B. G., Mosier, A., & Rypdal, K. (2006). *2006 IPCC Guidelines for National Greenhouse Gas Inventories—Volume 4 Agriculture, Forestry and Other Land Use—Chapter 11 : N_2O Emissions from Managed Soils, and CO_2 Emissions from Lime and Urea Application*. Intergovernmental Panel on Climate Change.

Dean, J. V., & Harper, J. E. (1986). Nitric Oxide and Nitrous Oxide Production by Soybean and Winged Bean during the *in Vivo* Nitrate Reductase Assay. *Plant Physiology*, *82*(3), 718-723. https://doi.org/10.1104/pp.82.3.718

Deemer, B. R., Harrison, J. A., Li, S., Beaulieu, J. J., DelSontro, T., Barros, N., Bezerra-Neto, J. F., Powers, S. M., dos Santos, M. A., & Vonk, J. A. (2016). Greenhouse Gas Emissions from Reservoir Water Surfaces : A New Global Synthesis. *BioScience*, *66*(11), 949-964. https://doi.org/10.1093/biosci/biw117

DelSontro, T., Beaulieu, J. J., & Downing, J. A. (2018). Greenhouse gas emissions from lakes and impoundments : Upscaling in the face of global change. *Limnology and Oceanography Letters*, *3*(3), 64-75. https://doi.org/10.1002/lol2.10073

Diaz, R. J. (Ed.). (2016). Anoxia, Hypoxia, And Dead Zones. In *Encyclopedia of Estuaries* (p. 19-26). Springer Netherlands. https://doi.org/10.1007/978-94-017-8801-4

Domogalla, B. P., Fred, E. B., & Peterson, W. H. (1926). Seasonal Variations in the Ammonia and Nitrate Content of Lake Waters. *Journal - American Water Works Association*, *15*(4), 369-385. https://doi.org/10.1002/j.1551-8833.1926.tb12541.x

Downing, J. A., Prairie, Y. T., Cole, J. J., Duarte, C. M., Tranvik, L. J., Striegl, R. G., McDowell, W. H., Kortelainen, P., Caraco, N. F., Melack, J. M., & Middelburg, J. J. (2006). The global abundance and size distribution of lakes, ponds, and impoundments. *Limnology and Oceanography*, *51*(5), 2388-2397. https://doi.org/10.4319/lo.2006.51.5.2388

Duarte, C. M., Conley, D. J., Carstensen, J., & Sánchez-Camacho, M. (2009). Return to Neverland : Shifting Baselines Affect Eutrophication Restoration Targets. *Estuaries and Coasts*, *32*(1), 29-36. https://doi.org/10.1007/s12237-008-9111-2

Elser, J. J., Bracken, M. E. S., Cleland, E. E., Gruner, D. S., Harpole, W. S., Hillebrand, H., Ngai, J. T., Seabloom, E. W., Shurin, J. B., & Smith, J. E. (2007). Global analysis of nitrogen and phosphorus limitation of primary producers in freshwater, marine and terrestrial ecosystems. *Ecology Letters*, *10*(12), 1135-1142. https://doi.org/10.1111/j.1461-0248.2007.01113.x

Erisman, J. W., Sutton, M. A., Galloway, J., Klimont, Z., & Winiwarter, W. (2008). How a century of ammonia synthesis changed the world. *Nature Geoscience*, *1*, 636-639. https://doi.org/10.1038/ngeo325

García-Lledó, A., Vilar-Sanz, A., Trias, R., Hallin, S., & Baneras, L. (2011). Genetic potential for N_2O emissions from the sediment of a free water surface constructed wetland. *Water Research*, *45*(17), 5621-5632. https://doi.org/10.1016/j.watres.2011.08.025

Garrido-Amador, P., Kniaziuk, M., Vekeman, B., & Kartal, B. (2021). Learning from microorganisms : Using new insights in microbial physiology for sustainable nitrogen management. *Current Opinion in Biotechnology*, *67*, 42-48. https://doi.org/10.1016/j.copbio.2020.12.017

Gérin, S., Mathy, G., Blomme, A., Franck, F., & Sluse, F. E. (2010). Plasticity of the mitoproteome to nitrogen sources (nitrate and ammonium) in Chlamydomonas reinhardtii : The logic of Aox1 gene localization. *Biochimica et Biophysica Acta (BBA) - Bioenergetics*, *1797*(6-7), 994-1003. https://doi.org/10.1016/j.bbabio.2010.02.034

Glibert, P. M. (2017). Eutrophication, harmful algae and biodiversity—Challenging paradigms in a world of complex nutrient changes. *Marine Pollution Bulletin*, *124*(2), 591-606. https://doi.org/10.1016/j.marpolbul.2017.04.027

Glibert, P. M., Fullerton, D., Burkholder, J. M., Cornwell, J. C., & Kana, T. M. (2011). Ecological Stoichiometry, Biogeochemical Cycling, Invasive Species, and Aquatic Food Webs : San Francisco Estuary and Comparative Systems. *Reviews in Fisheries Science*, *19*(4), 358-417. https://doi.org/10.1080/10641262.2011.611916

Glibert, P. M., Maranger, R., Sobota, D. J., & Bouwman, L. (2014). The Haber Bosch–harmful algal bloom (HB–HAB) link. *Environmental Research Letters*, *9*(10), 105001. https://doi.org/10.1088/1748-9326/9/10/105001

Goldberg, C. S., Turner, C. R., Deiner, K., Klymus, K. E., Thomsen, P. F., Murphy, M. A., Spear, S. F., McKee, A., Oyler-McCance, S. J., Cornman, R. S., Laramie, M. B., Mahon, A. R., Lance, R. F., Pilliod, D. S., Strickler, K. M., Waits, L. P., Fremier, A. K., Takahara, T., Herder, J. E., & Taberlet, P. (2016). Critical considerations for the application of environmental DNA methods to detect aquatic species. *Methods in Ecology and Evolution*, *7*(11), 1299-1307. https://doi.org/10.1111/2041-210X.12595

Gonzalez-Ballester, D., Camargo, A., & Fernandez, E. (2004). Ammonium transporter genes in Chlamydomonas : The nitrate-specific regulatory gene Nit2 is involved in Amt1;1 expression. *Plant Molecular Biology*, *56*(6), 863-878. https://doi.org/10.1007/s11103-004-5292-7

Grossman, A. R., & Aksoy, M. (2015). Algae in a phosphorus-limited landscape. In W. C. Plaxton & H. Lambers (Eds.), *Annual Plant Reviews Volume 48* (p. 337-374). John Wiley & Sons, Inc. https://doi.org/10.1002/9781118958841.ch12

Guieysse, B., Plouviez, M., Coilhac, M., & Cazali, L. (2013). Nitrous Oxide (N_2O) production in axenic *Chlorella vulgaris* microalgae cultures : Evidence, putative pathways, and potential environmental impacts. *Biogeosciences*, *10*(10), 6737-6746. https://doi.org/10.5194/bg-10-6737-2013

Guildford, S. J., & Hecky, R. E. (2000). Total nitrogen, total phosphorus, and nutrient limitation in lakes and oceans : Is there a common relationship? *Limnology and Oceanography*, *45*(6), 1213-1223. https://doi.org/10.4319/lo.2000.45.6.1213

Guillard, R. R., & Sieracki, M. S. (2005). Counting cells in cultures with the light microscope. In *Algal culturing techniques* (p. 239-252). Elsevier.

Hahn, J., & Junge, C. (1977). *Atmospheric Nitrous Oxide : A Critical Review*. 190-214.

Hakata, M., Takahashi, M., Zumft, W., Sakamoto, A., & Morikawa, H. (2003). Conversion of the Nitrate Nitrogen and Nitrogen Dioxide to Nitrous Oxides in Plants. *Acta Biotechnologica*, *23*(23), 249-257. https://doi.org/10.1002/abio.200390032

Hallin, S., Philippot, L., Löffler, F. E., Sanford, R. A., & Jones, C. M. (2018). Genomics and Ecology of Novel N_2O-Reducing Microorganisms. *Trends in Microbiology*, *26*(1), 43-55. https://doi.org/10.1016/j.tim.2017.07.003

Hamilton, B. (2003). *A review of short-term management options for Lakes Rotorua and Rotoiti* (p. 69). Ministry for the Environment.

Hamilton, J. F., & Lewis, A. C. (2006). Chromatographic Methods. In D. E. Heard (Ed.), *Analytical Techniques for Atmospheric Measurement* (p. 361-405). Blackwell Publishing. https://doi.org/10.1002/9780470988510.ch8

Han, P., Wu, D., Sun, D., Zhao, M., Wang, M., Wen, T., Zhang, J., Hou, L., Liu, M., Klümper, U., Zheng, Y., Dong, H.-P., Liang, X., & Yin, G. (2021). N_2O and NO_y production by the comammox bacterium Nitrospira inopinata in comparison with canonical ammonia oxidizers. *Water Research*, *190*, 116728. https://doi.org/10.1016/j.watres.2020.116728

Hanson, M. J., & Stefan, H. G. (1984). Side effects of 58 years of copper sulfate treatment of the Fairmont Lakes, Minnesota. *Journal of the American Water Resources Association*, *20*(6), 889-900. https://doi.org/10.1111/j.1752-1688.1984.tb04797.x

Harris, E. H. (2009). Chlamydomonas in the laboratory. In *The Chlamydomonas Sourcebook : Introduction to Chlamydomonas and Its Laboratory Use* (Vol. 1, p. 241-292). Academic Press.

Hatzenpichler, R. (2012). Diversity, Physiology, and Niche Differentiation of Ammonia-Oxidizing Archaea. *Applied and Environmental Microbiology*, *78*(21), 7501-7510. https://doi.org/10.1128/AEM.01960-12

Hayatsu, M., Tago, K., & Saito, M. (2008). Various players in the nitrogen cycle : Diversity and functions of the microorganisms involved in nitrification and denitrification. *Soil Science and Plant Nutrition*, *54*(1), 33-45. https://doi.org/10.1111/j.1747-0765.2007.00195.x

Hergoualc'h, K., Akiyama, H., Bernoux, M., Chirinda, N., del Prado, A., Kasimir, Å., MacDonald, J. D., Ogle, S. M., Regina, K., & van der Weerden, T. J. (2019). *2019 Refinement to the 2006 IPCC Guidelines for National Greenhouse Gas Inventories—Volume 4 Agriculture, Forestry and Other Land Use—Chapter 11 : N_2O Emissions from Managed Soils, and CO_2 Emissions from Lime and Urea Application*. Intergovernmental Panel on Climate Change.

Higgins, S. A., Welsh, A., Orellana, L. H., Konstantinidis, K. T., Chee-Sanford, J. C., Sanford, R. A., Schadt, C. W., & Löffler, F. E. (2016). Detection and Diversity of Fungal Nitric Oxide Reductase Genes (*p450nor*) in Agricultural Soils. *Applied and Environmental Microbiology*, *82*(10), 2919-2928. https://doi.org/10.1128/AEM.00243-16

Howarth, R. W., & Marino, R. (2006). Nitrogen as the limiting nutrient for eutrophication in coastal marine ecosystems : Evolving views over three decades. *Limnology and Oceanography*, *51*(1part2), 364-376. https://doi.org/10.4319/lo.2006.51.1_part_2.0364

Hu, M., Chen, D., & Dahlgren, R. A. (2016). Modeling nitrous oxide emission from rivers : A global assessment. *Global Change Biology*, *22*(11), 3566-3582. https://doi.org/10.1111/gcb.13351

Huang, F., Pan, L., He, Z., Zhang, M., & Zhang, M. (2020). Identification, interactions, nitrogen removal pathways and performances of culturable heterotrophic nitrification-aerobic denitrification bacteria from mariculture water by using cell culture and metagenomics. *Science of The Total Environment*, *732*, 139268. https://doi.org/10.1016/j.scitotenv.2020.139268

Huang, J., Zhang, Y., Arhonditsis, G. B., Gao, J., Chen, Q., & Peng, J. (2020). The magnitude and drivers of harmful algal blooms in China's lakes and reservoirs : A national-scale characterization. *Water Research*, *181*, 115902. https://doi.org/10.1016/j.watres.2020.115902

Hudson, J. J., Taylor, W. D., & Schindler, D. W. (2000). Phosphate concentrations in lakes. *Nature*, *406*(6791), 54-56. https://doi.org/10.1038/35017531

Huszar, V. L. M., Caraco, N. F., Roland, F., & Cole, J. (2006). Nutrient–chlorophyll relationships in tropical– subtropical lakes : Do temperate models fit? *Biogeochemistry*, *79*, 239-250. https://doi.org/10.1007/s10533-006-9007-9

Jacoby, J. M., Lynch, D. D., Welch, E. B., & Perkins, M. A. (1982). Internal phosphorus loading in a shallow eutrophic lake. *Water Research*, *16*(6), 911-919. https://doi.org/10.1016/0043-1354(82)90022-7

Janssen, A. B. G., Teurlincx, S., Beusen, A. H. W., Huijbregts, M. A. J., Rost, J., Schipper, A. M., Seelen, L. M. S., Mooij, W. M., & Janse, J. H. (2019). PCLake+ : A process-based ecological model to assess the trophic state of stratified and non-stratified freshwater lakes worldwide. *Ecological Modelling*, *396*, 23-32. https://doi.org/10.1016/j.ecolmodel.2019.01.006

Jansson, B. P. M., Malandrin, L., & Johansson, H. E. (2000). Cell Cycle Arrest in Archaea by the Hypusination Inhibitor N^1 -Guanyl-1,7-Diaminoheptane. *Journal of Bacteriology*, *182*(4), 1158-1161. https://doi.org/10.1128/JB.182.4.1158-1161.2000

Jetoo, S., Grover, V., & Krantzberg, G. (2015). The Toledo Drinking Water Advisory : Suggested Application of the Water Safety Planning Approach. *Sustainability*, *7*(8), 9787-9808. https://doi.org/10.3390/su7089787

Jin, X., Wang, S., Pang, Y., Zhao, H., & Zhou, X. (2005). The adsorption of phosphate on different trophic lake sediments. *Colloids and Surfaces A: Physicochemical and Engineering Aspects*, *254*(1-3), 241-248. https://doi.org/10.1016/j.colsurfa.2004.11.016

Jokel, M., Johnson, X., Peltier, G., Aro, E.-M., & Allahverdiyeva, Y. (2018). Hunting the main player enabling *Chlamydomonas reinhardtii* growth under fluctuating light. *The Plant Journal*, *94*(5), 822-835. https://doi.org/10.1111/tpj.13897

Jokel, M., Kosourov, S., Battchikova, N., Tsygankov, A. A., Aro, E. M., & Allahverdiyeva, Y. (2015). *Chlamydomonas* Flavodiiron Proteins Facilitate Acclimation to Anoxia During Sulfur Deprivation. *Plant and Cell Physiology*, *56*(8), 1598-1607. https://doi.org/10.1093/pcp/pcv085

Jung, M.-Y., Gwak, J.-H., Rohe, L., Giesemann, A., Kim, J.-G., Well, R., Madsen, E. L., Herbold, C. W., Wagner, M., & Rhee, S.-K. (2019). Indications for enzymatic denitrification to N_2O at low pH in an ammonia-oxidizing archaeon. *The ISME Journal*, *13*(10), 2633-2638. https://doi.org/10.1038/s41396-019-0460-6

Kalff, J. (1983). Phosphorus limitation in some tropical African lakes. *Hydrobiologia*, *100*(1), 101-112. https://doi.org/10.1007/BF00027425

Kamp, A., Stief, P., Knappe, J., & de Beer, D. (2013). Response of the Ubiquitous Pelagic Diatom Thalassiosira weissflogii to Darkness and Anoxia. *PLoS ONE*, *8*(12), e82605. https://doi.org/10.1371/journal.pone.0082605

Kampschreur, M. J., Poldermans, R., Kleerebezem, R., van der Star, W. R. L., Haarhuis, R., Abma, W. R., Jetten, M. S. M., & van Loosdrecht, M. C. M. (2009). Emission of nitrous oxide and nitric oxide from a full-scale single-stage nitritation-anammox reactor. *Water Science and Technology*, *60*(12), 3211-3217. https://doi.org/10.2166/wst.2009.608

Kar, D. (2013). *Wetlands and Lakes of the World*. Springer India. https://doi.org/10.1007/978-81-322-1023-8

Kaye, Y., Huang, W., Clowez, S., Saroussi, S., Idoine, A., Sanz-Luque, E., & Grossman, A. R. (2019). The mitochondrial alternative oxidase from Chlamydomonas reinhardtii enables survival in high light. *Journal of Biological Chemistry*, *294*(4), 1380-1395. https://doi.org/10.1074/jbc.RA118.004667

Kim, S.-W., Fushinobu, S., Zhou, S., Wakagi, T., & Shoun, H. (2009). Eukaryotic nirK Genes Encoding Copper-Containing Nitrite Reductase : Originating from the Protomitochondrion? *Applied and Environmental Microbiology*, *75*(9), 2652-2658. https://doi.org/10.1128/AEM.02536-08

Kock, A., Arévalo-Martínez, D. L., Löscher, C. R., & Bange, H. W. (2016). Extreme N_2O accumulation in the coastal oxygen minimum zone off Peru. *Biogeosciences*, *13*(3), 827-840. https://doi.org/10.5194/bg-13-827-2016

Kuypers, M. M. M., Marchant, H. K., & Kartal, B. (2018). The microbial nitrogen-cycling network. *Nature Reviews Microbiology*, *16*(5), 263-276. https://doi.org/10.1038/nrmicro.2018.9

Lake Horowhenua Water Quality. (2021). Land, Air, Water Aotearoa (LAWA). https://www.lawa.org.nz/explore-data/manawatū-whanganui-region/lakes/lake-horowhenua/

Lake Trophic Level Index. (2020). Land, Air, Water Aotearoa (LAWA). https://www.lawa.org.nz/learn/factsheets/lake-trophic-level-index/

Land Cover. (2021). Land, Air, Water Aotearoa (LAWA). https://www.lawa.org.nz/explore-data/land-cover/

Lauerwald, R., Regnier, P., Figueiredo, V., Enrich-Prast, A., Bastviken, D., Lehner, B., Maavara, T., & Raymond, P. (2019). Natural Lakes Are a Minor Global Source of N_2O to the Atmosphere. *Global Biogeochemical Cycles*, *33*(12), 1564-1581. https://doi.org/10.1029/2019GB006261

Li, J., Wang, Z., Cao, X., Wang, Z., & Zheng, Z. (2015). Effect of orthophosphate and bioavailability of dissolved organic phosphorous compounds to typically harmful cyanobacterium Microcystis aeruginosa. *Marine Pollution Bulletin*, *92*(1-2), 52-58. https://doi.org/10.1016/j.marpolbul.2015.01.001

Liu, L., & Xu, M. (2016). Microbial biomass in sediments affects greenhouse gas effluxes in Poyang Lake in China. *Journal of Freshwater Ecology*, *31*(1), 109-121. https://doi.org/10.1080/02705060.2015.1046511

Löscher, C. R., Kock, A., Könneke, M., LaRoche, J., Bange, H. W., & Schmitz, R. A. (2012). Production of oceanic nitrous oxide by ammonia-oxidizing archaea. *Biogeosciences*, *9*(7), 2419-2429. https://doi.org/10.5194/bg-9-2419-2012

Maavara, T., Lauerwald, R., Laruelle, G. G., Akbarzadeh, Z., Bouskill, N. J., Van Cappellen, P., & Regnier, P. (2019). Nitrous oxide emissions from inland waters : Are IPCC

estimates too high? *Global Change Biology*, *25*(2), 473-488. https://doi.org/10.1111/gcb.14504

Mahan, K. M., Odorn, O. W., & Herrin, D. L. (2005). Controlling fungal contamination in *Chlamydomonas reinhardtii* cultures. *BioTechniques*, *39*(4), 457-458. https://doi.org/10.2144/000112022

Masson-Delmotte, V., Zhai, P., Pirani, A., Connors, S. L., Péan, Berger, S., Caud, N., Chen, Y., Goldfarb, L., Gomis, M. I., Huang, M., Leitzell, K., Lonnoy, E., Matthews, J. B. R., Maycock, T. K., Waterfield, T., Yelekçi, O., Yu, R., & Zhou, B. (2021). IPCC, 2021 : Summary for Policymakers. In *Climate Change 2021 : The Physical Science Basis. Contribution of Working Group I to the Sixth Assessment Report of the Intergovernmental Panel on Climate Change* (Cambridge University Press).

McCauley, E., Downing, J. A., & Watson, S. (1989). Sigmoid Relationships between Nutrients and Chlorophyll among Lakes. *Canadian Journal of Fisheries and Aquatic Sciences*, *46*(7), 1171-1175. https://doi.org/10.1139/f89-152

McCrackin, M. L., & Elser, J. J. (2011). Greenhouse gas dynamics in lakes receiving atmospheric nitrogen deposition : GREENHOUSE GASES IN LAKES. *Global Biogeochemical Cycles*, *25*(4). https://doi.org/10.1029/2010GB003897

Mehner, T., Benndorf, J., Kasprzak, P., & Koschel, R. (2002). Biomanipulation of lake ecosystems : Successful applications and expanding complexity in the underlying science: *Biomanipulation today - summary and review*. *Freshwater Biology*, *47*(12), 2453-2465. https://doi.org/10.1046/j.1365-2427.2002.01003.x

Mengis, M., Gächter, R., & Wehrli, B. (1997). Sources and sinks of nitrous oxide (N_2O) in deep lakes. *Biogeochemistry*, *38*, 281-301. https://doi.org/10.1023/A:1005814020322

Meybeck, M. (1995). Global Distribution of Lakes. In A. Lerman, D. M. Imboden, & J. R. Gat (Eds.), *Physics and Chemistry of Lakes* (p. 1-35). Springer Berlin Heidelberg. https://doi.org/10.1007/978-3-642-85132-2_1

Miao, Y., Huang, J., Duan, H., Meng, H., Wang, Z., Qi, T., & Wu, Q. L. (2020). Spatial and seasonal variability of nitrous oxide in a large freshwater lake in the lower reaches of the Yangtze River, China. *Science of The Total Environment*, *721*, 137716. https://doi.org/10.1016/j.scitotenv.2020.137716

Ministry for the Environment. (2022). *New Zealand's Greenhouse Gas Inventory 1990–2020*. Wellington: Ministry for the Environment.

Ministry for the Environment, & Stats NZ. (2020). *New Zealand's Environmental Reporting Series : Our freshwater 2020* (ME 1490). Ministry for the Environment. https://www.mfe.govt.nz/sites/default/files/media/Environmental%20reporting/our-freshwater-2020.pdf

Morell, J. M., Capella, J., Mercado, A., Bauzá, J., & Corredor, J. E. (2001). Nitrous oxide fluxes in Caribbean and tropical Atlantic waters : Evidence for near surface production. *Marine Chemistry*, *74*(2-3), 131-143. https://doi.org/10.1016/S0304-4203(01)00011-1

Morgenstern, U., Daughney, C. J., Leonard, G., Gordon, D., Donath, F. M., & Reeves, R. (2015). Using groundwater age and hydrochemistry to understand sources and dynamics of nutrient contamination through the catchment into Lake Rotorua, New Zealand. *Hydrology and Earth System Sciences*, *19*(2), 803-822. https://doi.org/10.5194/hess-19-803-2015

Nalewajko, C., & Murphy, T. P. (2001). Effects of temperature, and availability of nitrogen and phosphorus on the abundance of Anabaena and Microcystis in Lake Biwa, Japan : An experimental approach. *Limnology*, *2*(1), 45-48. https://doi.org/10.1007/s102010170015

Naqvi, S. W. A., Bange, H. W., Farías, L., Monteiro, P. M. S., Scranton, M. I., & Zhang, J. (2009). *Coastal hypoxia/anoxia as a source of CH_4 and N_2O* [Preprint]. Biogeochemistry: Coastal Ocean. https://doi.org/10.5194/bgd-6-9455-2009

Nevison, C. D., Weiss, R. F., & Erickson, D. J. (1995). Global oceanic emissions of nitrous oxide. *Journal of Geophysical Research*, *100*(C8), 15809. https://doi.org/10.1029/95JC00684

National Policy Statement for Freshwater Management, (2020) (testimony of New Zealand Government).

New Zealand & Ministry for the Environment. (2003). *Microbiological water quality guidelines for marine and freshwater recreational areas*. Ministry for the Environment.

Oudot, C., Andrie, C., & Montel, Y. (1990). Nitrous oxide production in the tropical Atlantic Ocean. *Deep-Sea Research*, *37*, 183-202. https://doi.org/10.1016/0198-0149(90)90123-D

Paerl, H. W. (2009). Controlling Eutrophication along the Freshwater–Marine Continuum : Dual Nutrient (N and P) Reductions are Essential. *Estuaries and Coasts*, *32*(4), 593-601. https://doi.org/10.1007/s12237-009-9158-8

Paerl, H. W., Fulton, R. S., Moisander, P. H., & Dyble, J. (2001). Harmful Freshwater Algal Blooms, With an Emphasis on Cyanobacteria. *The Scientific World JOURNAL*, *1*, 76-113. https://doi.org/10.1100/tsw.2001.16

Paerl, H. W., Scott, J. T., McCarthy, M. J., Newell, S. E., Gardner, W. S., Havens, K. E., Hoffman, D. K., Wilhelm, S. W., & Wurtsbaugh, W. A. (2016). It Takes Two to Tango : When and Where Dual Nutrient (N & P) Reductions Are Needed to Protect Lakes and Downstream Ecosystems. *Environmental Science & Technology*, *50*(20), 10805-10813. https://doi.org/10.1021/acs.est.6b02575

Paerl, H. W., Xu, H., McCarthy, M. J., Zhu, G., Qin, B., Li, Y., & Gardner, W. S. (2011). Controlling harmful cyanobacterial blooms in a hyper-eutrophic lake (Lake Taihu, China) : The need for a dual nutrient (N & P) management strategy. *Water Research*, *45*(5), 1973-1983. https://doi.org/10.1016/j.watres.2010.09.018

Papista, E., Acs, E., & Böddi, B. (2002). Chlorophyll-a determination with ethanol – a critical test. *Hydrobiologia*, *485*, 191-198. https://doi.org/10.1023/A:1021329602685

Petroutsos, D., Busch, A., Janßen, I., Trompelt, K., Bergner, S. V., Weinl, S., Holtkamp, M., Karst, U., Kudla, J., & Hippler, M. (2011). The Chloroplast Calcium Sensor CAS Is Required for Photoacclimation in *Chlamydomonas reinhardtii*. *The Plant Cell*, *23*(8), 2950-2963. https://doi.org/10.1105/tpc.111.087973

Pham, L., Lambie, T., & Taiuru, K. (2019). Three Perspectives on Canterbury Freshwater Management. *Policy Quarterly*, *15*(3). https://doi.org/10.26686/pq.v15i3.5686

Pierotti, D., & Rasmussen, R. A. (1980). Nitrous oxide measurements in the eastern tropical Pacific Ocean. *Tellus*, *32*(1), 56-72. https://doi.org/10.1111/j.2153-3490.1980.tb01722.x

Piña-Ochoa, E., & Álvarez-Cobelas, M. (2006). Denitrification in Aquatic Environments : A Cross-system Analysis. *Biogeochemistry*, *81*(1), 111-130. https://doi.org/10.1007/s10533-006-9033-7

Pinay, G., Gascuel, C., Ménesguen, A., Souchon, Y., Le Moal, M., Levain, A., Etrillard, C., Moata, F., Pannard, A., & Souchu, P. (2018). *L'eutrophisation. Manifestations, causes, conséquences et prédictibilité*. éditions Quae. https://doi.org/10.35690/978-2-7592-2757-0

Plouviez, M. (2017). *N_2O synthesis by microalgae : Pathways, significance and mitigations*. Massey University.

Plouviez, M., Chambonnière, P., Shilton, A., Packer, M. A., & Guieysse, B. (2019b). Nitrous oxide (N_2O) emissions during real domestic wastewater treatment in an outdoor pilot-scale high rate algae pond. *Algal Research*, *44*, 101670. https://doi.org/10.1016/j.algal.2019.101670

Plouviez, M., Fernández, E., Grossman, A. R., Sanz-Luque, E., Sells, M., Wheeler, D., & Guieysse, B. (2021). Responses of *Chlamydomonas reinhardtii* during the transition from P-deficient to P-sufficient growth (the P-overplus response) : The roles of the vacuolar transport chaperones and polyphosphate synthesis. *Journal of Phycology*, jpy.13145. https://doi.org/10.1111/jpy.13145

Plouviez, M., & Guieysse, B. (2020). Nitrous oxide emissions during microalgae-based wastewater treatment : Current state of the art and implication for greenhouse gases budgeting. *Water Science and Technology*, *82*(6), 1025-1030. https://doi.org/10.2166/wst.2020.304

Plouviez, M., Shilton, A., Packer, M. A., & Guieysse, B. (2017b). N_2O emissions during microalgae outdoor cultivation in 50 L column photobioreactors. *Algal Research*, *26*, 348-353. https://doi.org/10.1016/j.algal.2017.08.008

Plouviez, M., Shilton, A., Packer, M. A., & Guieysse, B. (2019a). Nitrous oxide emissions from microalgae : Potential pathways and significance. *Journal of Applied Phycology*, *31*(1), 1-8. https://doi.org/10.1007/s10811-018-1531-1

Plouviez, M., Wheeler, D., Shilton, A., Packer, M. A., McLenachan, P. A., Sanz-Luque, E., Ocaña-Calahorro, F., Fernández, E., & Guieysse, B. (2017a). The biosynthesis of nitrous oxide in the green alga *Chlamydomonas reinhardtii*. *The Plant Journal*, *91*(1), 45-56. https://doi.org/10.1111/tpj.13544

Powell, N., Shilton, A., Pratt, S., & Chisti, Y. (2011). Luxury uptake of phosphorus by microalgae in full-scale waste stabilisation ponds. *Water Science and Technology*, *63*(4), 704-709. https://doi.org/10.2166/wst.2011.116

Prosser, J. I., Hink, L., Gubry-Rangin, C., & Nicol, G. W. (2020). Nitrous oxide production by ammonia oxidizers : Physiological diversity, niche differentiation and potential mitigation strategies. *Global Change Biology*, *26*(1), 103-118. https://doi.org/10.1111/gcb.14877

Qin, W., Meinhardt, K. A., Moffett, J. W., Devol, A. H., Virginia Armbrust, E., Ingalls, A. E., & Stahl, D. A. (2017). Influence of oxygen availability on the activities of ammonia-oxidizing archaea : Influence of oxygen availability. *Environmental Microbiology Reports*, *9*(3), 250-256. https://doi.org/10.1111/1758-2229.12525

Rapson, T. D., & Dacres, H. (2014). Analytical techniques for measuring nitrous oxide. *TrAC Trends in Analytical Chemistry*, *54*, 65-74. https://doi.org/10.1016/j.trac.2013.11.004

Ravishankara, A. R., Daniel, J. S., & Portmann, R. W. (2009). Nitrous Oxide (N_2O) : The Dominant Ozone-Depleting Substance Emitted in the 21st Century. *Science*, *326*(5949), 123-125. https://doi.org/10.1126/science.1176985

Reay, D. S., Smith, K. A., & Edwards, A. C. (2003). Nitrous oxide emission from agricultural drainage waters : N_2O IN AGRICULTURAL DRAINAGE WATER. *Global Change Biology*, *9*(2), 195-203. https://doi.org/10.1046/j.1365-2486.2003.00584.x

Reid, R. J., Mimura, T., Ohsumi, Y., Walker, N. A., & Smith, F. A. (2000). Phosphate uptake in *Chara* : Membrane transport via Na/Pi cotransport. *Plant, Cell & Environment*, *23*(2), 223-228. https://doi.org/10.1046/j.1365-3040.2000.00524.x

Ren, Y., Ngo, H. H., Guo, W., Ni, B.-J., & Liu, Y. (2019). Linking the nitrous oxide production and mitigation with the microbial community in wastewater treatment : A review. *Bioresource Technology Reports*, *7*, 100191. https://doi.org/10.1016/j.biteb.2019.100191

Revised 1996 IPCC Guidelines for National Greenhouse Gas Inventories : Reference Manual (Volume 3). (1997). Intergovernmental Panel on Climate Change.

Rigler, F. (1966). *Radiobiological analysis of inorganic phosphorus in lakewater*. *16*, 465-470. https://doi.org/10.1080/03680770.1965.11895717

Ritalahti, K. M., Cruz-García, C., Padilla-Crespo, E., Hatt, J. K., & Löffler, F. E. (2010). RNA Extraction and cDNA Analysis for Quantitative Assessment of Biomarker Transcripts in Groundwater. In K. N. Timmis (Ed.), *Handbook of Hydrocarbon and Lipid Microbiology* (p. 3671-3685). Springer Berlin Heidelberg. https://doi.org/10.1007/978-3-540-77587-4_289

Roberts, J. J., Höök, T. O., Ludsin, S. A., Pothoven, S. A., Vanderploeg, H. A., & Brandt, S. B. (2009). Effects of hypolimnetic hypoxia on foraging and distributions of Lake Erie yellow perch. *Journal of Experimental Marine Biology and Ecology*, *381*, S132-S142. https://doi.org/10.1016/j.jembe.2009.07.017

Ruttenberg, K. C. (2014). The Global Phosphorus Cycle. In *Treatise on Geochemistry* (p. 499-558). Elsevier. https://doi.org/10.1016/B978-0-08-095975-7.00813-5

Santoro, A. E., Buchwald, C., McIlvin, M. R., & Casciotti, K. L. (2011). Isotopic Signature of N_2O Produced by Marine Ammonia-Oxidizing Archaea. *Science*, *333*(6047), 1282-1285. https://doi.org/10.1126/science.1208239

Santos-Beneit, F. (2015). The Pho regulon : A huge regulatory network in bacteria. *Frontiers in Microbiology*, *6*. https://doi.org/10.3389/fmicb.2015.00402

Sanz-Luque, E., Bhaya, D., & Grossman, A. R. (2020a). Polyphosphate : A Multifunctional Metabolite in Cyanobacteria and Algae. *Frontiers in Plant Science*, *11*. https://doi.org/10.3389/fpls.2020.00938

Sanz-Luque, E., Chamizo-Ampudia, A., Llamas, A., Galvan, A., & Fernandez, E. (2015a). Understanding nitrate assimilation and its regulation in microalgae. *Frontiers in Plant Science*, *6*. https://doi.org/10.3389/fpls.2015.00899

Sanz-Luque, E., & Montaigu, A. de. (2018). Phenol-based Extraction of RNA from Chlamydomonas reinhardtii. *Bio-protocol*, *8*(13), e2910. https://doi.org/10.21769/BioProtoc.2910

Sanz-Luque, E., Ocaña-Calahorro, F., de Montaigu, A., Chamizo-Ampudia, A., Llamas, Á., Galván, A., & Fernández, E. (2015b). THB1, a truncated hemoglobin, modulates nitric oxide levels and nitrate reductase activity. *The Plant Journal*, *81*(3), 467-479. https://doi.org/10.1111/tpj.12744

Sanz-Luque, E., Saroussi, S., Huang, W., Akkawi, N., & Grossman, A. R. (2020b). Metabolic control of acclimation to nutrient deprivation dependent on polyphosphate synthesis. *Science Advances*, *6*(40), eabb5351. https://doi.org/10.1126/sciadv.abb5351

Saroussi, S., Karns, D. A. J., Thomas, D. C., Bloszies, C., Fiehn, O., Posewitz, M. C., & Grossman, A. R. (2019). Alternative outlets for sustaining photosynthetic electron transport during dark-to-light transitions. *Proceedings of the National Academy of Sciences*, *116*(23), 11518-11527. https://doi.org/10.1073/pnas.1903185116

Sartory, D. P., & Grobbelaar, J. U. (1984). Extraction of chlorophyll a from freshwater phytoplankton for spectrophotometric analysis. *Hydrobiologia*, *114*(3), 177-187. https://doi.org/10.1007/BF00031869

Schindler, D. W. (1977). Evolution of Phosphorus Limitation in Lakes. *Science*, *195*(4275), 260-262. https://doi.org/10.1126/science.195.4275.260

Schindler, D. W., & Hecky, R. E. (2009). Eutrophication : More Nitrogen Data Needed. *Science*, *324*(5928), 721-725. https://doi.org/10.1126/science.324_721a

Schindler, D. W., Hecky, R. E., Findlay, D. L., Stainton, M. P., Parker, B. R., Paterson, M. J., Beaty, K. G., Lyng, M., & Kasian, S. E. M. (2008). Eutrophication of lakes cannot be controlled by reducing nitrogen input : Results of a 37-year whole-ecosystem experiment. *Proceedings of the National Academy of Sciences*, *105*(32), 11254-11258. https://doi.org/10.1073/pnas.0805108105

Shoun, H., Fushinobu, S., Jiang, L., Kim, S.-W., & Wakagi, T. (2012). Fungal denitrification and nitric oxide reductase cytochrome P450nor. *Philosophical Transactions of the Royal Society B: Biological Sciences*, *367*(1593), 1186-1194. https://doi.org/10.1098/rstb.2011.0335

Smart, D. R., & Bloom, A. J. (2001). Wheat leaves emit nitrous oxide during nitrate assimilation. *Proceedings of the National Academy of Sciences*, *98*(14), 7875-7878. https://doi.org/10.1073/pnas.131572798

Smith, C. J., DeLaune, R. D., & Patrick, W. H. (1983). Nitrous oxide emission from Gulf Coast wetlands. *Geochimica et Cosmochimica Acta*, *47*(10), 1805-1814. https://doi.org/10.1016/0016-7037(83)90028-5

Smith, C. J., & Osborn, A. M. (2009). Advantages and limitations of quantitative PCR (Q-PCR)-based approaches in microbial ecology : Application of Q-PCR in microbial ecology. *FEMS Microbiology Ecology*, *67*(1), 6-20. https://doi.org/10.1111/j.1574-6941.2008.00629.x

Smith, F. A. (1966). Active phosphate uptake by Nitella translucens. *Biochimica et Biophysica Acta (BBA) - Biophysics Including Photosynthesis*, *126*(1), 94-99. https://doi.org/10.1016/0926-6585(66)90040-9

Smith, V. H., Tilman, G. D., & Nekola, J. C. (1999). Eutrophication : Impacts of excess nutrient inputs on freshwater, marine, and terrestrial ecosystems. *Environmental Pollution*, *100*, 179-196.

Smith, V., Wood, S., McBride, C., Atalah, J., & Hamilton, D. (2016). Phosphorus and nitrogen loading restraints are essential for successful eutrophication control of Lake Rotorua, New Zealand. *Inland Waters*, *6*(2), 273-283. https://doi.org/10.5268/IW-6.2.998

Smolders, A. J. P., Lamers, L. P. M., Lucassen, E. C. H. E. T., Van Der Velde, G., & Roelofs, J. G. M. (2006). Internal eutrophication : How it works and what to do about it—a review. *Chemistry and Ecology*, *22*(2), 93-111. https://doi.org/10.1080/02757540600579730

Stein, L. Y., Klotz, M. G., Lancaster, K. M., Nicol, G. W., Qin, W., Schleper, C., Stahl, D., Ward, B. B., & Yoon, S. (2021). Comment on"A Critical Review on Nitrous Oxide Production by Ammonia-Oxidizing Archaea" by Lan Wu, Xueming Chen, Wei Wei, Yiwen Liu, Dongbo Wang, and Bing-Jie Ni. *Environmental Science & Technology*, *55*(1), 797-798. https://doi.org/10.1021/acs.est.0c06792

Sterner, R. W. (2008). On the Phosphorus Limitation Paradigm for Lakes. *International Review of Hydrobiology*, *93*(4-5), 433-445. https://doi.org/10.1002/iroh.200811068

Stief, P., Kamp, A., Thamdrup, B., & Glud, R. N. (2016). Anaerobic Nitrogen Turnover by Sinking Diatom Aggregates at Varying Ambient Oxygen Levels. *Frontiers in Microbiology*, *7*. https://doi.org/10.3389/fmicb.2016.00098

Stow, C. A., Walker, J. T., Cardoch, L., Spence, P., & Geron, C. (2005). N_2O Emissions from Streams in the Neuse River Watershed, North Carolina. *Environmental Science & Technology*, *39*(18), 6999-7004. https://doi.org/10.1021/es0500355

Taberlet, P., Bonin, A., Zinger, L., & Coissac, E. (2018). *Environmental DNA For Biodiversity Research and Monitoring* (Vol. 1). Oxford University Press. https://doi.org/10.1093/oso/9780198767220.001.0001

Tian, H., Xu, R., Canadell, J. G., Thompson, R. L., Winiwarter, W., Suntharalingam, P., Davidson, E. A., Ciais, P., Jackson, R. B., Janssens-Maenhout, G., Prather, M. J., Regnier, P., Pan, N., Pan, S., Peters, G. P., Shi, H., Tubiello, F. N., Zaehle, S., Zhou, F., … Yao, Y. (2020). A comprehensive quantification of global nitrous oxide sources and sinks. *Nature*, *586*(7828), 248-256. https://doi.org/10.1038/s41586-020-2780-0

Tian, L., Cai, Y., & Akiyama, H. (2019). A review of indirect N_2O emission factors from agricultural nitrogen leaching and runoff to update of the default IPCC values. *Environmental Pollution*, *245*, 300-306. https://doi.org/10.1016/j.envpol.2018.11.016

Timilsina, A., Bizimana, F., Pandey, B., Yadav, R. K. P., Dong, W., & Hu, C. (2020). Nitrous Oxide Emissions from Paddies : Understanding the Role of Rice Plants. *Plants*, *9*(2), 180. https://doi.org/10.3390/plants9020180

Timilsina, A., Zhang, C., Pandey, B., Bizimana, F., Dong, W., & Hu, C. (2020). Potential Pathway of Nitrous Oxide Formation in Plants. *Frontiers in Plant Science*, *11*, 1177. https://doi.org/10.3389/fpls.2020.01177

van Lis, R., Brugière, S., Baffert, C., Couté, Y., Nitschke, W., & Atteia, A. (2020). Hybrid cluster proteins in a photosynthetic microalga. *The FEBS Journal*, *287*(4), 721-735. https://doi.org/10.1111/febs.15025

Walker, J. T., Stow, C. A., & Geron, C. (2010). Nitrous Oxide Emissions from the Gulf of Mexico Hypoxic Zone. *Environmental Science & Technology*, *44*(5), 1617-1623. https://doi.org/10.1021/es902058t

Wang, H., Wang, W., Yin, C., Wang, Y., & Lu, J. (2006). Littoral zones as the "hotspots" of nitrous oxide (N_2O) emission in a hyper-eutrophic lake in China. *Atmospheric Environment*, *40*(28), 5522-5527. https://doi.org/10.1016/j.atmosenv.2006.05.032

Wang, J., Vine, C. E., Balasiny, B. K., Rizk, J., Bradley, C. L., Tinajero-Trejo, M., Poole, R. K., Bergaust, L. L., Bakken, L. R., & Cole, J. A. (2016). The roles of the hybrid cluster protein, Hcp and its reductase, Hcr, in high affinity nitric oxide reduction that protects anaerobic cultures of *E scherichia coli* against nitrosative stress : NO reduction by the *E. coli* hybrid cluster protein. *Molecular Microbiology*, *100*(5), 877-892. https://doi.org/10.1111/mmi.13356

Wang, L., Xiao, L., Yang, H., Chen, G., Zeng, H., Zhao, H., & Zhu, Y. (2020). Genome-Wide Identification, Expression Profiling, and Evolution of Phosphate Transporter Gene Family in Green Algae. *Frontiers in Genetics*, *11*, 590947. https://doi.org/10.3389/fgene.2020.590947

Wang, R., Zhang, H., Zhang, W., Zheng, X., Butterbach-Bahl, K., Li, S., & Han, S. (2020). An urban polluted river as a significant hotspot for water–atmosphere exchange of CH_4 and N_2O. *Environmental Pollution*, *264*, 114770. https://doi.org/10.1016/j.envpol.2020.114770

Ward, B. B., Arp, D. J., Klotz, M. G., & American Society for Microbiology (Eds.). (2011). *Nitrification*. ASM Press.

Weathers, P. (1984). N_2O evolution by green algae. *Applied and Environmental Microbiology*, *48*, 1251-1253. https://doi.org/10.1128/aem.48.6.1251-1253.1984

Weathers, P. J., & Niedzielski, J. J. (1986). Nitrous oxide production by cyanobacteria. *Archives of Microbiology*, *146*(2), 204-206. https://doi.org/10.1007/BF00402352

Webb, J. R., Clough, T. J., & Quayle, W. C. (2021). A review of indirect N_2O emission factors from artificial agricultural waters. *Environmental Research Letters*. https://doi.org/10.1088/1748-9326/abed00

Wenk, C. B., Frame, C. H., Koba, K., Casciotti, K. L., Veronesi, M., Niemann, H., Schubert, C. J., Yoshida, N., Toyoda, S., Makabe, A., Zopfi, J., & Lehmann, M. F. (2016). Differential N_2O dynamics in two oxygen-deficient lake basins revealed by stable isotope and isotopomer distributions : Differential N_2O Dynamics in Two Lake Basins. *Limnology and Oceanography*, *61*(5), 1735-1749. https://doi.org/10.1002/lno.10329

Wetzel, R. G. (2001a). RIVERS AND LAKES—THEIR DISTRIBUTION, ORIGINS, AND FORMS. In *Limnology* (p. 15-42). Elsevier. https://doi.org/10.1016/B978-0-08-057439-4.50007-1

Wetzel, R. G. (2001b). SHALLOW LAKES AND PONDS. In *Limnology* (p. 625-630). Elsevier. https://doi.org/10.1016/B978-0-08-057439-4.50024-1

White, E., Law, K., Payne, G., & Pickmere, S. (1985). Nutrient demand and availability among planktonic communities—An attempt to assess nutrient limitation to plant growth in 12 central volcanic plateau lakes. *New Zealand Journal of Marine and Freshwater Research*, *19*(1), 49-62. https://doi.org/10.1080/00288330.1985.9516074

Wiedner, C., Rücker, J., Brüggemann, R., & Nixdorf, B. (2007). Climate change affects timing and size of populations of an invasive cyanobacterium in temperate regions. *Oecologia*, *152*(3), 473-484. https://doi.org/10.1007/s00442-007-0683-5

Wintermans, J. F. G. M., & De Mots, A. (1965). Spectrophotometric characteristics of chlorophylls a and b and their pheophytins in ethanol. *Biochimica et Biophysica Acta*, *109*, 448-453.

Wood, S. A., Briggs, L. R., Sprosen, J., Ruck, J. G., Wear, R. G., Holland, P. T., & Bloxham, M. (2006). Changes in concentrations of microcystins in rainbow trout, freshwater mussels, and cyanobacteria in Lakes Rotoiti and Rotoehu. *Environmental Toxicology*, *21*(3), 205-222. https://doi.org/10.1002/tox.20174

Wood, S. A., Maier, M. Y., Puddick, J., Pochon, X., Zaiko, A., Dietrich, D. R., & Hamilton, D. P. (2017). Trophic state and geographic gradients influence planktonic cyanobacterial diversity and distribution in New Zealand lakes. *FEMS Microbiology Ecology*, *93*(2), fiw234. https://doi.org/10.1093/femsec/fiw234

Wood, S. A., New Zealand, Ministry for the Environment, New Zealand, & Ministry of Health. (2009). *New Zealand guidelines for cyanobacteria in recreational fresh waters : Interim guidelines.* Ministry for the Environment.

Wrage, N., Velthof, G. L., van Beusichem, M. L., & Oenema, O. (2001). Role of nitrifier denitrification in the production of nitrous oxide. *Soil Biology, 33*, 1723-1732.

Wu, L., Chen, X., Wei, W., Liu, Y., Wang, D., & Ni, B.-J. (2020). A Critical Review on Nitrous Oxide Production by Ammonia-Oxidizing Archaea. *Environmental Science & Technology*, *54*(15), 9175-9190. https://doi.org/10.1021/acs.est.0c03948

Wykoff, D. D., Grossman, A. R., Weeks, D. P., Usuda, H., & Shimogawara, K. (1999). Psr1, a nuclear localized protein that regulates phosphorus metabolism in Chlamydomonas. *Proceedings of the National Academy of Sciences*, *96*(26), 15336-15341. https://doi.org/10.1073/pnas.96.26.15336

Xu, H., Paerl, H. W., Qin, B., Zhu, G., & Gaoa, G. (2010). Nitrogen and phosphorus inputs control phytoplankton growth in eutrophic Lake Taihu, China. *Limnology and Oceanography*, *55*(1), 420-432. https://doi.org/10.4319/lo.2010.55.1.0420

Yang, S., Chang, B. X., Warner, M. J., Weber, T. S., Bourbonnais, A. M., Santoro, A. E., Kock, A., Sonnerup, R. E., Bullister, J. L., Wilson, S. T., & Bianchi, D. (2020). Global reconstruction reduces the uncertainty of oceanic nitrous oxide emissions and reveals a vigorous seasonal cycle. *Proceedings of the National Academy of Sciences*, *117*(22), 11954-11960. https://doi.org/10.1073/pnas.1921914117

Yang, X., Wu, X., Hao, H., & He, Z. (2008). Mechanisms and assessment of water eutrophication. *Journal of Zhejiang University SCIENCE B*, *9*(3), 197-209. https://doi.org/10.1631/jzus.B0710626

Zhou, T., Cao, H., Zheng, J., Teng, F., Wang, X., Lou, K., Zhang, X., & Tao, Y. (2020). Suppression of water-bloom cyanobacterium Microcystis aeruginosa by algaecide hydrogen peroxide maximized through programmed cell death. *Journal of Hazardous Materials*, *393*, 122394. https://doi.org/10.1016/j.jhazmat.2020.122394

Zhu, G., Qin, B., Gao, G., Zhang, L., Luo, L., & Zhang, Y. (2007). Effects of hydrodynamics on phosphorus concentrations in water of Lake Taihu, a large, shallow, eutrophic lake of China. In *Eutrophication of Shallow Lakes with Special Reference to Lake Taihu, China* (p. 53-61). Springer Netherlands.

Zhu-Barker, X., Cavazos, A. R., Ostrom, N. E., Horwath, W. R., & Glass, J. B. (2015). The importance of abiotic reactions for nitrous oxide production. *Biogeochemistry*, *126*(3), 251-267. https://doi.org/10.1007/s10533-015-0166-4

Zumft, W. G. (1997). Cell biology and molecular basis of denitrification. *Microbiology and Molecular Biology Reviews : MMBR*, *61*(4), 533-616. https://doi.org/10.1128/.61.4.533-616.1997

9. Appendices

Appendix A. Sources and sinks of N_2O

Table 17: Sources and sinks of N_2O (Tian et al., 2020)

SOURCES	
Anthropogenic	
Direct emissions from agricultural N	Direct soil emissions
	Manure left on pasture
	Manure management
	Aquaculture
Other direct anthropogenic sources	Biomass burning
	Fossil fuels and industry
	Waste and wastewater
Indirect emissions	Atmospheric N deposition on land
	Atmospheric N deposition on ocean
	Estuaries, inland and coastal waters
Perturbed fluxes caused by changes in climate and land cover	Climate effect
	Post deforestation pulse effect
Natural	
Natural soils	
Lightning and atmospheric production	
Estuaries, inland and coastal waters	
Oceans	
SINKS	
Anthropogenic	
Perturbed fluxes caused by changes in CO_2 and land cover	Long-term effect of reduced mature forest area
	CO_2 effects
Natural	
Atmospheric chemical sink	Photolysis
	Reaction with electronically excited atomic oxygen
Surface sink	

Appendix B. Emissions from managed lands

Regarding the indirect emissions due to managed lands, two indirect pathways are considered for the anthropogenic input of N to water bodies: (i) the volatilization of NH_3 and oxides of N and their deposition on water surface and (ii) the leaching and runoff of N from managed land. The IPCC's methodology is based on the three-tiered approach previously described and uses two EFs, one for each pathway, to estimate indirect N_2O emissions from waterbodies that receive (N)-laden flux. The N_2O emissions are calculated as a fraction of the N flux to the aquatic body that is further converted into N_2O using the set of equations described in the Box 3. The indirect emissions due to N leaching and runoffs from agricultural soils takes into account the N_2O originating from 3 types of water bodies: (i) groundwater[17] and surface drainage (e.g. tile drainage, drainage ditches); (ii) rivers and others[18]; and (iii) estuaries[19] (*Revised 1996 IPCC Guidelines for National Greenhouse Gas Inventories : Reference Manual (Volume 3)*, 1997).

[17] including springs and upstream emissions corresponding to the degassing of groundwater
[18] including lakes, ponds and downstream emissions from the nitrification/denitrification of degassed water
[19] excluding outer estuaries and coastal waters

Box 3: Indirect N_2O emissions from managed soils (De Klein et al., 2006; Hergoualc'h et al., 2019).

Indirect N_2O emissions from managed soils are calculated as a fraction of the nitrogen flux reaching the aquatic body. The N sources included are synthetic and organic fertilizers, urine and dung from grazing animals in pastures, crop residues and N mineralization following land use change.

- Tier 1 method:

The indirect N_2O emissions from atmospheric deposition of N volatilised from managed soils are calculated as follow:

$$N_2O_{(ATD)} - N = [(F_{SN} \cdot Frac_{GASF}) + (F_{ON} + F_{PRP}) \cdot Frac_{GASM}] \cdot EF_4$$

Where $N_2O_{(ATD)}$ – N is the annual amount of N_2O – N produced from atmospheric deposition of N volatilised from managed soils (kg N_2O –N·yr^{-1}), F_{SN} is the annual amount of synthetic fertilizer N applied to soils (kg N·yr^{-1}), F_{ON} is the annual amount of organic N additions applied to soils (kg N·yr^{-1}), F_{PRP} is the annual amount of urine and dung N deposited by grazing animals (kg N·yr^{-1}), $Frac_{GASF}$ (default = 0.11 kg N volatilised·kg of N applied^{-1}) is the fraction of synthetic fertiliser N that volatilises as NH_3 and NO_x (kg N volatilised·kg of N applied^{-1}), $Frac_{GASM}$ (default = 0.21 kg N volatilised·kg of N applied or deposited^{-1}) is the fraction of applied organic N fertiliser materials and of urine and dung N deposited by grazing animals that volatilises as NH_3 and NO_x (kg N volatilised·kg of N applied or deposited^{-1}) and EF_4 (default = 0.010 kg N–N_2O·kg NH_3–N + NO_x–N volatilised^{-1}) is the emission factor for N_2O emissions from atmospheric deposition of N on soils and water surfaces (kg N–N_2O·kg NH_3–N + NO_x–N volatilised^{-1}).

The indirect N_2O emissions from leaching and runoff can be calculated using the equation below:

$$N_2O_{(L)} - N = (F_{SN} + F_{ON} + F_{PRP} + F_{CR} + F_{SOM}) \cdot Frac_{LEACH-(H)} \cdot EF_5$$

Where $N_2O_{(L)}$ – N is the annual amount of N_2O – N produced from leaching and runoff of N additions to managed soils (kg N_2O – N·yr^{-1}), F_{CR} is the amount of N in crop residues (kg N·yr^{-1}), F_{SOM} is the annual amount of N mineralised as a result of changes to land use or management (kg N·yr^{-1}), $Frac_{LEACH-(H)}$[20] (default = 0.24 kg N·kg of N additions^{-1}) is the fraction of all N added to/mineralised in managed soils (kg N·kg of N additions or deposition by grazing animals^{-1}) and EF_5 (default = 0.011 kg N_2O – N·kg N leached and runoff^{-1}) is the emission factor for N_2O emissions from N leaching and runoff (kg N – N_2O·kg N leached and runoff^{-1}).

The conversion of $N_2O_{(ATD)}$ – N and $N_2O_{(L)}$ – N emissions to N_2O is done using the equations:

$$N_2O_{(ATD)} = N_2O_{(ATD)} - N \cdot \frac{44}{28} \text{ and } N_2O_{(L)} = N_2O_{(L)} - N \cdot \frac{44}{28}$$

Where $\frac{44}{28}$ is the conversion factor of kg N_2O – N into kg N_2O.

- Tier 2 method

A similar equation as for Tier 1 can be adopted using country-specific values for emission factors and partitioning fractions for each N source. For instance, $N_2O_{(ATD)}$ – N would be calculated as follow:

$$N_2O_{(ATD)} - N = \left\{\sum_i (F_{SN_i} \cdot Frac_{GASF_i}) + [(F_{ON} + F_{PRP}) \cdot Frac_{GASM}]\right\} \cdot EF_4$$

Where F_{SN_i} is the annual amount of synthetic fertilizer N applied to soils under different conditions *i* (kg N·yr^{-1}) and $Frac_{GASF_i}$ is the fraction of synthetic fertiliser N that volatilises as NH_3 and NO_x under different conditions *i* (kg N volatilised·kg of N applied^{-1}). The conversion of $N_2O_{(ATD)}$ – N emissions to N_2O emissions is similar to the one used in Tier 1.

[20] In dry climate regions where no irrigation is used or where rainfall – evaporation does not exceed the soil water-holding capacity, the default value for $Frac_{LEACH-(H)}$ is 0.

Appendix C. Natural N_2O emissions from aquatic environments

C.1. Inland and coastal waters (lakes, reservoirs, rivers, estuaries)

Tian et al. (2020) estimated that natural emissions from inland and coastal waters were 500 (200 – 700)[21] kt N-N_2O·year^{-1} from 2007 to 2016. Most papers compared their estimations to the 2006 IPCC value of 600 kt N-N_2O·year^{-1}. To simplify, we decided to adjust the comparisons to the most recent value from Tian et al. (2020).

Based on the data from 223 studies, DelSontro et al. (2018) used a model combining lakes size and primary productivity to specifically estimate the annual N_2O emissions from lakes and impoundments. These authors estimated these emissions at 190-450 kt N-N_2O·year^{-1}. Following a different approach, Maavara et al. (2019) used a mass balance mechanistic model to estimate emissions from rivers, estuaries and coastal zones and assessed that these emissions were about half of the estimations from Tian et al. (2020), at around 148 – 277 kt N-N_2O·year^{-1}, from which 42.5 – 71.5 kt N-N_2O·year^{-1} would be emitted by reservoirs (which does not include lakes, wetlands and coastal aquaculture ponds). That last value is close to the 30 kt N-N_2O·year^{-1} estimated by Deemer et al. (2016) for all reservoirs. Using the same model as Maavara et al. (2019), Lauerwald et al. (2019) estimated that 63 kt N-N_2O·year^{-1} were emitted by all natural lakes and reservoirs, which is 5 times less than the estimation from DelSontro et al. (2018). These authors also noted that reservoirs were responsible for half of these emissions even though their area represents only 9% of the total area for all natural lakes and reservoirs. The suggested reason behind this observation is that reservoirs are more prone to N and P influxes due to their proximity to urban and agricultural zones. As can be seen, the values found in the literature differ greatly depending on the approach used and the aquatic ecosystems considered.

A better understanding of the drivers of N_2O production is needed to improve estimates of N_2O emissions from lentic[8] waters. Miao et al. (2020) noticed a significant seasonality and spatial variation of N_2O emissions from lake Chaohu in China, with the highest N_2O flux originating from the most nutrient-polluted zones during summer. The emissions of N_2O are thus under the control of different factors. These authors suggested that this phenomenon could be partially explained by the variation of the average transfer velocity of N_2O, the water temperature and the dissolved oxygen (DO) concentration as the DO influences nitrification and denitrification processes.

[21] The values written in brackets correspond to the lower and higher end of range.

C.2. Oceans

The IPCC estimates that oceans naturally emit 3,800 (1,800 - 9,400)[21] kt N-N_2O $year^{-1}$, which represents around 35% of all natural N_2O emissions in 2006 (Ciais et al., 2013). Similar estimates of 4,000 (1,200 - 6,800) [21] kt N-N_2O.$year^{-1}$ and 4,200 ± 1,000 kt N-N_2O.$year^{-1}$ were proposed by Nevison et al. (1995) and Yang et al. (2020), respectively.

N_2O distribution in the ocean is related to oxygen distribution (Kock et al., 2016). The highest N_2O emissions are generally recorded at the boundaries of oxygen minimum zones (OMZ) of the ocean (Arévalo-Martínez et al. 2015a). These zones are mostly located on the west coast of continents, mainly in tropical zones, and are found at different depths. Their distribution is determined by the water surface temperature, the large-scale ocean currents circulation, and the biological and chemical processes occurring in the ocean. Oxygen solubility decreases with water temperature and the ocean areas located between gyres[22] are less mixed and, therefore, less oxygenated. The high biological activity occurring in the upwelling areas is also responsible for oxygen depletion in OMZs. This low oxygen level could explain the partial denitrification during which the conversion of N_2O to N_2 does not take place (Arévalo-Martínez et al., 2015a; Arévalo-Martínez et al., 2015b). However, N_2O is consumed in anoxic waters, such as in the core of the OMZ (Arévalo-Martínez et al., 2015a). Besides, Yang et al. (2020) observed that N_2O emissions from the ocean show a strong seasonality, as reported for other ecosystems such as lakes. These authors used over 158,000 measurements from the ocean to reconstruct climatological N_2O emissions and determined that the seasonality is mostly due to the variations in wind speed and the disequilibrium between air and water N_2O concentrations. They also demonstrated that the seasonality of the N_2O concentration disequilibrium was associated to the chlorophyll concentration, the subsurface apparent oxygen utilization (AOU) and, to a lesser extent, sea-surface temperature (SST) and mixed-layer depth. The nature of the correlation was dependent on the regions considered and is presented in Table 18. N_2O emissions seasonality could be explained at over 66% by changes in the N_2O disequilibrium and by changes in wind speed at 33%. The Arctic Ocean and, occasionally, the subtropical gyres were predicted to consume N_2O while the upwelling regions (e.g. Peruvian upwelling), the subpolar Pacific Ocean and the Southern Ocean were predicted as main producers. Thus, upwelling regions representing only 3% of oceanic areas could be responsible for 20% of all N_2O oceanic emissions (840 kt N-N_2O.$year^{-1}$) (Yang et al., 2020).

[22] Large system of circulating ocean currents.

Table 18: Regimes and empirical drivers of N_2O disequilibrium seasonality (Yang et al., 2020)

	Regimes of N_2O disequilibrium seasonality			
	Upwelling	**Mixed-layer**	**Solubility**	**Productivity-driven**
Location	Tropical and northern Indian Ocean, eastern tropical Pacific and Atlantic Oceans, parts of the Southern Ocean	Southern Ocean Polar Front, subpolar Atlantic and Pacific	Ocean's subtropical gyres	Other parts of the ocean
Empirical drivers positively correlated to N_2O supersaturation	Chlorophyll, subsurface AOU	AOU, mixed-layer depth	SST	Chlorophyll
Empirical drivers negatively correlated to N_2O supersaturation	SST	Chlorophyll, SST	Chlorophyll, AOU, mixed-layer depth	

Apart from OMZ, hypoxia[23] can occur in the ocean due to eutrophication. These hypoxic zones are often found near coasts and are contributing to N_2O emissions (Naqvi et al., 2009). For example, N_2O emissions of 25 - 287 nmole·m^{-2}·h^{-1} were reported in the Gulf of Mexico hypoxic zone receiving nutrients-rich fluxes from the Mississippi and Atchafalaya Rivers (Walker et al., 2010).

[23] Oxygen-depleted condition triggered by the aerobic biodegradation of exogenous organic matter and/or endogenous respiration.

Appendix D. General lake characteristics

Lakes can be classified according to their location (polar, temperate, or tropical), origin (glacial, volcanic, riverine, etc.), circulation and mixing patterns, or trophic state. The main definitions related to thermal stratification and the different mixing patterns are illustrated in Box 4.

Box 4: Thermal stratification and mixing patterns of lakes.

When a lake shows a thermal stratification, the surface layer, called epilimnion and the lowest layer, called hypolimnion are separated by a transition layer called the thermocline. The layers can mix during the year and the different mixing patterns found in lakes are described below.

- *Polymictic lake: Non-stratified lake, the water is mixed all the year.*

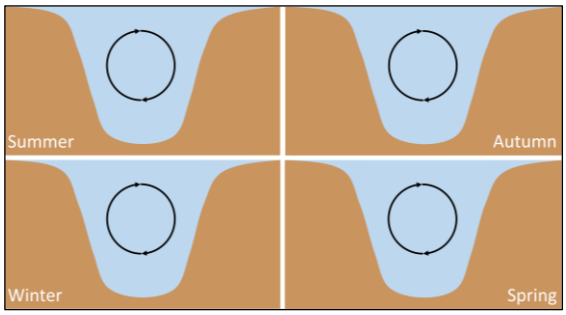

- *Oligomictic lake: Lake that rarely mixes.*

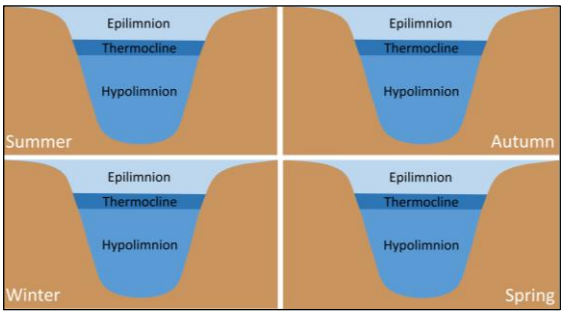

- *Monomictic lake: Lake that mixes only once a year. The lake is either warm monomictic if the mixing occurs during winter or cold monomictic if it occurs during summer months.*

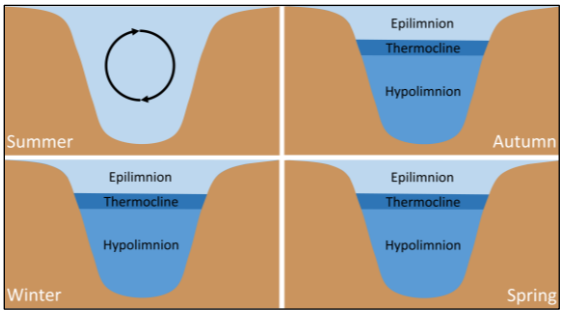

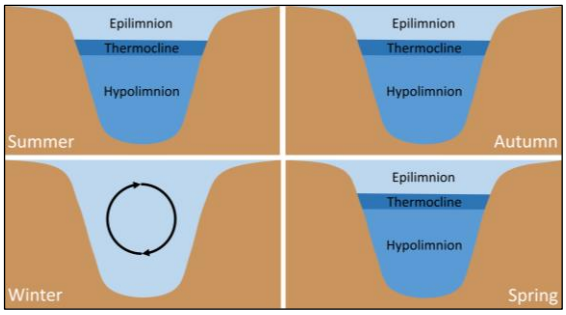

- *Dimictic lake: Lake that mixes twice a year.*

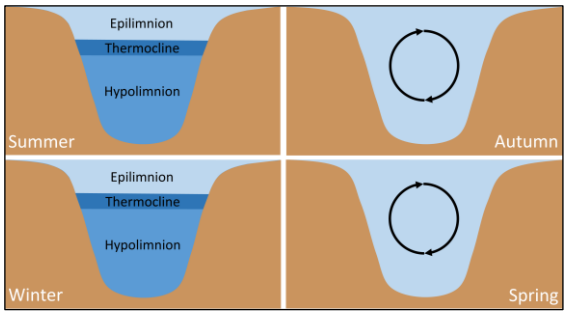

- *Amictic lake: Lake that never mixes and are isolated by an ice layer on top.*

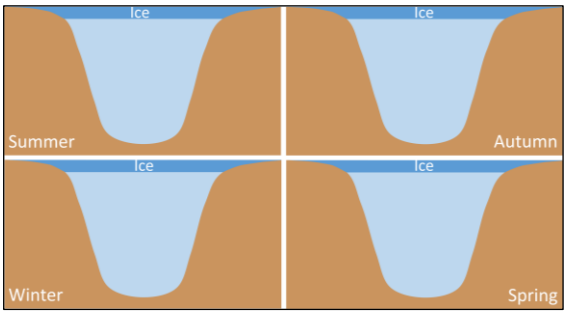

Appendix E. TLI score calculation

Box 5: TLI score.

Annual average values of chlorophyll a (Chla) concentration, Secchi depth (SD), total phosphorous (TP) concentration and total nitrogen (TN) concentration of 24 New Zealand lakes measured over a period of two to four years were used by Burns et al. (2000) to elaborate the TLI. The average annual values are used to normalise the data by suppressing the variability due to the different seasons over the year.

First, Burns et al. (2000) chose to base the TLI score on the Chla concentration: the TLI values of 3, 4 and 6 were assigned to Chla concentrations of 2, 5 and 30 $mg \cdot m^{-3}$ based on the description of New Zealand lake trophic classes made by Vant (Davies-Colley et al., 1993). A plot of the 3 TLI values against the base-10 logarithm of the 3 Chla concentrations followed by an ordinary least squares (OLS) regression gives the equation for the trophic level index of Chla called TLc:

$$TLc = 2.22 + 2.54 \log(Chla) \quad (1)$$

Using equation (1), the average annual TLc are calculated from the average annual Chla concentration values for each lake. Then, the plot of TLc against the base-10 logarithm of TN and TP values followed by an OLS regression gives the equations for the trophic level indexes of TN and TP, respectively TLn and TLp, assuming that TLc = TLn = TLp:

$$TLn = -3.61 + 3.01 \log(TN) \quad (2)$$

$$TLp = 0.218 + 2.92 \log(TP) \quad (3)$$

The SD being inversely proportional to the trophic state, it is necessary to first transform this variable before following the same calculation method as for TLn and TLp to determine TLs. The transformation applied by Chapra & Dobson (1981) using the Beer-Lambert law for light extinction was employed, and the extinction coefficient due to water itself was adapted to the highest SD reported in New Zealand. The new SD expression considered was $\frac{1}{SD} - \frac{1}{40}$. Then, assuming that TLc = TLs, the expression obtained for TLs was:

$$TLs = 5.10 + 2.27 \log(\frac{1}{SD} - \frac{1}{40}) \quad (4)$$

Finally, the average TLI can be calculated as the average value of the four trophic level indexes:

$$TLI = \frac{1}{4} (TLc + TLs + TLp + TLn) \quad (5)$$

Appendix F. Potential sampling sites list

Table 19: Potential sampling sites list

	Lake	Mixing pattern	TLI in 2019	Trophic state	Geomorphic Type	Distance from Massey (km)	Area (ha)	Max Depth (m)	Depth (Lakes380) (m)	Altitude (m)	Authorization required
Eutrophic lake	Lake Koputara	Polymictic	8	Eutrophic	Aeolian	40.7					Maori-owned lake
	Omanuka lagoon	Polymictic	5.7	Eutrophic	Aeolian	43.3				29	Maori-owned lake
	Pukepuke lagoon	Polymictic	7.2	Eutrophic	Aeolian	44.5	15	2	1	10	Anyone visiting the wetland requires a (free) permit from the local DOC office.
	Lake Alice	Polymictic	5.8	Eutrophic	Aeolian	45.7	12	3.5		116	
	Lake Horowhenua	Polymictic	6.7	Eutrophic	Aeolian	47.8	389	2			Maori-owned lake
	Lake William	Polymictic	6.6	Eutrophic	Aeolian	48.2	7		9.8	105.8	
	Lake Heaton	Polymictic	7.1	Eutrophic	Aeolian	49.3	14		5.00	97	
	Lake Dudding	Stratified	5.6	Eutrophic	Aeolian	50.7	8	12	7.3	92	No
	Lake Herbert	Polymictic	6.2	Eutrophic	Aeolian	50.9					
	Lake Koitiata	Polymictic	4.8	Eutrophic	Aeolian	58.8	10	5	1.60	18	
	Lake Waipu	Polymictic	6.3	Eutrophic	Aeolian	64.8	7		4.3	20	
	Lake Pauri	Stratified	5.6	Eutrophic	Aeolian	73.2	19	8	14.2	58	No
	Lake Wiritoa	Stratified	4.9	Eutrophic	Aeolian	77.7	22	20	19	51	No
	Lake Kohata	Stratified	4.9	Eutrophic	Aeolian	78.2	10	5			
	Lake Westmere	Polymictic	6.7	Eutrophic	Aeolian	87.2	8	5	6	96	
	Lake Kawau					33.5	1		1.10	71	
	Karere lagoon					15.7	3		1.60	12.6	
	Voss lagoon					18.6	5		1.6	10.6	
Clean lake	Turitea Dams			Mesotrophic	River dam	6.8	12	10		170	Yes
	Upper Karori Lake			Mesotrophic	River dam	141	0.1	9		169	
	Ohakune lakes			Oligotrophic	Volcanic	174	2	5		579	
	Lake Rotorangi	Stratified	4	Mesotrophic	River dam	197	290	60		111	
	Lake Opunake			Mesotrophic	River dam	212	10	5		19	No
	Lake Otamangakau			Oligotrophic	River dam	220	150	10		617	No
	Lake Ratapiko			Mesotrophic	River dam	222	24	10		205	No
	Lake Okareka	Stratified	3.1	Mesotrophic	Volcanic	346	334	34		355	No
	Lake Tikitapu	Stratified	2.7	Oligotrophic	Volcanic	346	144	28		418	No
	Lake Waikaremoana			Oligotrophic	Landslide	347	5574	248		585	No
	Lake Tarawera		3.1	Oligotrophic	Volcanic	353	4115	88		299	No
	Lake Waikareiti			Oligotrophic	Landslide	355	1371	50		900	No
	Lake Okataina	Stratified	2.7	Oligotrophic	Volcanic	357	1073	79	78	311	No
	Lake Rotoiti	Stratified	4	Mesotrophic	Volcanic	358	3369	126	126	297	No
	Lake Rotoma	Stratified	2.5	Oligotrophic	Volcanic	373					No

Appendix G. Comparison between different methods of quantification

In microbiology, the chlorophyll concentration is often used as an indicator of the cell concentration in a sample. In engineering, the cell concentration is preferably expressed in unit of mass of cells per unit of volume. To easily switch from one unit to the other, the main objective of this experiment was to check the relationship between different quantification units: chlorophyll a and b concentration, cell concentration, cell optical density and dry cell weight.

For this experiment, axenic *Chlamydomonas* cultures were grown in similar conditions than the batch assays set-up and biological triplicates were used. We tested the strain 6145c in TAP and minimal media, M3 in TAP and HSM and CMJ030 in HSM.

As expected, the values of the triplicate cultures were similar during the week. However, the cell counting method is the least accurate method because the cells are not always distributed in a homogeneous manner on the scales. The values of the DCW at time 0 are not very reliable because the weight differences between the filters alone and the filters with cells were not significant. The correlations between the different quantification methods are good with a $R^2 > 0,97$ for all of them for the culture of 6145c in TAP medium (Figure 19).

The results for the other strains and conditions are shown in Figure 20 - Figure 23. The experiments must be repeated to improve the results by taking more mid-point values. Besides, the cell growth is much slower in MM and HSM compared to TAP medium which increases the errors as the daily values are all similar.

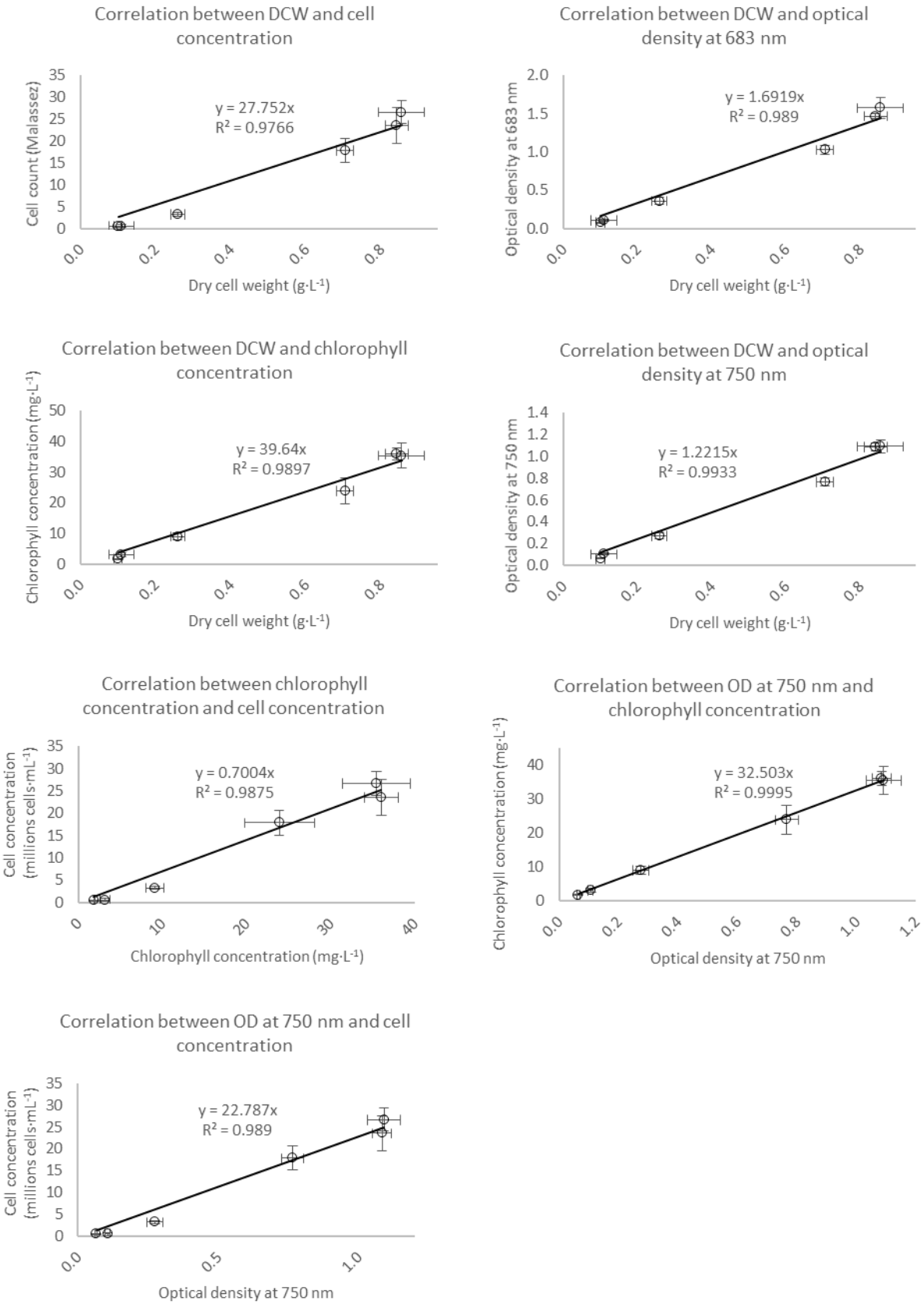

Figure 19: Correlation between the chlorophyll concentration, dry cell weight, optical densities at 750 nm and 683 nm and cell concentration of C. reinhardtii 6145c cultures in TAP medium.

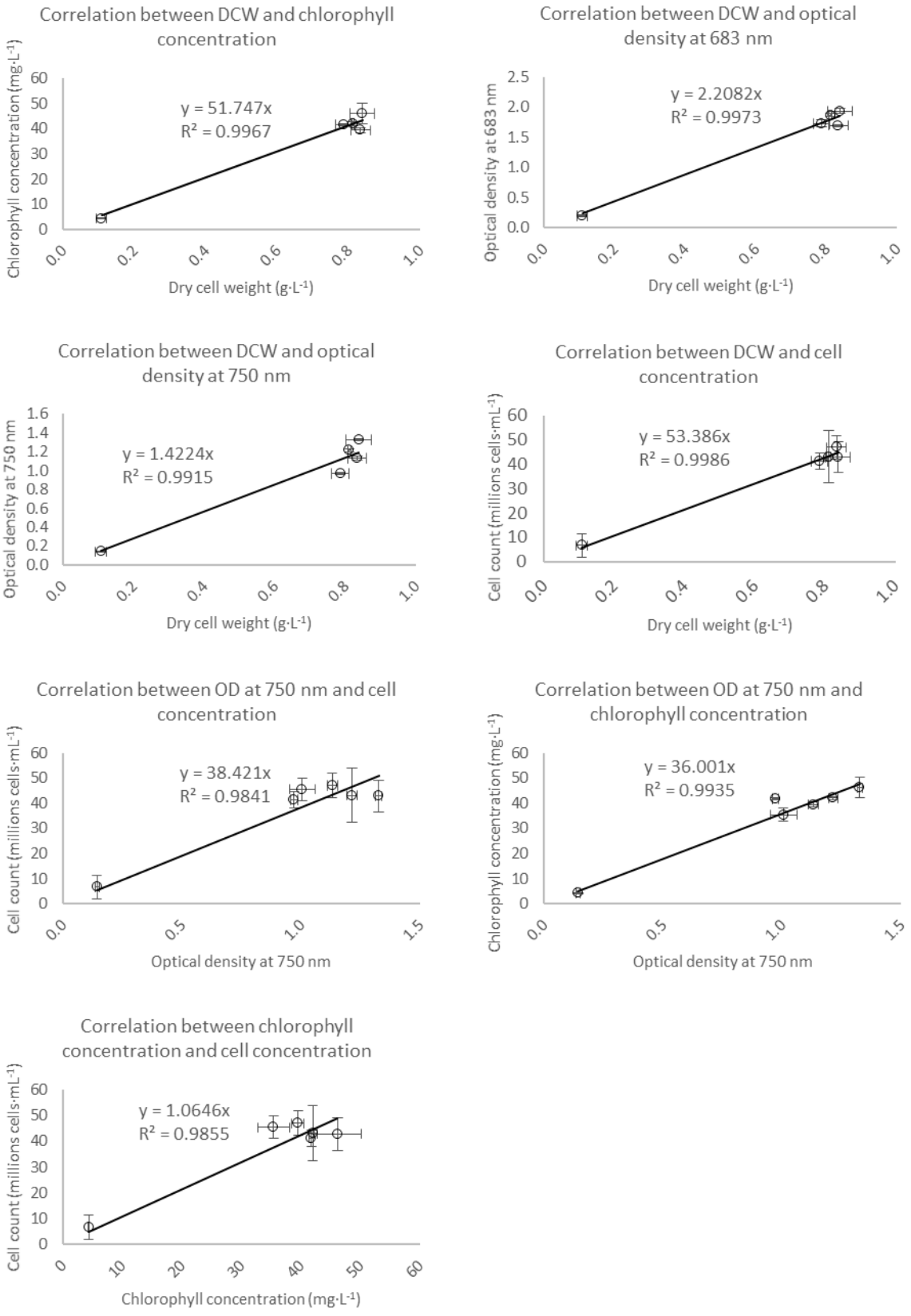

Figure 20: Correlation between the chlorophyll concentration, dry cell weight, optical densities at 750 nm and 683 nm and cell concentration of C. reinhardtii M3 cultures in TAP medium.

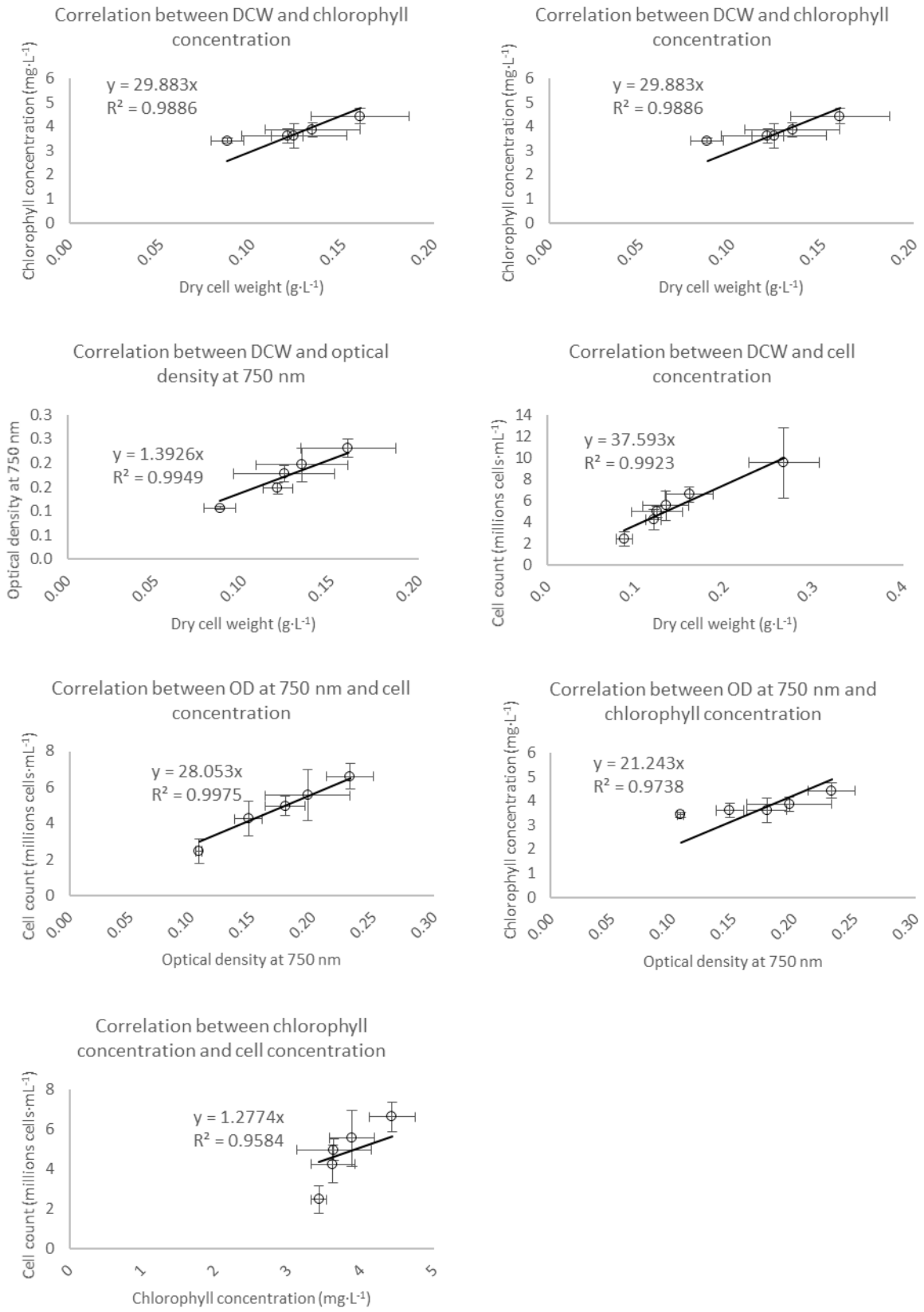

Figure 21: Correlation between the chlorophyll concentration, dry cell weight, optical densities at 750 nm and 683 nm and cell concentration of C. reinhardtii 6145c cultures in MM.

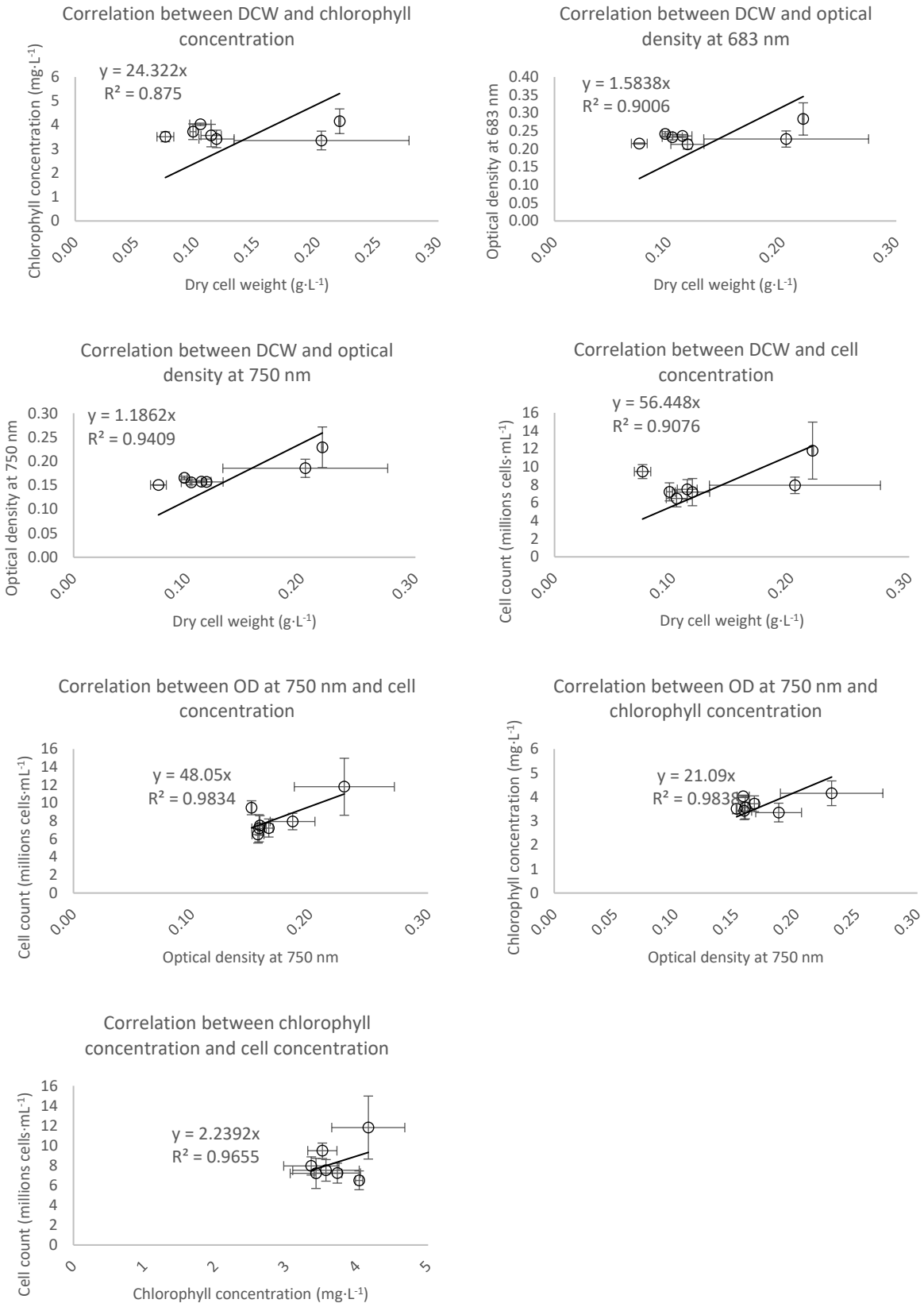

Figure 22: Correlation between the chlorophyll concentration, dry cell weight, optical densities at 750 nm and 683 nm and cell concentration of C. reinhardtii CMJ030 cultures in HSM.

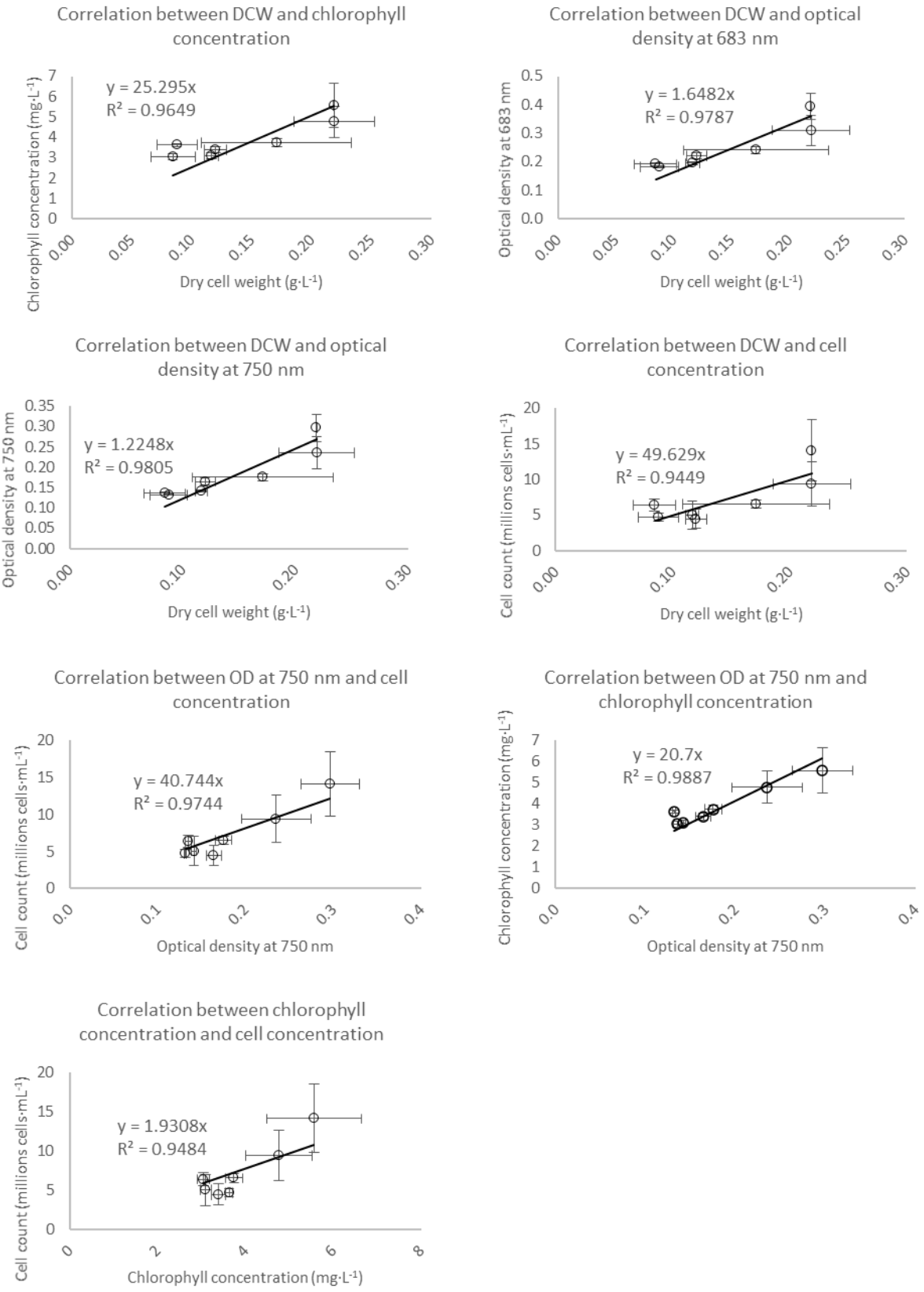

Figure 23: Correlation between the chlorophyll concentration, dry cell weight, optical densities at 750 nm and 683 nm and cell concentration of C. reinhardtii M3 cultures in HSM.

Appendix H. Cell extract preparation

Each method has been tested in triplicates. We have chosen the method n°4 for the cell extract preparation because this method does not require to take a large volume of sample compared to the method n°1 which means we can use the same set-up as the batch assays. This method is also more practical to carry out than the method n°2 and still gives an acceptable RNA concentration. The method n°3 has been disregarded due to its poor extraction rate.

Table 20: Cell extract preparation methods and results.

Method	Description of the method	Ratio 260/280	RNA concentration ($\mu g \cdot mL^{-1}$)
1	Collect 50 mL of cells Centrifuge for 2 min at 2,000 x g Resuspend the pellet in 800 µL of lysis buffer Add 75 µL of SDS 20% Freeze at -80°C	2.16	1022
2	Collect 10 mL of cells Cool down quickly with liquid nitrogen Centrifuge for 2 min at 2,000 x g Freeze the pellet at -80°C	2.12	185.1
3	Collect 10 mL of cells Flash-freeze with liquid nitrogen Freeze at -80°C Thaw the sample at 4°C Centrifuge for 2 min at 2,000 x g to get the pellet	2.19	20
4	Collect 10 mL of cells Centrifuge for 1 min at 2,000 x g Flash-freeze the pellet with liquid nitrogen Freeze at -80°C	2.19	99.7

Appendix I. N_2O batch assays abiotic control

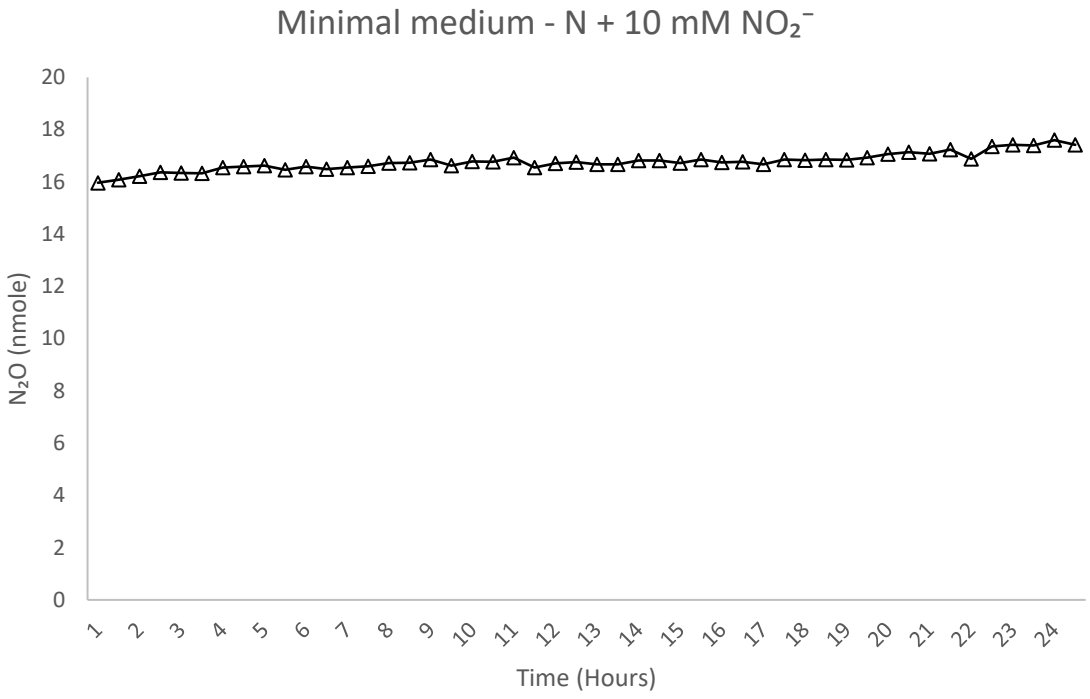

Figure 24: N_2O batch test, Minimal medium + 10 mM NO_2^- without cells.

Appendix J. RNA concentration and 260/280 ratio after RNA extraction and DNA removal

Table 21: RNA concentration and 260/280 ratio after RNA extraction and DNA removal.

Conditions	RNA concentration after precipitation (ng/µL)	260/280 ratio after RNA precipitation	RNA concentration after DNA removal (ng/µL)	260/280 ratio after DNA removal
M3 in HSM-N +10 mM NO_2^- t 0h	74.4	2.13	179.6	2.46
M3 in HSM-N +10 mM NO_2^- t 1h	89.1	2.04	513.6	2.3
M3 in HSM-N +10 mM NO_2^- t 3h	644.4	2.21	147.7	2.39
M3 in HSM-N +10 mM NO_2^- t 6h	248.3	2.11	493.5	2.29
M3 in HSM-N +10 mM NO_2^- t 17h	1566.7	2.17	67.9	2.42
M3 in HSM-N +10 mM NO_2^- t 24h	601.5	2.04	235.1	2.36
M3 in HSM-N t 0h	12.9	2.1	11.2	1.97
M3 in HSM-N t 1h	154.1	2.11	384.8	2.35
M3 in HSM-N t 3h	226.4	2.11	347.7	2.33
M3 in HSM-N t 6h	79	1.96	166.1	2.34
M3 in HSM-N t 17h	87	2.17	304.3	2.32
M3 in HSM-N t 24h	56.5	1.92	229.7	2.41
CMJ030 in HSM-N +10 mM NO_2^- t 0h	538.2	2.3	538.9	2.1
CMJ030 in HSM-N +10 mM NO_2^- t 1h	793.6	2.45	521.5	2.14
CMJ030 in HSM-N +10 mM NO_2^- t 3h	667.5	2.51	555.2	2.12
CMJ030 in HSM-N +10 mM NO_2^- t 6h	616.3	2.43	324.5	2.17
CMJ030 in HSM-N +10 mM NO_2^- t 17h	455.4	2.39	531.1	2.13
CMJ030 in HSM-N +10 mM NO_2^- t 24h	348.5	2.34	594.6	2.14
CMJ030 in HSM-N t 0h	900.1	2.16	563.4	2.13
CMJ030 in HSM-N t 1h	1797.9	2.17	344.6	2.18
CMJ030 in HSM-N t 3h	1071.1	2.17	397.7	2.16
CMJ030 in HSM-N t 6h	677.1	2.16	470	2.15
CMJ030 in HSM-N t 17h	473.5	2.13	531.6	2.12
CMJ030 in HSM-N t 24h	184.4	2.16	386.9	2.16

Appendix K. Melting peak charts

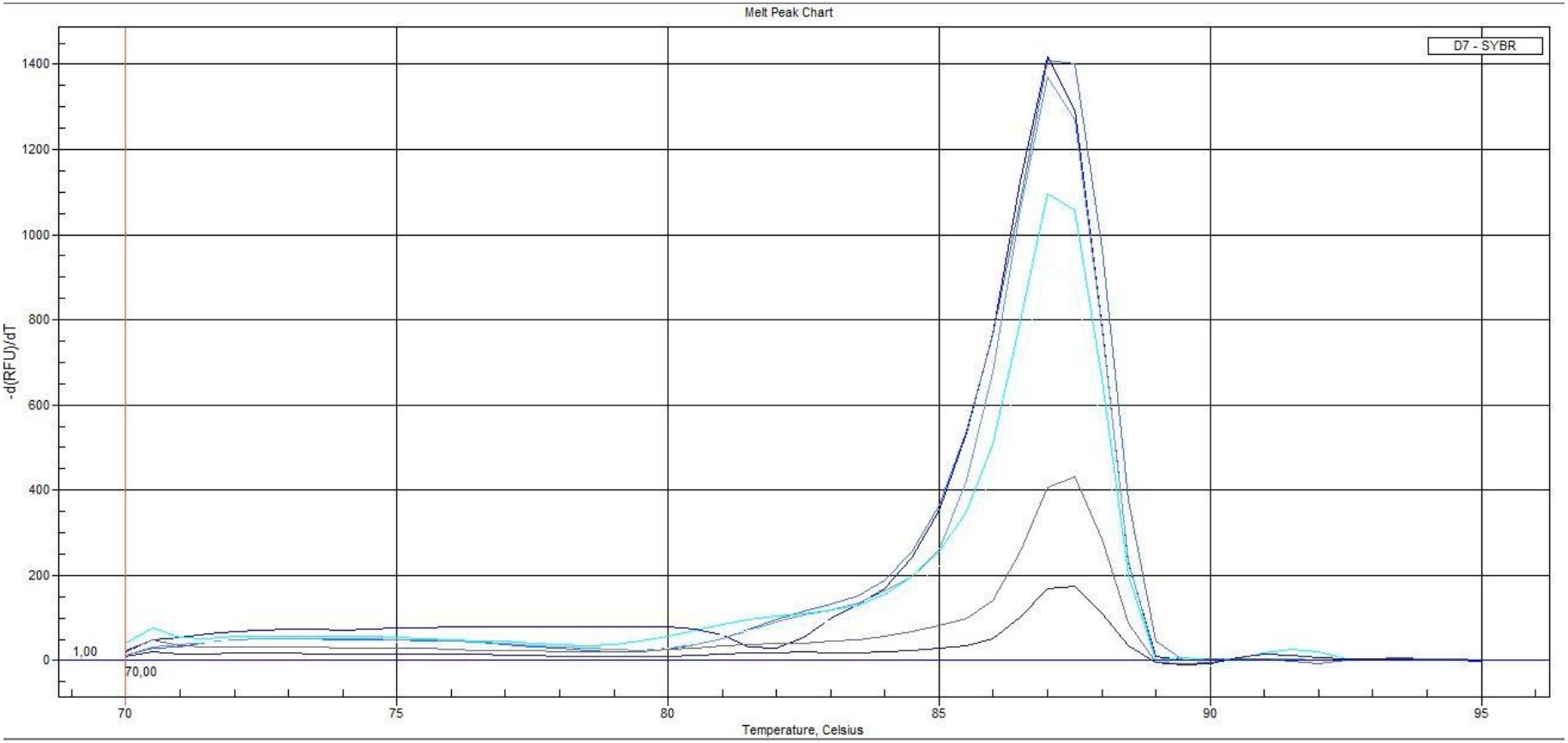

Figure 25: Melting peak chart of different dilutions of FLVB primer.

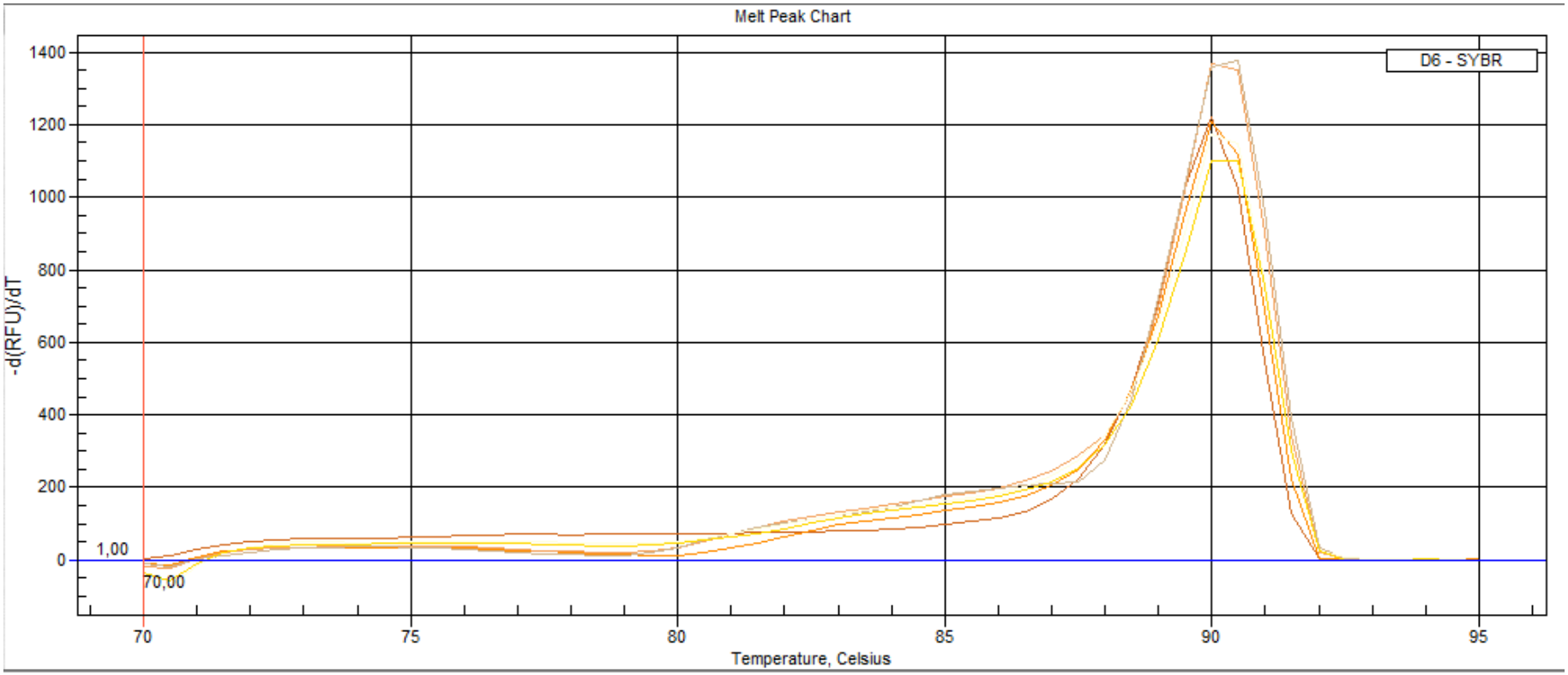

Figure 26: Melting peak chart of different dilutions of CBLP primer.

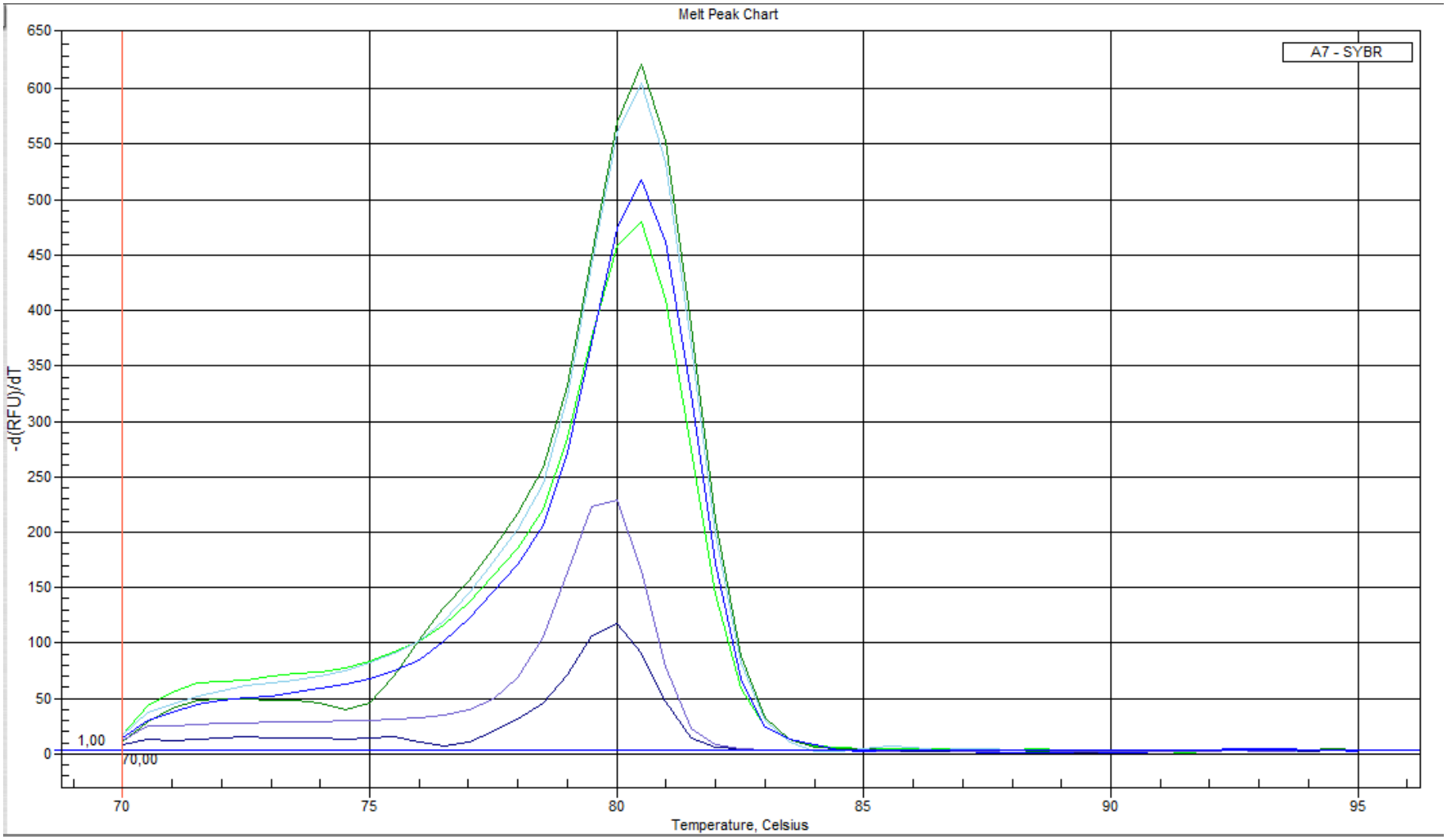

Figure 27: Melting peak chart of different dilutions of FLVA primer.

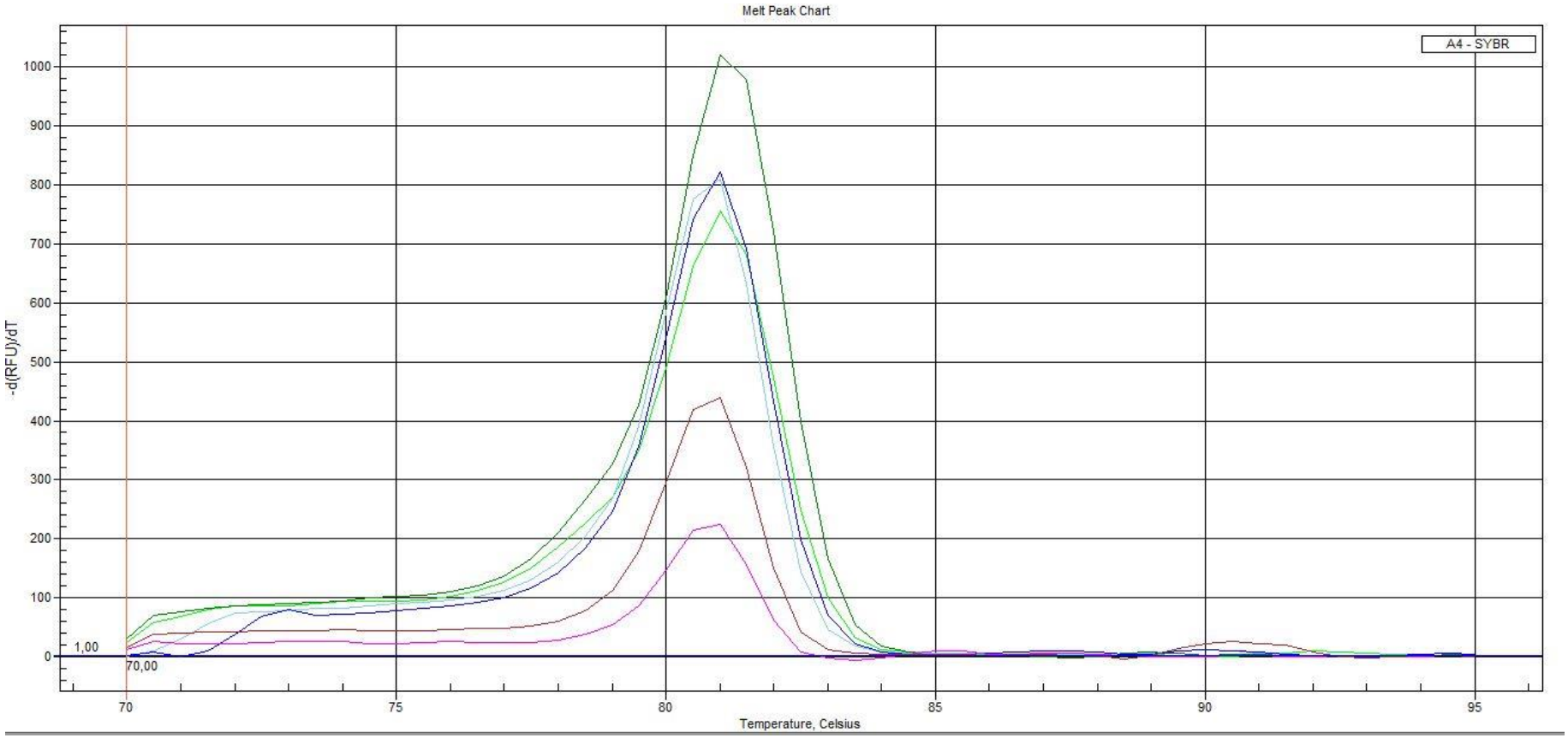

Figure 28: Melting peak chart of different dilution of NIRK primer.

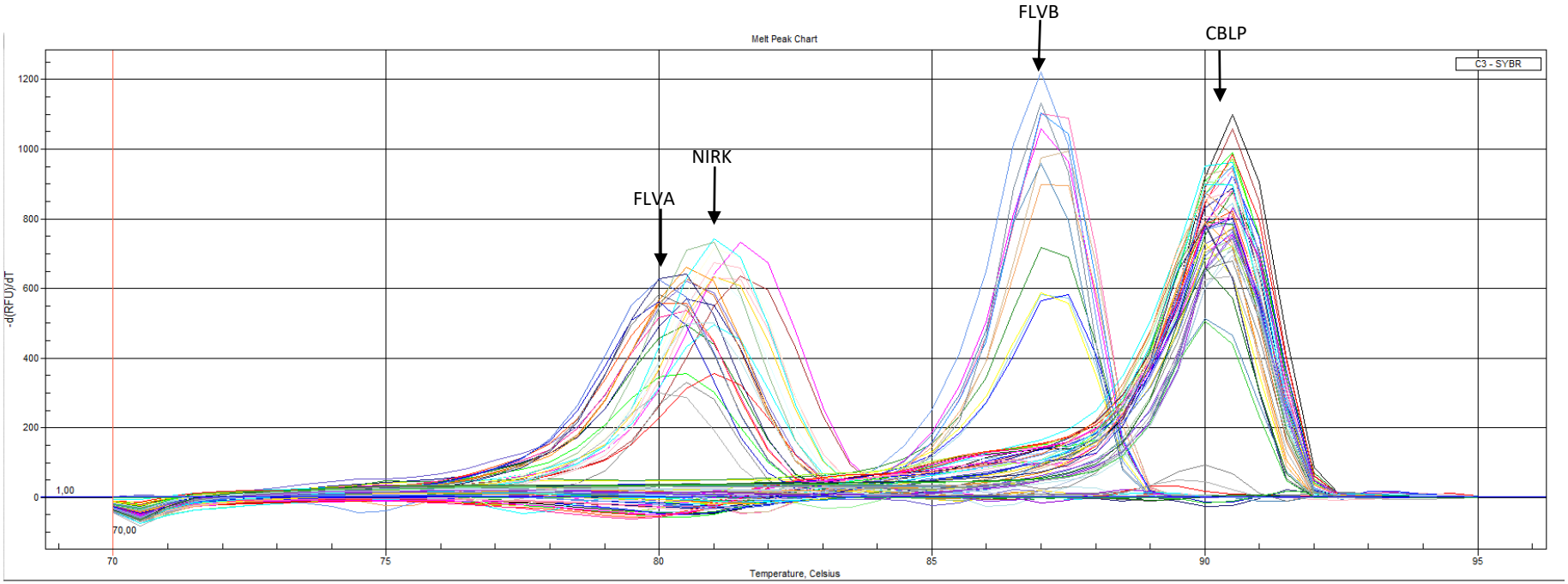

Figure 29: Melting peak chart: PCR from the 27/01/2021.

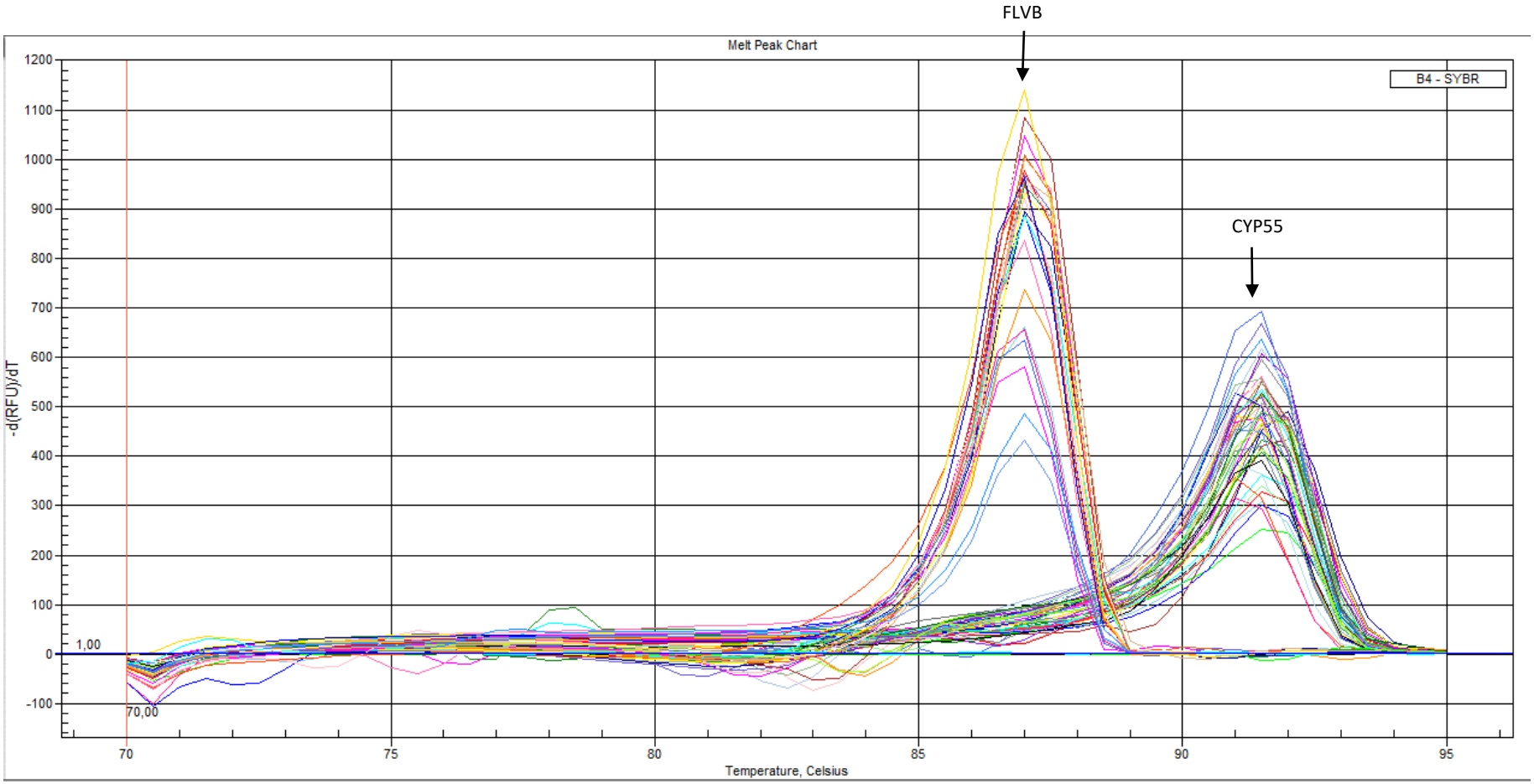

Figure 30: Melting peak chart: PCR from the 27/01/2021.

Appendix L. Media used

L.1. TAP (Tris Ammonium Phosphate) medium

Chemical	Concentration ($g.L^{-1}$)
NH_4Cl	0.40
$CaCl_2 \cdot 2H_2O$	0.05
$MgSO_4 \cdot 7H_2O$	0.10
Tris Acetate	2.42
KH_2PO_4	0.056
K_2HPO_4	0.108
Glacial Acetic Acid	950 µL
Trace Elements	1 mL
Trace elements	**Concentration ($g.L^{-1}$)**
EDTA	50
BO_3H_3	11.4
$ZnSO_4.7H_2O$	22
$MnCl_2.4H_2O$	5.1
$FeSO_4.7H_2O$	5
$CoCl_2.6H_2O$	1.6
$CuSO_4.5H_2O$	1.6
$MoO_4Na_2.2H_2O$	0.214

Table 22: TAP medium

L.2. TAP medium without nitrogen

Chemical	Concentration ($g.L^{-1}$)
$CaCl_2 \cdot 2H_2O$	0.05
$MgSO_4 \cdot 7H_2O$	0.10
Tris Acetate	2.42
KH_2PO_4	0.056
K_2HPO_4	0.108
Glacial Acetic Acid	950 µL
Trace Elements	1 mL
Trace elements	**Concentration ($g.L^{-1}$)**
EDTA	50
BO_3H_3	11.4
$ZnSO_4.7H_2O$	22
$MnCl_2.4H_2O$	5.1
$FeSO_4.7H_2O$	5
$CoCl_2.6H_2O$	1.6
$CuSO_4.5H_2O$	1.6
$MoO_4Na_2.2H_2O$	0.214

Table 23: TAP medium without nitrogen

L.3. TAP without nitrogen and sulfur

Chemical	Concentration ($g.L^{-1}$)
$CaCl_2 \cdot 2H_2O$	0.05
$MgCl_2 \cdot 6H_2O$	0.0824
Tris Acetate	2.42
KH_2PO_4	0.056
K_2HPO_4	0.108
Glacial Acetic Acid	950 µL
Trace Elements	1 mL
Trace elements	**Concentration ($g.L^{-1}$)**
EDTA	50
BO_3H_3	11.4
$ZnSO_4.7H_2O$	22
$MnCl_2.4H_2O$	5.1
$FeSO_4.7H_2O$	5
$CoCl_2.6H_2O$	1.6
$CuSO_4.5H_2O$	1.6
$MoO_4Na_2.2H_2O$	0.214

Table 24: TAP medium without nitrogen and sulfur

L.4. Minimal medium

Chemical	Concentration ($g.L^{-1}$)
NH_4Cl	0.40
$CaCl_2 \cdot 2H_2O$	0.05
$MgSO_4 \cdot 7H_2O$	0.10
KH_2PO_4	0.56
K_2HPO_4	1.08
Trace Elements	1 mL
Trace elements	**Concentration ($g.L^{-1}$)**
EDTA	50
BO_3H_3	11.4
$ZnSO_4.7H_2O$	22
$MnCl_2.4H_2O$	5.1
$FeSO_4.7H_2O$	5
$CoCl_2.6H_2O$	1.6
$CuSO_4.5H_2O$	1.6
$MoO_4Na_2.2H_2O$	0.214

Table 25: Minimal medium.

L.5. HSM (High Salt medium)

Chemical	Concentration ($g.L^{-1}$)
NH_4Cl	0.50
$CaCl_2 \cdot 2H_2O$	0.01
$MgSO_4 \cdot 7H_2O$	0.02
KH_2PO_4	0.72
K_2HPO_4	1.44
Trace Elements	1mL
Trace elements	**Concentration ($g.L^{-1}$)**
EDTA	50
BO_3H_3	11.4
$ZnSO_4.7H_2O$	22
$MnCl_2.4H_2O$	5.1
$FeSO_4.7H_2O$	5
$CoCl_2.6H_2O$	1.6
$CuSO_4.5H_2O$	1.6
$MoO_4Na_2.2H_2O$	0.214

Table 26: HSM medium.

L.6. HSM without nitrogen

Chemical	Concentration ($g.L^{-1}$)
$CaCl_2 \cdot 2H_2O$	0.01
$MgSO_4 \cdot 7H_2O$	0.02
KH_2PO_4	0.72
K_2HPO_4	1.44
Trace Elements	1mL
Trace elements	**Concentration ($g.L^{-1}$)**
EDTA	50
BO_3H_3	11.4
$ZnSO_4.7H_2O$	22
$MnCl_2.4H_2O$	5.1
$FeSO_4.7H_2O$	5
$CoCl_2.6H_2O$	1.6
$CuSO_4.5H_2O$	1.6
$MoO_4Na_2.2H_2O$	0.214

Table 27: HSM medium without nitrogen.